universität
wien

DIPLOMARBEIT

Titel der Diplomarbeit

„Illuminating the functional role of PTPA via knock down analyses and determination of its subcellular localization"

Verfasserin

Sarah Maria Schönbauer

angestrebter akademischer Grad

Magistra der Naturwissenschaften (Mag.rer.nat.)

Wien, 2011

„Die Unwissenheit ist eine Situation, die den Menschen ebenso hermetisch abschließt wie ein Gefängnis."

Simone de Beauvoir

Abstract

Protein phosphorylation and dephosphorylation, carried out by kinases and phosphatases respectively, represent hallmarks of intracellular signalling cascades. One of the most abundant serine/threonine phosphatases PP2A, protein phosphatase 2A, fulfills distinct roles in cell cycle regulation, programmed cell death and signal transduction pathways. Active and specific PP2A is represented by heterotrimeric holoenzymes, which need to be tightly regulated to cope with various substrates. Different studies revealed posttranslational mechanisms, as for instance phosphorylation and methylation, to be key modifications for the regulation of PP2A.

PTPA, the p̲hosphtase t̲wo A p̲hosphatase a̲ctivator, was originally identified as an activator of the *in vitro* phosphotyrosyl phosphatase activity of PP2A [Cayla et al, 1990]. Furthermore, Fellner and coworkers showed a deletion of the yeast homologues of PTPA, *RRD1* and *RRD2*, to reduce catalytic activity, affect substrate specificity, protein stability and metal dependence of PP2A [Fellner et al., 2003]. Recently, inactive PP2A was shown to be reactivated by PTPA. Nevertheless, the identification of an exact function of PTPA in mammals is still missing. A conservation of function is emphasized through the ability of mammalian PTPA to complement the proliferation phenotype of a *rrd1Δ/rrd2Δ* yeast strain. Moreover, previous findings of apoptotic conditions, emerging upon knock down or due to overexpression of PTPA in mammalian cell lines, pinpointed towards an essential role of PTPA.

Therefore, we wanted to further elucidate the consequence of PTPA knock down in mammalian cells by the use of shRNA and siRNA. Single clones of HelaTRex cells, stably transfected with a vector coding for the inducible expression of a targeting shRNA against the mRNA of PTPA, were shown to efficiently reduce the protein to 15% of its normal amount. Furthermore, short interfering RNAs were applied and resulted in a PTPA protein knock down to 1/4 in comparison to normal amount. A combination of both methods, however, failed to decrease PTPA to lower levels. Despite these low amounts of PTPA, a significant alteration of phenotype could not be observed.

Furthermore, we intended to unravel the subcellular localization of PTPA by the use of different antibodies specific for mammalian PTPA, applied in subcellular fractionation experiments and immunofluorescence analyses. Upon the subdivision of Hela cells into nuclear and cytoplasmic fractions, a major distributrion of PTPA in the cytoplasm was confirmed by immuno blot analysis. As opposed to this, PTPA seemed to emerge mainly in nuclear compartments if analysed with immunofluorescence.

Abstract in German

Phosphorylierung und Dephosphorylierung von Proteinen repräsentieren wichtige Modifizie-rungen in intrazellulären Signalkaskaden, welche für die Aktivierung und Deaktivierung der jeweiligen Proteine verantwortlich sind. Eine der häufigsten Serin/Threonin Phosphatasen, PP2A, Protein Phosphatase 2A, erfüllt dabei eine wichtige Rolle in der Zellzyklusregulation, im programmierten Zelltod sowie in Signaltransduktionswegen. Heterotrimere Holoenzyme reprä-sentieren dabei das aktive und spezifische PP2A, welches wiederum sehr genau reguliert werden muss um die Interaktion mit verschiedenen Substraten bewerkstelligen zu können. Unterschied-liche Studien verdeutlichten bereits, dass sowohl Phosphorylierung als auch Methylierung wich-tige Modifikationen für die Funktion von PP2A darstellen.

PTPA, der P̲hosphtase 2̲ A P̲hosphatase A̲ktivator, wurde ursprünglich als Aktivator der *in vitro* Phosphotyrosin Phosphatase Aktivität von PP2A identifiziert [Cayla et al, 1990]. Zusätzlich zeigten Fellner und Kolleg_innen, dass eine Deletion der homologen Proteine von PTPA in He-fe, *RRD1* und *RRD2*, sowohl die katalytische Aktivität von PP2A reduziert als auch die Sub-stratspezifität, Proteinstabilität und Abhängigkeit von Metallionen beeinträchtigt. Kürzlich wur-de gezeigt, dass inaktives PP2A durch PTPA reaktiviert werden kann. Dennoch fehlt bisher die Charakterisierung der exakten Funktion von PTPA in Säugetieren. Der Umstand, dass Säuge-tier-PTPA den Wildtyp Phänotyp von einem *rrd1Δ/rrd2Δ* Hefestamm komplementieren kann, bestärkt die Hypothese einer konservierten und essentiellen Funktion von PTPA. Frühere Studi-en zeigten zudem, dass sowohl durch Überexprimierung als auch durch Knock-down von PTPA, apoptotische Bedingungen entstehen und dieses Protein insofern eine essentielle Rolle ein-nimmt.

Deshalb war es ein Teilziel dieser Arbeit mittels shRNA und siRNA weitere Konsequenzen ei-nes PTPA-Knock-down in Säugetierzellen zu untersuchen. Einzelzellklone einer HelaTRex Zelllinie, stabil transfiziert mit einem Vektor, der eine induzierbare Expression einer shRNA gegen die mRNA von PTPA kodiert, zeigten eine effiziente Reduktion des Proteins auf 15% der normalen Menge. Zusätzlich wurden siRNAs (short interfering RNAs) angewandt und erzielten einen PTPA Knock-down auf 1/4 der normalen Menge. Schließlich wurden beide Methoden kombiniert, konnten aber keine weitere Reduzierung der Proteinmenge von PTPA erreichen. Trotz geringer Mengen von PTPA, konnte keine signifikante Veränderung des Phänotyps beo-bachtet werden.

Darüber hinaus wollten wir mithilfe der Anwendung verschiedener PTPA spezifischer Antikör-per, in Experimenten der subzellulären Fraktionierung und Immunfluoreszenz, die subzelluläre Lokalisierung des Proteins aufdecken. Western-Blot-Analysen konnten in Hela-Zellen, welche in Kern- und Zytoplasmafraktionen unterteilt wurden, ein hauptsächliches Vorkommen von PTPA im Zytoplasma bestätigen. Im Gegensatz dazu trat PTPA in Analysen von Immunfluoreszenzen vorrangig im Kernkompartiment auf.

Index

1. Introduction

Protein phosphorylation and dephosphorylation represent hallmarks of intracellular signalling cascades. Many human proteins experience a regulation of their biological function via the mechanism of protein phosphorylation, carried out by a dynamic and highly regulated class of enzymes [Honkanen and Golden, 2002]. As a consequence of their importance, these enzymes have been intensively studied over the last years.

Phosphorylation regulates a large variety of cellular processes, like signal transduction, cell cycle regulation or apoptosis. It represents a fast and reversible mechanism to activate enzymes, label proteins for degradation, facilitate protein-protein interactions or determine the subcellular localization of proteins. Phosphorylation occurs primarily on three amino acids: Serine, threonine and tyrosine, with serine as the most frequently phosphorylated (~98%) amino acid. Furthermore, kinases catalyse phosphorylation and phosphatases operate as antagonists.

Until recently, 518 putative protein kinases have been identified [Johnson and Hunter, 2005], which can be divided into 90 tyrosine and 428 serine/threonine kinases. Surprisingly, 107 protein tyrosine phosphatases and [Alonso et al., 2004] but only 30 serine/threonine phosphatases accomplish the function of dephosphorylation. The phosphatases can be subdivided based on their substrate specificity into: serine/threonine specific (PSTPs), tyrosine specific (PTPs) and dual specificity phosphatases (DSPs). PSTPs possess a catalytic core structure distinct to the core of PTPs and DSPs and hence use distinct catalytic mechanisms for the hydrolysis of the phosphoester bond [Fellner et al., 2003]. PSPs are different from PTPs/DSPs, which are more similar to each other regarding the catalytic mechanism. PSPs comprise three major families: PPMs, metal-dependent protein phosphatases, FCP/SCPs, aspartate-based phosphatases and PPPs, phosphoprotein phosphatases, [Yigong Shi, 2009]. Whereas PPM and PPPs both need metal ions for their catalytic activity, FCP/SCP use an aspartate-based mechanism. In contrast to the PPM family, which contains additional domains to determine substrate specificity, PPPs do have a multisubunit architecture with catalytic and regulatory subunits. Moreover, the PPP and PPM family differ in their sensitivity for inhibitors, which was important for the discrimination between type 1 versus type 2 phosphatases [Ingebritsen and Cohen, 1983]. The PPP family includes PP1, PP2A, PP2B, PP4, PP5, PP6 and PP7.

This study focuses on protein phosphatase 2A, PP2A, a member of the PPP family, and its activator protein, phosphatase 2A phosphatase activator, PTPA.

PP2A fulfills various roles in cell cycle regulation, programmed cell death and signal transduction pathways, as for instance in the MAP-Kinase and the TOR pathway, respectively [Di Como et al., 1996, Jiang et al., 1999, Sontag et al., 1993].

As a consequence of its multisubunit architecture, embodied in three core subunits, PP2A is able to cope with a variety of substrates in different cellular localizations.

1.1. Structure and subunits of protein phosphatase 2A (PP2A)

PP2A is a serine/threonine phosphatase, which is highly conserved between yeast and human and represents one of the most abundant cellular proteins in some tissues. It exhibits a multisubunit architecture with three major subunits, determining its specificity. The heterodimeric core enzyme is characterized through a 65 kDa structural A subunit and a 37 kDa catalytic C subunit. Together with one of many different regulatory B subunits, more than 72 different heterotrimeric holoenzymes can be formed. Via this mechanism substrate specificity as well as cellular localization can be determined.
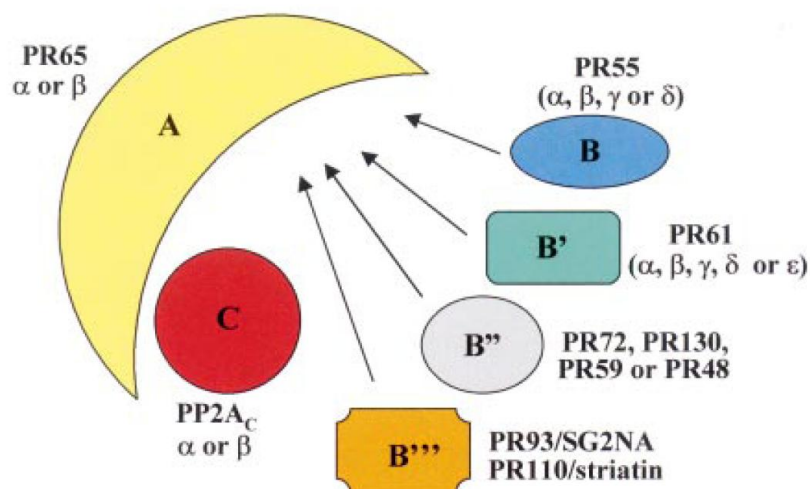
Figure 1: Structure of PP2A; adapted from "Protein phosphatase 2A, a highly regulated familiy of serine/threonine phosphatases implicated in cell growth and signaling"; Veerle Janssens and Jozef Goris (2001) Biochem J **353**(Pt 3): 417-39.

Figure 1 displays an illustration of the A subunit, which forms the core enzyme together with the C subunit [Goris et al., 2001]. Together with the B subunit, which originates from one of the four identified families, B (B55R55), B´ (B56/PR61), B´´ (PR48, PR59, PR72/130) and B´´´(PR93/PR110/striatin/SG2NA), the substrate specific holoenzyme is formed.

1.1.1. The structural subunit

Two constitutively expressed isoforms, α and β, exist, sharing 86% sequence identity [Hemmings et al., 1990]. The structure of the A subunit consists of 15 HEAT (huntingtin-elongation-A subunit TOR) repeats with each HEAT repeat defined by two antiparallel α-helices connected by an intra-repeat loop and adjacent repeats connected by inter-repeat loops. The conformation of the A subunit resembles a hook shaped structure before binding to the C subunit. When building a heterodimeric complex, the structural subunit changes to a more closed structure, upon interaction between HEAT repeats 11 and 15 with the C subunit [Cho et al., 2007].

Interestingly, Aβ isoform was identified as a putative tumor suppressor. Somatic alterations of the β isoform were found in certain cancers [Wang et al., 1998, Ruediger et al., 2001] and the loss of functional Aβ was contributed to transformation [Sablina et al., 2007].

1.1.2. The catalytic subunit

Within its catalytic domain, the C subunit reveals sequence homology to other Serine/Threonine phosphatases, like PP1, PP2B, PP4 and PP6. Similar to the structural subunit, the catalytic subunit exhibits 97% of sequence identity between the two isoforms, α and β, which are both constitutively expressed in brain and heart [Stone et al., 1988, Arino et al., 1988, Green et al., 1987]. However, the α-isoform is up to 10 fold more abundant than the β-isoform [Khew-Goodall and Hemmings, 1988]. A deletion of the α-isoform in mice was found to be embryonically lethal without the β-isoform being able to compensate the loss [Götz et al., 1998]. The heterodimeric core enzyme is assembled via A and C subunit interactions which are mediated through intra-repeat loops and inner helices of A subunit HEAT repeats 11-15. The importance of this interaction for a functional holozyme is underlined by the fact that some missense mutations inhibiting this AC core dimer interaction are cancer-associated [Cho et al., 2007]. Furthermore, PP2A-specific inhibitors like okadaic acid and microcystin can bind to the catalytic subunit and interact with amino acids surrounding the active site [Xing et al., 2006].

Finally, the C subunit contains a highly conserved C-terminal domain, featuring a critical role in the regulation of PP2A, as it recruits the B subunit to the core enzyme possibly through a neutralization of the charge-charge repulsion and subsequent binding of the B56 subunit to the C terminal tail [Cho et al., 2007]. Furthermore, methylation of the highly conserved C-terminal domain was suggested to enhance the affinity of the PP2A core enzyme for some regulatory

subunits and therefore influence the formation of a PP2A holoenzyme [Ikehara et al., 2007, Xing et al., 2006].

1.1.3. The regulatory subunits

As mentioned before, the regulatory subunits determine specificity and localization of the PP2A holoenzyme. The B subunit comprises four families, with each of them containing two to five isoforms and multiple splice variants: B (PR55), B´(PR61), B´´(PR48/PR72/PR130) and B´´´(PR93/PR110). Examples for the diverse functions of PP2A holoenzymes, containing distinct regulatory subunits, are the dephosphorylation of microtubule-binding protein tau, mediated by a PP2A holoenzyme with the B subunit (PR55) [Drewes et al., 1993, Gong et al., 1994, Xu et al., 2008], and the suggested interaction of B´subunit (PR61) with shugoshin [Kitajima et al., 2006, Riedel et al., 2006, Tang et al., 2006].

A PP2A holoenzyme containing regulatory B´ subunit was found to make interactions with A and C subunits to a greater extend than a PP2A holoenzyme containing B subunit. A shared feature of PP2A holoenzymes containing B or B´ regulatory subunits is that their potential substrate-binding site is on the top face and in close vicinity to the active site of the catalytic subunit [Yigong Shi, 2009]. All regulatory subunits, except the last family, interact directly with the PP2A core enzyme and do not share sequence similarity. The B´´´family shares a conserved epitope with the B´subunit and contains WD40-repeats for the interaction with the PP2A core enzyme [Janssens and Goris, 2001]. Finally, their expression patterns vary greatly in different tissues as well as interaction with substrates [Yigong Shi, 2009].

1.2. Protein phosphatase 2A in yeast

The serine/threonine phosphatase PP2A is widely distributed in eukaryotes and highly conserved from yeast to human. Therefore, PP2A was studied extensively using deletion mutant analysis in Saccharomyces cerevisiae. The catalytic subunit is composed of two isoforms, PPH21 and PPH22, exhibiting 74% amino acid sequence identity to the mammalian C subunit [Sneddon et al., 1990]. A double disruption of both isoforms leads to severe growth defects and to lethality, if *PPH3*, a related Ppase gene, is not present. Furthermore, *pph21/pph22* mutants led to an abnormal morphology of cells and smaller buds [Ronne et al., 1991]. The A subunit is

represented by TPD3, which is in yeast also required for the production of tRNA. S.cerevisiae lacking TPD3 exhibits multi-budded and multinucleated cells [van Zyl et al., 1989]. Finally, the mammalian regulatory subunits B (PR55) and B´(PR61), are in yeast represented by CDC55 and RTS1. A heterotrimeric complex of PP2A with CDC55 has multiple roles in mitosis, with mutants lacking a functional kinetochore/spindle assembly checkpoint, while PP2A holoenzyme with RTS1 takes part in the cellular stress response [Chan et al., 2009, Queralt et al., 2008]. Additionally, knockout studies revealed that the two subunits are not interchangeable [Healy, Zolnierowicz et al., 1991, Shu, Yang et al., 1997, Zhao et al., 1997].

1.3. A potential model for PP2A biogenesis

PP2A can make up to 1% of all enzymes in some tissues, fulfills multiple functions in signalling pathways and is likely to act as a tumor suppressor [Mumby, 2007]. Therefore, its activity and inactivity need to be tightly regulated. This regulation takes place on different levels: First, the assembly of the PP2A holoenzyme is dependent on the availability of specific regulatory subunits as well as their expression patterns. Second, an autoregulatory mechanism, which acts on the translational level, was found to adjust a constant level of catalytic subunit [Schönthal et al., 1998]. Furthermore, a regulatory circuit could result in activation and inactivation of PP2A, through the removal and loading of metal ions [Fellner et al., 2003].

And in addition to these mechanisms, posttranslational mechanisms, as phosphorylation and methylation, take their part in the formation of an active and specific PP2A holoenzyme.

First, phosphorylation is an important mechanism initiated through various stimuli and leading to diverse effects. The C-terminal part of the catalytic subunit of PP2A was shown to be phosphorylated *in vitro* by the pp60[v-src] and pp56[lck] kinases, leading to inactivation of the enzyme [Chen et al., 1992]. *In vivo*, phosphorylation of Tyrosine[307] in the C-terminal has been detected in T-cells and fibroblasts. Further, phosphorylation occurs due to stimuli of the epidermal growth factor, serum and in response to IL-1, TNFα or insulin [Chen et al., 1994, Guy et al., 1995, Srinivasan and Begum, 1994, Begum and Ragolia, 1996 and 1999]. Additionally, phosphorylation of the regulatory subunits, especially the B´family, resulted in altered substrate specificity (PR61δ) and increased activation (PR61α) of them [Xu et al., 2000, Usui et al., 1998].

Second, methylation was shown to play an essential role in holoenzyme assembly. Demethylation performs an opposing effect and changes in methylation control the binding of B subunits to the core dimer [Tolstykh et al, 2000]. Furthermore, the PP2A holoenzyme was found destabilized in strains lacking methyltransferase [Wu et al, 2000]. The methylation of the C-terminus of the C subunit can have different consequences.

Reversible methylation of the C-terminal Leucine309 in the conserved TPDYFL309 motif of the catalytic subunit controls the recruitment of some regulatory subunits to the PP2A core enzyme [Ikehara et al., 2007, Xing et al., 2006]. Mutational analyses of the carboxy terminus of the C subunit revealed its importance for the binding of B subunit [Ogris et al, 1997]. Furthermore, the methylated core enzyme could exhibit a higher binding affinity for the regulatory subunit, methylation could serve as an assembly signal for the PP2A holoenzyme or it could recruit other proteins facilitating the holoenzyme assembly [Yigong Shi, 2009].

Two conserved enzymes are counteractive for the methylation of PP2A: LCMT1, a leucine carboxyl methyltransferase, catalyses methylation of PP2A C subunit, and PME-1, PP2A methylesterase, catalyses the removal of the methyl group [Ogris et al, 1997, De Baere et al., 1999, Lee et al., 1996 and 1993]. Furthermore, evidence was gathered that PME-1 associates with two inactive mutants of PP2A [Ogris et al., 1999]. While PP2A was inactive through stable binding of PME-1, it could be reactivated by PTPA, the phosphatase two A phosphatase activator [Longin et al., 2004]. So, LCMT1, which fulfills methylation, and PTPA, reactivating inactive PP2A, oppose the function of PME-1.

1.4. Phosphatase 2A phosphatase activator, PTPA

In this study, PTPA, the phosphatase two A phosphatase activator, and its functional role in mammalian cell cycle is the subject of interest. PTPA is ubiquitously expressed and highly conserved in a variety of species, emphasized through the fact that the PTPA primary structures of rabbits and humans share more than 96% of sequence identity [Van Hoof et al., 1994 and 1998, Cayla et al., 1994]. Originally, PTPA was characterized to stimulate the phosphotyrosyl activity of PP2A [Cayla et al., 1990, Van Hoof et al., 1994]. Later on, RRD proteins, the PTPA homologues in yeast, were shown to be required for an active and P-Ser/P-Thr specific C subunit of PP2A in vivo [Fellner et al., 2003]. However, after revealing the potential of PTPA to reactivate the serine/threonine phosphatase activity of an inactive form of PP2A, which was in a complex

with the methylesterase PME-1 [Longin et al., 2004, Van Hoof et al., 2005], it was renamed the phosphatase two A phosphatase activator.

1.4.1. Structure of PTPA

Human PTPA is encoded by a single gene mapped on chromosome 9q34 and is organized into 10 exons and 9 introns [Van Hoof et al., 1995, Janssens et al., 2000]. Seven transcripts are possible due to alternative splicing, with all of them including exons 5-10 (Figure 2). All transcripts are expressed from the same TATA-less promoter, regulated by the yin yang 1 (YY1) transcription factor, which binds to two sides within the minimal promoter [Janssens et al., 2000]. All isoforms contain exon 1 and thus could be generated from a single pre-RNA by alternative splicing, which is suggested to represent a potential target for the regulation of PTPA. However, not all of the isoforms lead to a functional product. PTPAα, with a molecular weight of ~37kDa, is the most abundant isoform expressed, followed by PTPAβ and PTPAδ [Janssens et al., 2000, Magnusdottir et al., 2006].

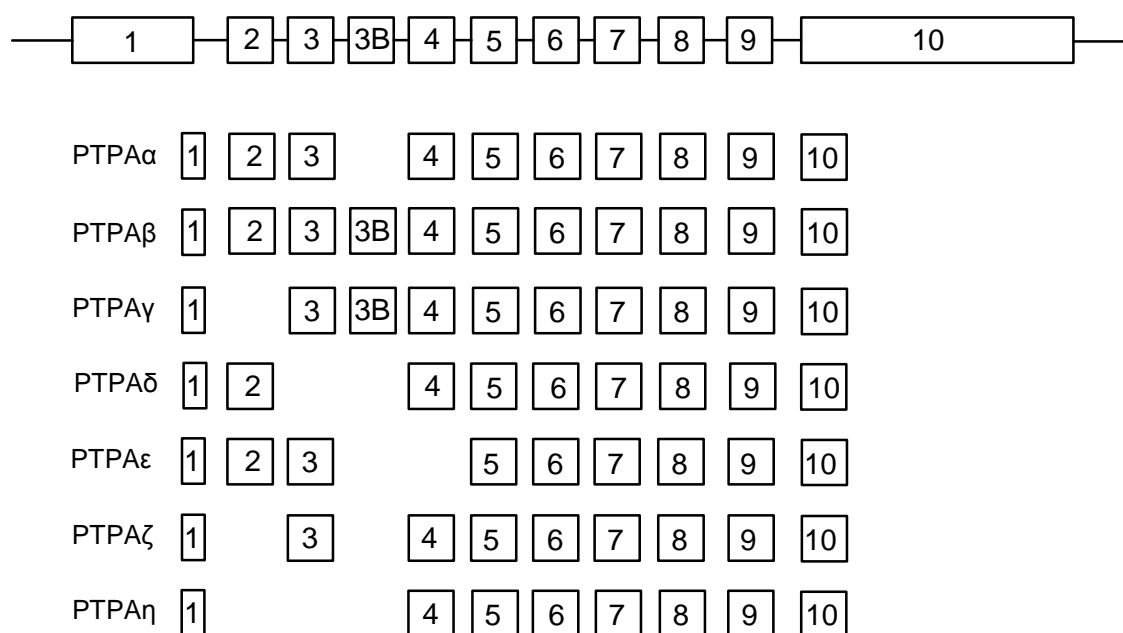**Figure 2: PTPA splice variants:** PTPA gene is represented by the top line with the 5´UTR and 3´UTR on the left and right side, respectively (3´UTR is not drawn to scale). Small boxes repesent exons. The isoform structure of PTPA results from RT-PCR reactions of total RNA from human HepG2 and Saos-2 cells and subsequent sequencing. Adapted from Janssens et al., 2000, Eur J Biochem. **267**(14):4406-4413.

The full length human PTPA contains 323 amino acids and exhibits a crystal structure at 1.9 A. The mostly α-helical compact structure, including 17 α helices and four short β-sheets, was divided into three subdomains: core, lid and linker. A highly conserved surface patch or cleft, surrounding the border between lid and linker domain was found to be a potential region for the interaction of peptide segments [Magnusdottir et al., 2006] or responsible for interacting with PP2A [Chao et al.. 2006]. If ATP binding is possible in the deep pocket and moreover, might enhance the interaction between PTPA and PP2A [Chao et al., 2006], or if ATP is unlikely to be a cofactor/substrate for PTPA [Magnusdottir et al., 2006, Leulliot et al., 2006] remains unsolved. Furthermore, *in vivo* PTPA activity and *in vitro* activation of PP2A was shown to be influenced by mutations on the surface of the peptide binding pocket, emphasising the importance of the conserved region [Leulliot et al., 2006].

1.4.2. Functions of PTPA in yeast

Originally, PTPA was identified as an activator of the *in vitro* phosphotyrosyl phosphatase activity of PP2A in an ATP/Mg^{2+} dependent reaction [Cayla et al., 1990]. Later, it was found to be required for active and specific PP2A [Fellner et al., 2003]. Recently, it was renamed, due to its potential to reactivate inactive PP2A, bound to PME-1 (for references, see above). PTPA is highly conserved from yeast to human.

In yeast, PTPA is encoded by two genes, termed *RRD1* and *RRD2* (rapamycine resistance deletion), since the phenotype of their deletion causes rapamycin resistance [Rempola et al., 2000]. Double deletion of RRD genes leads to synthetic lethality, while single deletion yeast strains exhibit an altered proliferation rate, aberrant bud morphology and a defective spindle checkpoint [Rempola et al., 2000, Van Hoof et al., 2001]. Furthermore, evidence was found that deletion of *RRD1* and *RRD2* generated a catalytic subunit of PP2A, differing from the wild-type enzyme in terms of substrate specificity, protein stability and metal dependance. As the catalytic subunit of PP2A, despite the RRD deletions, still assembles with A and B subunits, RRD functions are not required for holoenzyme assembly, but for the formation of an active PP2A enzyme with correct substrate specificity for phospho-serine/threonine over phospho-tyrosine [Fellner et al., 2003]. Interestingly, RRD functions are not completely redundant, as a deletion of *RRD1* results in a more severe phenotype compared to *RRD2* deletion, including aberrant bud morphology, abnormal actin distribution and growth defects [Jordens et al., 2006]. An additional study implied, that *RRD1* mutants display hypersensitivity to oxidative DNA damage [Ramotar et al., 1998].

Furthermore, *RRD1* was indicated to serve as an activator/regulator of SIT4 catalytic activity, probably responsible for the more severe phenotype of a *RRD*1 deletion strain, due to less activity of SIT4 [Fellner et al., 2003]. Moreover, *RRD2* is suggested to interact with PPH21/PPH22 and human PP2A C subunit expressed in yeast *in vivo*, as its deletion caused a larger decrease in catalytic activity than in a *RRD1* deletion strain. Additionally, recombinant expression of *RRD2* in a RRD deletion strain regenerated PP2A activity more efficiently than *RRD1* [Fellber et al., 2003]. Once more, this partial redundancy might be due to a high degree of conservation of PP2A and RRD/PTPA [Fellner et al., 2003]. Due to the fact, that PTPA is represented by one protein in mammals, whereas two proteins are necessary in yeast, an evolutionary shift regarding the function of PTPA has been proposed.

Recently, PTPA was reported to be a novel peptidyl-prolyl *cis/trans*-isomerase (PPIase), targeting *Pro190* in the catalytic subunit of PP2A. ATP hydrolysis and a conformational change in the C subunit should regulate the activity of PP2A [Jordens et al., 2006]. Interestingly, the PPIase activity was not exclusively due to the presence of ATP/Mg^{2+}, as the proline isomerase activity was measurable as well without ATP/Mg^{2+}.

These findings can be summarized in models for PTPA/RRD mode of action (see figure 3A and B). PTPA/RRD induces a conformational change in the catalytic site of the C subunit of PP2A, narrowing the possibility of entry for bulky P-Tyr substrates (indicated by pNPP in Figure 3A). P-Ser/Thr substrates enter and produce a PP2A catalytic core with a high affinity for metal ions (figure 3A). Hombauer and coworkers proposed a potential model for PP2A biogenesis, dependent on the function of RRD/PTPA (see figure 3B). RRD2 and TPD3 interact with an inactive demethylated form of the C subunit. Subsequently, PPM1 can methylate the catalytic subunit and the regulatory subunit binds to the complex, forming an active heterotrimeric PP2A. PPE1 could carry out a surveillance function of the TPD3/RRD2-dependent C subunit maturation, as it could prevent the premature generation of active C subunit and holoenzyme assembly.

Moreover, Chao and coworkers proposed a different model with PTPA acting as an ATPase, responsible for the pNPPase activity of PP2A and thus, the change of substrate specificity to P-Tyr substrates [Chao et al., 2006]. This is controversial, as ATP and Mg^{2+} were shown to activate the phosphotyrosyl phosphatase activity of PP2A on their own [Fellner et al., 2003].
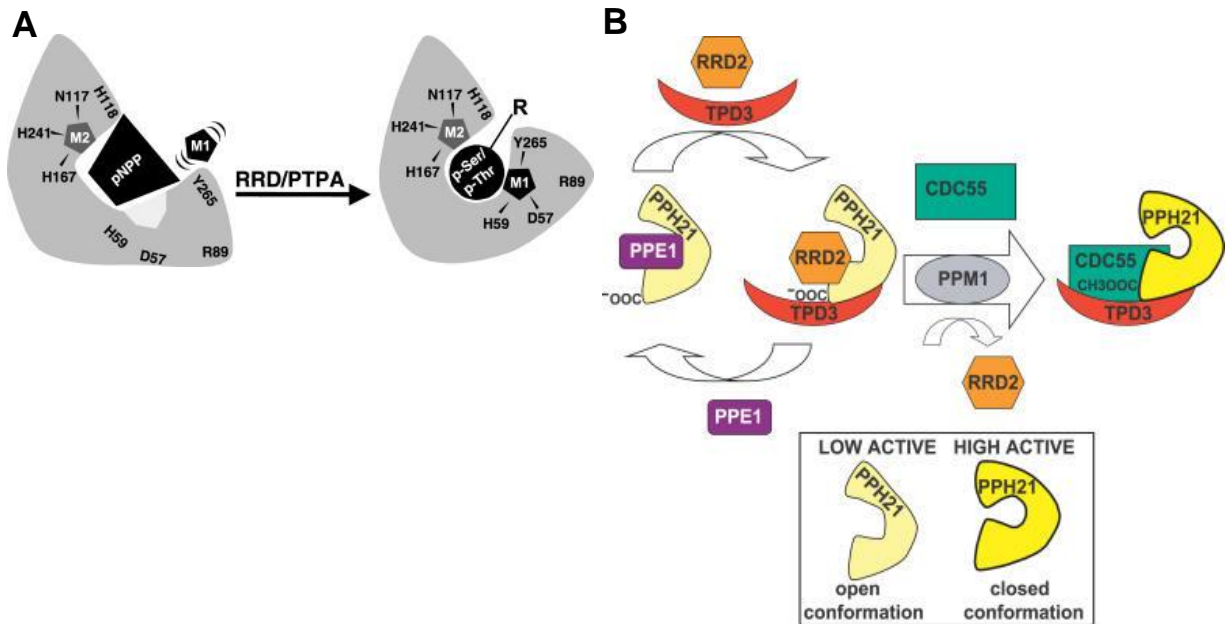
Figure 3: Models of RRD/PTPA function. A) PTPA/RRD induces a conformational change in PP2Ac. Para-nitrophenyl phosphate (pNPP) represents a bulky P-Tyr-like substrate. (P-Ser-R) phospho-serine substrate; (P-Thr-R) phospho-threonine substrate. M1 and M2 indicate metal ion 1 and metal ion 2, respectively, located in the catalytic core of the catalytic subunit of PP2A. The indicated amino acid residues represent amino acids of the PP2A catalytic subunit that are required for metal ion coordination and catalysis. (D) Asp; (H) His; (N) Asn; (R) Arg; (Y) Tyr. Adapted from Fellner et al. 2003; Genes Dev. **17**(17): 2138-50. **B) Potential model of PP2A biogenesis.** RRD2/TPD3 (TPD3 = A subunit in yeast) interacts preferentially with the demethylated and inactive form of the C subunit by targeting the PPH21:PPE1 complex. With the help of PPE1, premature generation of active C subunit and holoenzyme assembly is prevented. A heterotrimeric fully active and specific holoenzyme is built after dissociation of RRD2 and association of the regulatory subunit. Hombauer et al. (2007) PLoS Biol. **5**(6):e155.

1.4.3. Functions of PTPA in mammals

Interestingly, mammalian PTPA was shown to complement the proliferation phenotype in a *rrd1∆/rrd2∆* yeast strain, indicating a conservation of functions [Fellner et al., 2003]. But still, little is known about the mechanism by which PTPA activates or interacts with PP2A. Two studies provided evidence for an important function of PTPA. First, Fellner *et al.* determined the effects of downregulated PTPA on cell survival in Hela cells. Hela cells were transiently transfected with either a targeting vector, PTPA-RNAi, expressing a short interfering RNA against the coding sequence of PTPA, an empty pSUPER vector or a vector expressing a nonsense oligonucleotide, NS-RNAi. 48 hours after transfection, Hela cells containing the PTPA-RNAi con-

struct undergo apoptotic cell death, as demonstrated by nuclear fragmentation and caspase-3 staining, a marker for apoptotic conditions. In comparison, cells transfected with NS-RNAi or the pSUPER vector did not reveal signs of apoptotic conditions.

In a different study by Azam and co-workers [Azam et al., 2007], ectopic overexpression of PTPA-GFP induced cell death as indicated by morphological changes, activation of caspase-3 and detection of annexin V staining, without involving p53 or MAP kinases in the apoptotic pathway. Further, upon overexpression of a PTPA-GFP fusion protein in HCT116 cells, the localization of PTPA was determined to occur mainly in the nucleus (figure 4B, arrows indicating nucleus). The observed cytoplasmic staining was attributed to the overexpression of PTPA-GFP. To summarize, a correct balance of PTPA seems to be necessary for the homeostasis of the cell, as both studies detected apoptotic behaviour due to a shift in the cellular level of PTPA.
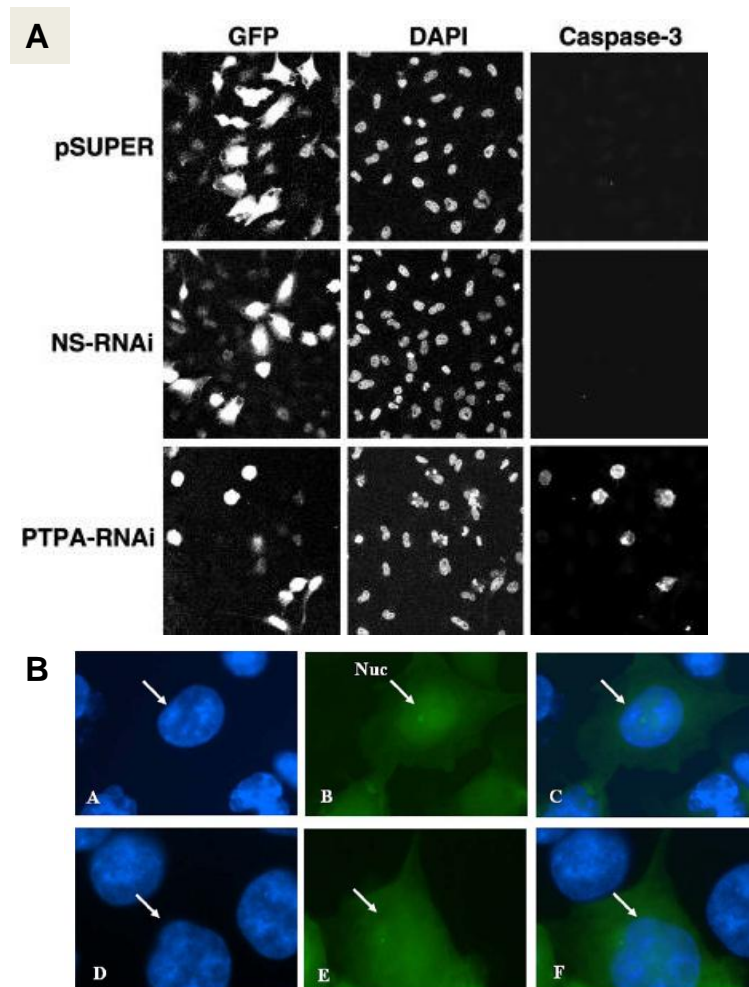

Figure 4: Suppression of PTPA expression by RNAi triggers apoptotic cell death in mammalian cells. A) HeLa cells were cotransfected with a vector containing a puromycin resistance marker and the green fluorescence protein (GFP) and either an empty vector as negative control (pSUPER), pSUPER-

NS-PTPA containing a "nonsense"-targeting sequence (NS-RNAi) , or pSUPER-PTPA containing a tar-geting sequence against PTPA. (PTPA-RNAi). 48 h after transfection, cells were stained with an antibody specific for active caspase-3 and counterstained with DAPI. Co-transfected cells are indicated by GFP-staining. Adapted from Fellner et al. 2003; Genes Dev. **17**(17): 2138-50. **B) Localization of PTPA.** Cells were transiently transfected for 24 hours in HCT116 cells with either pPTPA-GFP (panels A-C) or the empty pEYFP vector (panels D-F). Cells were counterstained with DAPI (A and D); localization of pPTPA-GFP and GFP is shown in B and E, respectively, and merged picture in C and F. Arrows point to the nucleus (Nuc). Adapted from Azam et al. (2007) Apoptosis. **12**(7):1243-55.

1.5. Aim of this study

1.5.1. Knockdown of mammalian PTPA

Primarily, the project aimed to investigate the potential involvement of PTPA in the manifesta-tion of Alzheimer´s disease. A dominant feature of this neurodegenerative disease is hyperphos-phorylation of the microtubule-associated protein tau, which results in neurofibrillar tangles that trigger neuronal death [Virshup and Shenolikar, 2009]. PP2A is a main regulator of the dephos-phorylation of tau and as such, is responsible for a pathological hyperphosphorylation when inhibited in cultured cells or in mice expressing a mutant form of the catalytic subunit Cα of PP2A [Kins et al., 2001, Sontag et al., 1996, Iqbal et al., 2005]. Furthermore, Sontag and co-workers could link defective Bα subunit expression with the phospho-tau pathology together with a reduced PP2A catalytic activity in affected brain regions [Sontag et al., 1999 and 2004]. Because our data in yeast showed, that RRD/PTPA is essential for the biogenesis of active PP2A holoenzyme, including the yeast homologue of B/PR55 subunit, we hypothesized, that the decreased loss of PTPA would reduce PP2A activity and further enhance the hyperphosphoryla-tion of tau. As the reason for the dysfunction of PP2A holoenzyme remained unclear, the effect of PTPA on the biogenesis of PP2A and further the effect of its downregulation on the phos-phorylation of tau was still a matter of debate.

Recently, apoptotic cell death was demonstrated to occur after suppression of human PTPA in Hela cells due to transient transfections with a constitutive pSUPER vector system expressing RNAi against the coding sequence of PTPA [Fellner et al., 2003].

Based on this result, an essential role for PTPA in mammalian cell survival was proposed. How-ever, the reason for the apoptotic cell death remained unclear. As biochemical analyses were

missing, we wanted to investigate the role of PTPA in the biogenesis of PP2A and confirm or abandon the hypothesis of a potential involvement of PTPA in the manifestation of the Alzheimer disease. Thus, further studies using Neuronal cells were performed (see thesis of Martina Mitterhuber). As the constitutive expression of RNAi causes apoptosis, an inducible vector system allowing the production of RNAi under control of an inducible promoter, was preferred. Due to time-dependent induction, different levels of protein are achievable and possible phenotypic effects can be monitored in inducible vector systems. A schematic representation of the Tet Repressor system, used in this study, is shown in figure 5.
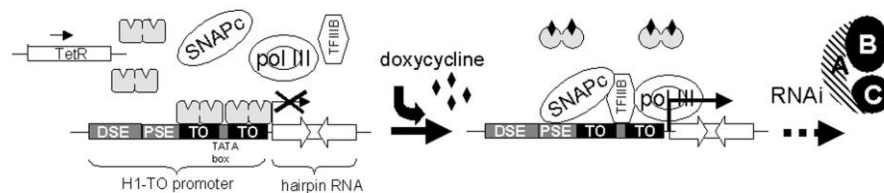
Figure 5: pNTO vector containing the Tet Repressor system. The pNTOneo vector with TO (Tetracycline Operator) and H1 promotor. After addition of doxycycline, the Tet Repressor dissociates from the promoter and transcription of shRNA can start. Adapted from Stefan Strack et al. (2004) J Biol Chem. **279**(46):47732-9.

In the absence of doxycycline, a tetracycline analogue, repressor proteins bind to the Tet operator and block transcription. Following the addition of doxycycline, which binds to the repressor proteins, the repressor proteins dissociate and shRNA gets transcribed under control of the RNA Pol III dependent H1 promoter. After synthesis of the shRNA in the nucleus, the transcript is processed by two enzymes, namely Drosha and DGCR8, producing 2nt 3´overhangs. After transport into the cytoplasm, the pre-shRNA is loaded into the Dicer complex, which leads to a product of 21-23 bp double-stranded siRNA. Subsequently, the siRNA targets the complementary mRNA by an unknown process and gets incorporated into the RNA-induced silencing complex (RISC). Finally, the mRNA is degraded and siRNA can be released for additional rounds of gene silencing [Rao et al., 2009, Lee et al., 2003, Zhang et al., 2002]. The pNTO vector (kindly provided by Stefan Strack, Strack et al., 2004) contains a neomycin resistance for selection of transfected cells and requires the native TetR for its function. Thus, stably expressing TetR cell lines have to be used.

Martina Mitterhuber generated stably transfected N2ATRex cell line with the pNTOneo vector. The vector contains a shRNA sequence, targeting the C-terminal part of the mRNA of PTPA, which is under the control of a doxycycline inducible promoter. Neither cell proliferation nor PP2A activity were altered after knockdown of PTPA to 50% of its wild type level. High leaky expression and low inducibility accompanied these experiments with N2ATRex cells [see diploma thesis of Martina Mitterhuber], and therefore, HEKTRex cells stable transfected with the same vector system were further analysed by Michaela Kugler. HEKTRex cells, an immortalized embryonic kidney cell line, express RNAi targeting the ORF I position 903-921 of human PTPA upon induction with doxycycline. In addition, cells transfected with the pNTOneo vector, expressing a missense PTPA RNAi, were used as control cells. The missense PTPA sequence contains three mismatches at positions 4, 10 and 16 of the PTPA targeting sequence, and is therefore unable to bind the PTPA mRNA. HEKTRex cells exhibited a knockdown of PTPA to approximately one fourth. However, the downregulation of PTPA did not seem to have an effect on PP2A complex assembly. Additional, HEKTRex cells with a low amount of PTPA did not even exhibit an effect on proliferation after 10 days of RNAi expression.

Because of the result of transient PTPA knockdown in Hela cells (see above), a HelaTRex cell line was (performed by Michaela Kugler) stably transfected with the pNTOneo vector, expressing either a missense PTPA RNAi or the PTPA targeting sequence. The same vectors as utilised in previous experiments were used. The knockdown of PTPA in HelaTrex cells was checked during my Wahlbeispiel and in this study. Since the previous studies (see above) did not result in unambiguous results we wanted to unravel the phenotype of downregulated PTPA in mammalian cells.

We hypothesized, that proliferation in PTPA knockdown cells would change and thus, a 6 days proliferation test was performed. Furthermore, flow cytometric analyses of PTPA knockdown cells were made after treatment with Nocodazole. We speculated, that cells with a low amount of PTPA and arrested in M phase due to treatment with Nocodazole could overcome the spindle assembly checkpoint.

Besides inducible cell lines expressing a shRNA, short interfering RNAs (siRNA) targeting the conserved C terminal part of PTPA were used for knockdown analysis in Hela and HEKTRex cells. The efficiency of PTPA downregulation by these methods was quantified via the LI-COR Odyssey system on protein level and via quantitative reverse transcription PCR on mRNA level. Moreover, a combination of shRNA and siRNA was used to knockdown PTPA below a critical

level. Due to fact, that apoptotic behaviour was shown to occur in some but not all cell lines (see diploma thesis of Michaela Kugler), we wanted to find an explanation why the knockdown of PTPA seemed to differ. Finally, the construction of a conditional knock-out vector was started, to make an inducible knock-out possible in further studies.

1.5.2. Subcellular localization of mammalian PTPA

Previously, Azam *et al.* indicated a mainly nuclear localization of mammalian PTPA (see figure 4B for details) based on the overexpression of GFP tagged PTPA in HCT116 cells. These authors further concluded that the cytoplasmic staining results from the overexpression of the protein. However, up till now further evidence is missing and the subcellular localization of PTPA remains unclear. Moreover, our biogenesis model would rather indicate a role for PTPA as a chaperone at the ribosome. Due to the fact, that Azam and coworkers made their assumption based on microscope analysis solely, we aimed to analyse the localization of PTPA by subcellular fractionation. In addition, we wanted to identify the subcellular localization with a second method and identify the localization and quantity of the protein in knockdown cells. To achieve this aim, I started, in collaboration with with Stefan Schüchner and Marko Roblek, the production of a monoclonal antibody against PTPA, and used two different monoclonal antibodies for immunofluorescence analysis.

2. Materials and Methods

2.1 Tissue culture

2.1.1. Cell lines and stable transfected single clones:

2.1.1.1. Cell lines used in this study:

Cell line	description	DMEM + FCS	Selective antibiotics
Hela	Human cervical cancer cell line	DMEM + 10%FCS	
HelaTRex	Human cervical cancer cell line stably expressing the Tet Repressor (kindly provided by Michael Glotzer)	DMEM + 10%FCS Tetfree	5µg/ml Blasticidin
HelaTRex-pNTOneo-CT/Mis	Human cervical cancer cell line stably expressing the Tet Repressor and stably transfected with the pNTOneo-vector (generated by Michaela Kugler)	DMEM + 10%FCS Tetfree	5µg/ml Blasticidin + 800µg/µl Neomycin
HEKTRex	Human embryonic kidney cell line stably expressing the Tet Repressor (kindly provided by Stefan Strack)	DMEM + 10%FCS Tetfree	5µg/ml Blasticidin
HEKTRex-pNTOneo-CT/Mis	Human embryonic kidney cell line stably expressing the Tet Repressor and stably transfected with the pNTOneo-vector (generated by Martina Mitterhuber)	DMEM + 10%FCS Tetfree	5µg/ml Blasticidin + 300µg/µl Neomycin
NIH3T3	Mouse fibroblast cell line	DMEM + 10%FCS	
BOSC23	Human kidney cell line derived from 293T cells	DMEM + 10%FCS	
Hela pWZL	Human cervical cancer cell line stably transfected with the pWZL-vector (kindly provided by Patrick Piribauer)	DMEM + 10%FCS	
X63.Ag8.653	Mouse myeloma cell line	X63 medium	

2.1.1.2. shRNA sequences:

shPTPA-1 forward (PTPA-CtfwPetra#630)	5´-GATCCCC-GTTCCCTGTGATCCAGCAC-TTCAAGAGA-GTGCTGGATCACAGGGAAC-TTTTTGGAAA-3´
shPTPA-1 reverse (PTPA-CtrevPetra#631)	5´-AGCTTTTCCAAAAA-GTTCCCTGTGATCCAGCAC-TCTCTTGAA-GTGCTGGATCACAGGGAAC-GGG-3´
shControl-1 forward (PTPA-Ctmisfw#632)	5´-GATCCCC-GTT$\underline{T}$CCTGT$\underline{A}$ATCCA$\underline{A}$CAC-TTCAAGAGA-GTGTTGGATTACAGGAAAC-TTTTTGGAAA-3´
shControl-1 reverse (PTPA-Ctmisrev#633)	5´-AGCTTTTCCAAAAA-GTTTCCTGTAATCCAACAC-TCTCTTGAA-GTG$\underline{T}$TGGAT$\underline{T}$ACAGG$\underline{A}$AAC-GGG-3´

The shRNA sequences [Fellner et al., 2003] were cloned by Martina Mitterhuber (see diploma thesis). "shPTPA-1forward" refers to "CT" in the following, as it represents the targeting sequence against the C-terminal part of mouse and human PTPA. "shControl-1reverse" is termed "Mis" in further, as it stands for the targeting sequence including 3 mismatches. Thus, the Mis-sequence is used as a non-binding control. The "CT-sequence" is 100% homologous to the mouse and human PTPA.

2.1.2. Solutions and media:

10xPBS: Dissolve 80g NaCl, 2g KCl, 2g KH_2PO_4 and 14,4g Na_2HPO_4 in ddH_2O, adjust to a final volume of 1l, adjust to pH 7.4, autoclave and store at RT.

DMEM (Gibco #31660-083): Dissolve one package in 5l ddH_2O and stir for 30min until completely dissolved. Add 30g $NaHCO_3$, stir until completely dissolved and add ddH_2O up to 10l. Filter sterilize through a membrane filter (0,2µm) and make aliquots of 450ml. Store at 4°C. Add glutamine, if stored longer than 2 weeks.

Trypsin: Dissolve 250mg Trypsin in 25ml 10xPBS and add water to a total of 245ml. Stir for 2 hours. Add 5ml 1% Na-EDTA (pH 7.4), mix and filter sterilize through a membrane filter (0,2µm). Store aliquots of 10ml at −20°C.

Blasticidin (Invitrogen #R210-01): Dissolve 50mg in 20ml ddH_2O, filter sterilize through a membrane filter (0,2µm), aliquot and store at –20°C. Use to an end concentration of 5µg/ml.

Hygromycin B (Calbiochem #400049): Dissolve 50mg/ml in ddH_2O, filter sterilize through a membrane filter (0.2µm), use to an end concentration of 200µg/ml for HekTRex cells (Calbiochem #400049).

Puromycin (Sigma #P-7255): Dissolve 100mg Puromycin in 10ml ddH_2O, filter sterilize through a membrane filter (0,2µm), aliquot and store at –20°C. Use to an end concentration of 1µg/ml for Hela-pWZL cells and 5µg/ml for NIH3T3 cells.

Doxycycline (Sigma #D-9891): Dissolve 10mg in 10ml ddH_2O, filter sterilize through a membrane filter (0,2µm), aliquot and store at –20°C. Use to an end concentration of 1µg/ml.

Geneticin (Gibco #11811-098): Dissolve 1g in 100ml DMEM +P/S, filter sterilize through a membrane filter (0,2µm), aliquot and store at –20°C. Use to an end concentration of 600µg/ml.

AB: 0.6g Penicillin-G; 1g Streptomycin-sulfate; 10ml 10x PBS. Add H_2O to 100ml, filter sterilize through a membrane filter (0,2µm) and store 5ml aliquots at -20°C.

DMSO (Dimethylsulfoxide, Applichem #A3672.0250)

FCS (fetal calf serum, Gibco #4023696J): Store 50ml aliquots at -20°C.

Polybrene (Hexadimethrine bromide, Sigma #C-6628): Dissolve 40mg Polybrene in 10ml ddH_2O, filter sterilize through a membrane filter (0,2µm) and store 1ml aliquots at -20°C.

Propidium Iodide (Roche #11348639001): 0.5mg/ml

RNAse Type I-A: Dissolve 10mg/ml RNAse A (Sigma #R-5125) in 10mM sodium acetate pH 5.2. Heat to 100°C for 15min and allow to cool slowly to RT. Adjust the pH by adding 0.1 volumes of 1M Tris-Cl pH 7.4. Store 1ml aliquots at -20°C.

Chloroquine (1000x): Dissolve 0.129g Chloroquine (Sigma #C-6628) in 10ml ddH_2O, filter sterilize through a membrane filter (0,2µm) and store aliquots at -20°C.

2xHBS: 280mM NaCl; 50mM Hepes pH 7.12 (AppliChem #A1069); 1.5mM Na_2HPO_4; Add ddH_2O to 100ml, autoclave and store at 4°C.

Polybrene (1000x): Dissolve 40mg Polybrene (Hexadimethrine bromide, Sigma #52495) in 10ml ddH$_2$O, filter sterilize through a membrane filter (0,2µm) and store 1ml aliquots at -20°C.

2.5M CaCl$_2$: dissolve 36.8g CaCl$_2$.2H$_2$O in 100ml ddH$_2$O, autoclave and store at 4°C.

X63 Medium: 435ml DMEM (Gibco #31660-083); 50ml FCS; 5ml P/S; 5ml Glutamine (Sigma); 5ml Natrium-Pyruvate (Sigma).

2.1.3. Cultivation and propagation:

Petri-dishes with 60mm/100mm/150mm diameter were used and all cells were grown in DMEM+10% FCS+P/S at 37° with 7.5%CO$_2$ except hybridoma cells, which were propagated at 5%CO$_2$. In order to split the cells, either for induction with doxycycline or propagation, they were washed with ~5ml of 1xPBS, trypsinized and resuspended in medium.

2.1.4. Counting of cells:

To determine the cell number, 50µl of cell suspension were diluted in 5ml CASY®ton solution and cells were counted with a CASY® (Schärfe System) cell counter. For transfections, immunofluorescences and doxycycline inductions, 50µl of cells were counted with a Bürker 0.1mm counting chamber (Optik Labor).

2.1.5. Freezing and thawing:

Cells were washed with 5ml of 1xPBS. Subsequently ~500µl Trypsin/p100 was used to detach the cells from the petri-dish, and 10ml of adequate medium was used to collect the cells. After centrifugation at 1200g, the pellet was resuspended in 1ml 10%DMSO + 90%FCS (freezing mix), stored at -80° for two weeks and transferred onto liquid nitrogen afterwards. For thawing, freezing stocks were put shortly on 37°C, diluted in DMEM + 10%FCS and centrifuged at 1200g. The supernatant was soaked off and the pellet resuspended in 10ml of DMEM + 10%FCS, which was preincubated for 1 hour at 37°C and 7.5%CO$_2$.

2.1.6. Induction of doxycycline with HelaTRex cells:

To test the knockdown of PTPA in HelaTRex-pNTOneo, mixed and single clones after induction with doxycycline, $1x10^6$ cells were seeded on a 100mm petri dish. To induce the production of RNAi, which is under control of a doxycycline inducible H1 promotor, 10µl of doxycyclin (1µg/ml) per 100mm petri-dish were added to the medium once every day for 96hours. For the determination of knockdown efficieny whole protein lysates of induced and uninduced negative controls were made afterwards.

2.1.7. Proliferation test:

Number of cells seeded
$3x10^6$ lyse on day 1
$3x10^6$ lyse on day 2
$1x10^6$ lyse on day 3
$1x10^6$ lyse on day 4
$5x10^5$ lyse on day 5
$1x10^5$ lyse on day 6

To test the proliferation behaviour of HelaTRex-pNTOneo-CT/Mis single clones over a period of 6 days, different amounts of cells were seeded on 100mm petri dishes and induced with 1µg/ml of doxycycline every day. After four days, a media change was made with all petri dishes. Whole cell lysates were made starting from day 1 with induced and uninduced samples and loaded on 10% SDS PAGE to determine the knockdown of PTPA. The cells were counted before lysis to analyse the corresponding cell count.

2.1.8. Propidium Iodide labelling and flow cytometry analysis:

In order to identify apoptotic behaviour, the DNA of the cells was stained with propidium iodide, an intercalating agent used for flow cytometry to evaluate cell viability and DNA content. HelaTRex single clones were induced with 1µg/ml doxycycline every 24 hours for 4 days and uninduced samples were taken as negative controls. After 96 hours, cell proliferation was analysed via flow cytometry analysis. $0.5x10^6 - 1x10^6$ cells were used for labelling with propidium iodide. Cells were washed one time with 5ml of 1xPBS, trypsinized and resuspended with 10ml of DMEM containing 10%FCS. Cells were counted with counting chamber (see 2.1.4.) and an appropriate volume transferred to a Falcon tube. The cell suspension was centrifuged for 5 minutes at 1200 rpm, supernatant was removed and the pellet resuspended in 500µl 1xPBS. 500µl of cold 95% ethanol (stored beforehand at -20°C) was added drop-wise while vortexing in

order to prevent clumping. Incubation was done for a minimum of 20 minutes on ice. Fixed samples can be stored over months before analysis. To pellet cells again, centrifugation was done at 1000rpm for 7 minutes at 4°C, supernatant was removed and pellet was resuspended in 500µl PI-RNAse solution. Dye solution contains 50µg/ml PI and 100µg/ml RNAse Type I-A in 1xPBS. Samples were mixed well, transferred to FACS-tubes, incubated at room temperature in the dark for a minimum of 20 minutes and analysed by flow cytometry with a FACS Calibur™ (BD Biosiences).

2.1.9. Nocodazole assay:

Nocodazole is a drug, affecting the spindle assembly and stops all cells in M-phase. As some cancer cell lines do often have a defective spindle assembly checkpoint, flow cytometry analysis has been performed after treatment as described in section2.1.8 with the following modifications. $1x10^6$ cells of HelaTRex-pNTOneo single clones were seeded, induced for 96 hours with 1µg/ml doxycycline and the uninduced cells were used as negative control. After 96 hours of induction, 0.5µg/ml Nocodazole (0.15mM; stock = 2.5mg/ml) was added to the medium and the cells were cultivated o/n either for 20 hours or 30 hours with Nocodazole treatment. Medium was poured off including detached cells and remaining cells were carefully washed with 5ml of 1xPBS. 1xPBS was poured off and added to the medium containing detached cells. Cells were trypsinized and resuspended in medium containing detached cells. Cells were counted with counting chamber (see 2.1.4.) and centrifuged at 1200 rpm for 5 minutes. To be able to check the knockdown on a protein level, whole cell lysates were made additionally, as the drug treatment was done in duplicates.

2.1.10. Preparation of Retroviral Supernatant and infection of cells:

For infection of mammalian cells with retrovirus containing supernatant, three different vectors were used: pRetroSuper$_{Stuffer}$-CT, pRetroSuper$_{Stuffer}$-Mis and pRetroSuper$_{Stuffer}$. After infection with the retroviral supernatant, cells were selected with puromycin. The shRNA targeting PTPA should be expressed constitutively. All pipet tips, tubes, glass pipettes and tissue culture plates were soaked in hypochlorit after usage.

2.1.10.1. Production of retroviral supernatant:

The production of retroviral supernatant was achieved using BOSC23 cells, which are a derived from 293T cells. The BOSC23 cell line is permanently transfected with a helper virus, providing all necessary components for creating a competent virus and furthermore is easy to transfect transiently with a retroviral vector. $5x10^6$ cells were seeded on p60 tissue culture plates. Before starting to transfect the cells, pasteur pipettes were shortly treated with a flame. The medium was sucked off and replaced very carefully by 4ml DMEM including 10% FCS and 25μM chloroquine. Subsequently, the transfection mix was prepared in a certain order: 450μl of sterile H_2O, 10μg of vector-DNA (see 2.4.9.) and 50μl 2.5M $CaCl_2$. The solution was mixed thoroughly by pipetting up and down a few times and added dropwise to 500μl 2xHBS while bubbling with a pasteur-pipette and a pipette boy. The final mix was added immediately and dropwise to the cells and left on for at least 9 hours. A change of medium was done afterwards with 4ml of DMEM and 10% FCS and left on o/n. Another change of medium was done the next day with 3ml of DMEM and 10% FCS and left on o/n again. The first retroviral supernatant was harvested by transferring the supernatant to a new tube. Medium was replaced and 24 hours later, the second retroviral supernatant could be harvested. Part of the volume of the retroviral supernatant was stored at -80°C whereas the other part was used immediately.

2.1.10.2. Infection of cells:

Two different cell lines have been used for infection, NIH3T3 and Hela-pWZL cells. NIH3T3 is a mouse fibroblast cell line, while Hela-pWZL is a cell line stably transfected with a vector, expressing ectropic mouse retrovirus receptor (P.Piribauer and E.Ogris, unpublished data).

The day before infection, $5x10^5$ cells/p100 were seeded on three tissue culture plates for the infection with pRetroSuper$_{Stuffer}$-CT, pRetroSuper$_{Stuffer}$-Mis and pRetroSuper$_{Stuffer}$. The medium was sucked off before infection and replaced with 3ml retroviral supernatant and 4μg/ml polybrene. If less supernatant should be taken, the volume can be filled up with DMEM and 10% FCS. The infectious supernatant was left on for a minimum of 3 hours and a maximum of 5 hours. Afterwards, the medium was carefully sucked off and disposed in hypochlorite. Subsequently 10ml DMEM and 10% FCS were added on the tissue culture plate. The day after, the cells from a p100 were split on three plates, in order to make whole cell lysates consecutively three days in a row and analyse via 10% SDS-PAGE and western blotting. Additionally, in-

fected cells were selected with 5µg/ml puromycin for each tissue culture plate of NIH3T3 cells and 1µg/ml for each tissue culture plate of Hela-pWZL cells, as the pRetroSuperStuffer vector contains a puromycin selection marker.

2.2. Working with proteins

2.2.1. Solutions and media:

30% Acrylamide: 292g acrylamide; 8g bisacrylamide. Fill up to 1l with ddH$_2$O. Add mixed-bed, ion-exchange resin (BioRad AG 501-X6) to the final solution and store in dark at 4°C.

1M Tris pH 8.8: Dissolve 242.3g Tris in 1l of ddH$_2$O. Adjust pH to pH 8.8 and fill up to 2l with ddH$_2$O, autoclave and store at 4°C.

1M Tris pH 6.8: Dissolve 60.5g Tris in ddH$_2$O. Adjust pH to pH 6.8 and fill up to 500ml with H2O, autoclave and store at 4°C.

20% SDS: Dissolve 40g SDS (Amresco #0227) in 100ml of ddH$_2$O, stir and slightly heat, fill up to 200ml with H$_2$O and store at RT.

10% APS: Dissolve 1g ammoniumperoxodisulfate (Merck #1201) in 10ml ddH$_2$O and store at 4°C.

TEMED (N,N,N',N'-Tetramethylenediamine, Fluka #87689)

10xRunning buffer: Dissolve 250mM Tris, 2M Glycine and 35mM SDS in 5l H$_2$O and store at RT.

Transfer buffer with Methanol: 25mM Tris; 190mM Glycine; 20% (v/v) Methanol. Dissolve Tris and Glycine in 8l H$_2$O and add Methanol, store at 4°C.

Ponceau S stock solution (10x): 2g Ponceau S (Serva #33429); 30g Trichloroacetic acid (AppliChem #A1431); 30g Sulfosalicylic acid (Merck #1.00691). Dissolve and fill up to 100ml with ddH$_2$O and store at RT.

Ponceau S working solution: Dilute Ponceau S stock solution 1:10 with ddH$_2$O.

20% Sodium-azide (Merck #67188): Dissolve 2g sodium-azide in 10ml ddH$_2$O and store in the dark at 4°C.

GSD stock (3x): 335mM DTT (Gerbu #1008); 230mM SDS; 4.5M Glycerol (Merck #1.04092); 20ml ddH$_2$O. Add a bit bromphenolblue (Amresco #0312) and a few drops 1M Tris pH 6.8 until solution appears blue. Store 2ml aliquots at -20°C. To obtain 1x GSD, dilute the stock with ddH$_2$O.

1% Thimerosal (Sigma #T-5125): Dissolve 0.5g Thimerosal in 50ml ddH$_2$O. Store in the dark at 4°C.

Prestained Protein Molecular Weight Standards (Biorad #161-0373): Store at -20°C. Use 4µl or 8µl for one lane on a small or large SDS-polyacrylamide gel, respectively.

10xPBS: 1.37M NaCl; 27mM KCl; 43mM Na$_2$HPO$_4$; 14mM KH$_2$PO$_4$. Dissolve in ddH$_2$O, adjust to pH 7.4 and autoclave.

1xPBS (working solution): 137mM NaCl; 2.7mM KCl; 4.3mM Na$_2$HPO$_4$; 1.4mM KH$_2$PO$_4$.

3% milk (blocking solution): 15g Non fat dry milk (NFDM); 50µl 20% sodium azide. Add PBS and 0.05% Tween20 to 500ml and store at 4°C.

0.5% milk (for incubation): 2.5g Non fat dry milk (NFDM); 500µl 1% Thimerosal. Add PBS + 0.05% Tween 20 to 500ml and store at 4°C.

Ni-NTA beads (Qiagen #30410)

PMSF-stock (100x): Dissolve 0.697g PMSF (Roche #837091) in 20ml isopropanol and store aliquots of 1ml at room temperature, protected from light.

Aprotinin-stock (200x): Store aliquots of 1ml Aprotinin (Sigma #A-6012) at 4°C.

Complete (25x): Dissolve one Complete^{TM} Protease Inhibitor cocktail tablet (Boehringer Mannheim #1836145) in 2ml IP-Lyse buffer and store at 4°C for a maximum of 2 weeks.

RNAse A (Sigma #R-5125) Dissolve 10mg/ml RNAse A in 10mM sodium acetate pH 5.2. Heat to 100°C for 15min and cool down to RT. Adjust the pH by adding 0.1 volumes of 1M Tris-Cl pH 7.4. Store 1ml aliquots at -20°C. Use to an end concentration of 10µg/ml.

0.1M Glycine buffer: Dissolve 3.76g glycine in 400ml H_2O. Adjust to pH 3.0 and add ddH_2O to 500ml. Store at 4°C.

Wash buffer (for Ni-NTA beads): 50mM NaH_2PO_4; 300 mM NaCl; 20mM imidazole. Adjust pH to pH 8.0 and add ddH_2O to 500ml.

Elution buffer (for Ni-NTA beads): 50mM NaH_2PO_4; 300 mM NaCl; 250 mM imidazole. Adjust pH to pH 8.0 and add ddH_2O to 500ml.

Coomassie-stock: Dissolve 2.5g Coomassie (Serva #17524) in 500ml methanol, stir over night, add 500ml ddH_2O and store at room temperature.

Coomassie working solution: 30% Ethanol; 30% Coomassie-stock; 10% acetic acid; 30% ddH_2O.

Destaining solution: 30% Ethanol; 60% ddH_2O; 10% acetic acid

IP Wash: 10% glycerol; 20mM Tris pH 8.0; 135 mM NaCl. Filter sterilize through a membrane filter (0,2µm) and store at 4°C.

IP Lyse: 450ml IP Wash; 50ml 1% NP-40.

Buffer F1: 20mM Tris pH7.6; 50mM β-mercaptoethanol; 0.1mM EDTA, 2mM $MgCl_2$; add protease inhibitors (Aprotinin, PMSF, Complete) and fill up to 100ml with ddH_2O.

2.2.2. Purification of soluble His-tagged proteins via Ni-agarose beads:

Bacteria of the strain Rosetta (-), expressing pB´His NP *SpHI/NcOI* PTPA#2), were lysed in IP-Lyse and sonicated (see 2.3.5.). Furthermore, the bacterial lysate was centrifuged for 30 minutes at 5000rpm at 4°C. The supernatant was collected and 100µl of Ni-NTA beads, which was equilibrated in 25mM Tris pH 8.4, was added to the supernatant from 100ml of a bacterial culture with OD_{550}=1. The suspension was shaked at 4°C for either 1-2 hours or o/n. Subsequently, the beads were washed 4 times with 25mM Tris pH8.4 (containing Aprotinin and PMSF) and 5 times with washing buffer (containing Aprotinin and PMSF). Centrifugation was done between every washing step for 1 minute at 1000rpm. The bound proteins were eluted with elution buffer for 1 hour at 4°C. The efficiency of elution was checked on a 10% SDS-PAGE.

2.2.3. Lysis of mammalian cells with IP-Lyse buffer:

Cells of a whole p100 were washed with 5ml of 1xPBS and afterwards with 5ml of IP Wash buffer. The buffer was sucked off and 500µl IP Lyse buffer (containing Aprotinin, PMSF and Complete) was added to a 100mm tissue culture dish. The dish was incubated on a rotator for 20 minutes at 4°C. The cells were collected with a rubber scrapper, homogenized by pipetting and centrifuged for 10 minutes at 14.000rpm at 4°C. The supernatant was taken to measure the protein concentration using the Bradford method (see 2.2.4.). Whole cell lysates were either stored at -80°C or mixed with GSD, denatured at 95°C for 5 minutes and used for SDS-PAGE immediately.

To lyse cells in smaller volumes of lysis buffer, cells were washed 1 time with 5ml of 1xPBS, trypsinized and resuspended in DMEM and 10% FCS. After centrifugation for 5 minutes at 1200rpm, cell pellet was washed again with 5ml of 1xPBS, centrifuged and the supernatant was sucked off. The pellet was resuspended in 50µl-200µl IP Lyse buffer (depending on pellet size and cell count) and incubated on a rotator for 20 minutes at 4°C. Centrifugation followed for 10 minutes at 4°C and the protein concentration of the supernatant could be measured.

2.2.4. Determination of protein concentration:

Bradford reagent (Bio-Rad Protein Assay Dye Reagent #500-0006) was diluted 1:5 with ddH$_2$O. 1µl of cell lysate or protein solution was added and incubated for at least 10 minutes at room temperature. The protein concentration was determined by measuring the absorption at 595nm. Each sample was measured at least two times.

2.2.5. SDS-PAGE (SDS-Polyacrylamide gel electrophoresis):

1xSeparating gel 10%	
30% Acrylamide	13.4ml
Tris pH 8.8	15ml
SDS 20%	200µl
ddH2O	11.7ml
APS 10%	134µl
TEMED	26µl

1xStacking gel	
30% Acrylamide	1.7ml
Tris pH 8.8	1.25ml
SDS 20%	50µl
ddH2O	7.1ml
APS 10%	50µl
TEMED	10µl

The gel unit was assembled together. Components were mixed together (without APS and TEMED) and degased to avoid air bubbles. 10% APS and TEMED were added, and the mixture was poured into the gel unit. The separation gel was covered with ddH$_2$O until polymerized. Subsequently, ddH$_2$O was sucked off, the stacking gel could be poured and the appropriate gel comb inserted. After polymerization of the stacking gel, the comb was removed and slots were washed with water before inserting into the running unit. 1xrunning buffer was added and air bubbles removed with a pasteur pipette. Boiled samples were loaded and the gel was run for either 8 mA o/n or 120 V for 1.5 hours.

2.2.6. Coomassie staining of gels:

SDS-PAG was stained with Coomassie staining solution for 1-2 hours, incubated in destaining solution for approximately 2 hours and dried for 3.5 hours at 80°C in a vacuum trap.

2.2.7. Western blotting:

The western sandwich was assembled in the following way: support pad, 3 sheets of 3MM Whatman paper, gel, nitrocellulose membrane (Whatman Protran Nitrocellulose Membrane Filters), 3 sheets of 3MM Whatman paper and suport pad. All components were soaked before in 1xtransfer buffer and air bubbles were avoided. The western sandwich was inserted into the transfer unit and the proteins were transferred at 4°C for either 3.5 hours at 500mA (big gel) or

1.5 hours at 250mA (small gel). After the transfer, the nitrocellulose membrane was washed shortly with ddH$_2$O and stained with 1xPonceau S. To remove Ponceau, the membrane was washed for 1 minute with 1xPBS-Tween and blocked afterwards with 3% NFDM for 1 hour at room temperature. After blocking, the membrane was washed once with 1xPBS-Tween and incubated with the appropriate primary antibody, diluted in 0.5% NFDM, o/n at 4°C. Before incubation with the secondary antibody, the nitrocellulose membrane was washed 3 times for 5 minutes with 1xPBS-Tween. The membrane was incubated with the appropriate HRP-coupled secondary antibody, diluted in 0.5% NFDM, for 1 hour at room temperature. All incubations were done on a shaker. After incubation with the secondary antibody, the membrane was washed 3 times for 10 minutes with 1xPBS-Tween. ECL solutions were mixed (oxidizing reagent and enhanced luminal reagent, Perkin Elmer) in equal amounts and the membrane was incubated for 1 minute, wrapped in a foil and exposed to X-ray films. Alternatively, immunodetection with the LI-COR infrared imaging system has been done for quantifying (see 2.2.8.).

2.2.8. Immunodetection with LI-COR infrared imaging system:

After incubation for 1 hour with an appropriate IR-dye coupled secondary antibody, the nitrocellulose membrane was washed three times with 1xPBS-Tween and scanned with the LI-COR Odyssey infrared imaging system. The adequate program, "Odyssey 2.1.", was used at medium resolution with an intensity of 5 at 700nm excitation wavelength. Afterwards the membrane could be either dried between Whatman papers or blocked again with 3% NFDM for 30 minutes and incubated with a different primary antibody.

2.2.9. Antibodies used for western blotting:

Primary as well as secondary antibodies have been diluted in 0.5%NFDM-PBS-Tween.

2.2.9.1. Primary antibodies:

Primary antibodies	Clone/Source	Dilution	Species	kDa
Anti-PTPA	R171, 5.bleed (Ingrid Mudrak; Fellner et al., 2003)	1:10.000	Rabbit polyclonal	40.6
Anti-β-tubulin	AA2 (upstate, #05-661)	1:10.000	Mouse monoclonal	50
Anti-GAPDH	MAB374 (millipore)	1:40.000	Mouse monoclonal	39
Anti-PTPA	5G3 (Ingrid Mudrak)	1:1000	Mouse monoclonal	40.6
Anti-His	(GE healthcare, #27471001)	1:10.000	Mouse monoclonal	
Anti-Lamin A/C	3A6-4C11 (Roblek et al., 2010)	1:1000	Mouse monoclonal	75
Anti-PTPA	132/10, 4.bleed (this study)	1:200	Rabbit polyclonal	40.6
Anti-PTPA	6G2 (this study)	1:20	Mouse polyclonal	40.6
Anti-PTPA	7F12-10B (this study)	1:20	Mouse monoclonal	40.6
Anti-PTPA	6G2-7F (this study)	1:20	Mouse monoclonal	40.6
Anti-EAPP	582 (Novy et al., 2005)	1:5.000	Rabbit polyclonal	36

2.2.9.2. Secondary antibodies:

Secondary antibodies	Source	Description	Dilution
HRP anti-mouse	Goat, Jackson #115-035-008	IgG, Fcγ fragment specific	1:5.000
HRP anti-rabbit	Goat, Jackson #111-035-008	IgG, Fcγ fragment specific	1:5000
Alexa 680 anti-mouse	Goat, Invitrogen A-21057	IgG heavy and light chain	1:20.000
Alexa 680 anti-rabbit	Goat, Invitrogen A-21076	IgG heavy and light chain	1:20.000

2.2.10. Immunofluorescence:

5×10^4 Hela cells (or Helatrex-pNTOneo single clones after 3x induction with doxycyline every 24 hours for 3 days) were seeded in a single well of a 6 well tissue culture plate. Helatrex-pNTOneo single clones were induced once again after seeding with 1µg/ml doxycycline. Cells were cultivated o/n. Medium was sucked off and cells were washed two times with 1xPBS. All following steps were performed at room temperature. Cells were fixed with 3.7% formaldehyde/PBS for 15 minutes and washed again three times with 1xPBS. Quenching was done with 50mM NH_4Cl/PBS for 15 minutes followed by two times washing with 1xPBS. Subsequently, cells were permeabilized with 0.1% Triton X-100/PBS and washed afterwards three times with 1xPBS. Cells were incubated with 3% BSA/PBS for 1 hour and incubated afterwards with the primary antibody, diluted in 1%BSA/PBS, for either 2 hours at room temperature or 4°C o/n. Afterwards, cells were washed three times and incubated with the fluorescence dye coupled secondary antibody (diluted in 1%BSA/PBS; absorption maximum was either 594 or 488nm) for 1 hour at room temperature. After three times of washing, cell nuclei were stained with Hoechst 33342/PBS (750ng/ml) for 10 minutes, washed once with 1xPBS and two times with ddH_2O. The cover slips were mounted with Vectashield (Vector Laboraties). Slides were stored at 4°C. Images were recorded using a Zeiss LSM 510 Meta confocal microscope.

2.2.11. Antibodies used in Immunofluorescence:

Secondary antibodies for immunofluorescence were diluted in 1%BSA/PBS. Primary antibodies were either diluted as well or used without dilution.

2.2.11.1. Primary antibodies for Immunofluorescence:

Primary antibody	Clone/Source	Dilution	Species
Anti-PTPA	5G3 (Ingrid Mudrak)	1:10	Mouse monoclonal
Anti-Lamin A/C	3A6-4C11 (Roblek et al., 2010)	1:100	Mouse monoclonal
Anti-PTPA	132/10, 4.bleed (this study)		Rabbit polyclonal
Anti-PTPA	6G2 (this study)		Mouse polyclonal
Anti-PTPA	7F12-10B (this study)		Mouse monoclonal
Anti-PTPA	6G2-7F (this study)		Mouse monoclonal

2.2.11.2. Secondary antibodies for Immunofluorescence:

Secondary antibodies	Source	Description	Dilution
Alexa Fluor 594 goat anti-mouse	Molecular probes, #A11005	594, IgG (H+L)	1:500
Alexa Fluor 488 goat anti-mouse	Molecular probes, #A11029	488, IgG (H+L)	1:500

2.2.12. Sub-cellular fractionation:

In order to analyse the localization of PTPA, Hela cell lysates were fractionated into cytoplasm and nucleus. Hela cells were cultivated on p100 tissue culture plates until they reached a confluent status. The cells were washed 1 time with 1xPBS, trypsinized, counted with a counting chamber and washed again 2 times with ice-cold PBS. Between all the washing steps centrifugation was done at 1200rpm for 5 minutes each. Cells were resuspended in 250µl Buffer F1 per $1x10^6$ cells and incubated at room temperature for 2 minutes. An incubation on ice followed for 10 minutes and afterwards, NP-40 was added to a final concentration of 1% (v/v). A whole cell lysate aliquot (50µl) was taken before homogenizing the sample by passing the solution carefully through a 20G needle for three times. The nuclei were pelleted by centrifugation at 600g for 5 minutes at 4°C and the supernatant was harvested as the cytoplasmic fraction. The nuclei were washed 3 times in Buffer F1 containing 1% NP-40 and resuspended afterwards in 200µl

Buffer F1 including 1% NP-40. Whole cell lysates, cytoplasmic and nuclear fractions were boiled in GSD-buffer for 5 minutes at 95°C and analysed by SDS-PAGE and Western blotting.

2.2.13. CIP-treatment of mammalian cell lysates:

Lysates of mammalian cells (Hela, HelaTRex, HEKTRex, NIH 3T3) were made with IP-Lyse buffer (see 2.2.3.) and either stored at -80°C for a short period or prepared freshly before the CIP-treatment. After determining the protein concentration (see 2.2.4.) with the Bradford method, 100µg of each sample was used for the phosphatase treatment and pipetted together with all components. NEBuffer 3 (New England Biolabs) and 5000 U of alkaline phosphatase (CIP, New England Biolabs, NEB #M0290S) was added and filled up to a final volume of 50µl with ddH$_2$O. The assay was incubated for 60 minutes at 37°C on a shaker. The reaction was stopped by the addition of GSD-buffer and samples were analysed by SDS-PAGE and Western blotting.

2.2.14. Purification of antibodies:

2.2.14.1. Purification of antibodies using the SulfoLink® Kit:

For the affinity purification of the polyclonal rabbit anti-PTPA antibody (R.171, 5.bleed), the SulfoLink® Kit (Pierce Biotechnology; #44895) was used. The guidelines provided by the supplier´s protocol were followed for the SulfoLink column coupled with peptid #5 (5.1.2000). The efficiency of elution was checked on a 10% SDS-PAG.

2.2.14.2. Affinity purification of antibodies:

For the affinity purification of three different monoclonal and polyclonal antibodies against PTPA, 7F12 10B (mouse monoclonal), 6G2 (mouse polyclonal) and 132/10 (rabbit polyclonal), His-tagged PTPA bound to a nitrocellulose membrane has been used. Full length His-tagged PTPA was purified as described under 2.2.2. and the protein concentration was determined using the Bradford method (see 2.2.4.). 100µg of PTPA-His was denatured in GSD-buffer at 95°C and loaded on a 10% SDS-PAG (see 2.2.5.) followed by Western blotting (see 2.2.7.). After transferring the protein to the nitrocellulose membrane, the membrane was stained with

1xPonceau S. The PTPA specific antigen band was cut out, chopped into small pieces with a broadness of approximately 1mm and put into 2ml eppendorf tubes. The membrane pieces were incubated for 2 days at 4°C on a rotator with 1ml of each serum, centrifuged shortly and the supernatant was removed and checked for the depletion of PTPA specific antibody. The membrane pieces were washed 1 time with 1ml of 10mM Tris pH8.0 and another time with 1ml of 10mM Tris pH8.0 including 10.5mM NaCl. For acidic elution, the membrane pieces with the bound antibody were incubated three times for 2 minutes each with 200µl of 100mM Glycin pH2.5, centrifuged in between and the supernatants were neutralized with 50µl of 1M Tris pH8.0 including sodium-azide (1:1000). All eluates were diluted 1:200 with 0.5% NFDM and analysed by western blotting together with unpurified antibodies, diluted 1:20 and 1:200 with 0.5%NFDM.

2.3. Working with Bacteria

2.3.1. Solutions and Media:

LB-medium: 5g Tryptone (AppliChem #A1553); 2.5g Yeast extract (AppliChem #A1552); 2.5g NaCl; Dissolve in 500ml ddH$_2$O, autoclave immediately and store at RT.

LB-agar plates: 5g Tryptone; 2.5g Yeast extract; 2.5g NaCl; 7.5g Agar (AppliChem #A0949); Dissolve in 500ml ddH$_2$O, autoclave immediately, cool to 50°C, add appropriate antibiotics, pour plates and store plates at 4°C.

Ampicillin-stock (100x) (Gerbu #1046): Dissolve 10mg/ml in ddH$_2$O. Filter sterilize through a membrane filter with a pore size of 0.2µm and store aliquots at -20°C.

Kanamycin-stock (200x) (Sigma #K-4000): Dissolve 10mg/ml in ddH$_2$O. Filter sterilize through a membrane filter with a pore size of 0.2µm and store aliquots at -20°C.

Chloramphenicol-stock (1000x) (Serva #16785): Dissolve 34mg/ml in 96% ethanol and store at -20°C.

200mM IPTG-stock: Dissolve 9.35g IPTG in 200ml of ddH$_2$O and store aliquots at -20°C.

Bacterial strains:

XL1blue: *recA1 endA1 gyrA96 hsdR17 supE44 relA1 lac* [F´*proAB lacI^{q}ZΔM15 Tn10* (Tet^R)]
The bacterial strain is tetracycline resistant.

Origami(DE3)pLysS: Δ*(ara-leu)7697 ΔlacX74 ΔphoA PvuII phoR araD139 ahpC galE galL rpsL* F´[*lac$^-$ lacI^q pro*] (DE3) *gor522::Tn10 trxB* pLysS (Cam^R, Str^R, Kan^R, Tet^R)
The bacterial strain is chloramphenicol, streptamycin, kanamycin and tetracyclin resistant.

Rosetta(DE3)pLysS: F´*ompThsdS$_B$($r_B^-$$m_B^-$) gal dcm lacYI(DE3)* pLysSRARE (Cam^R)
The bacterial strain is chloramphenicol resistant.

Rosetta^{TM}(DE3): F´*ompThsdS$_B$($r_B^-$$m_B^-$) gal dcm lacYI*(DE3) pRARE (Cam^R)
The bacterial strain is chloramphenicol resistant.

EL350: DY380 [(cro-bioA) <> araC-PBADcre]; The EL350 strain has no resistance and includes a genomically integrated Cre gene, which is inducible by a temperature switch from 32°C to 42°C. EL350 bacteria have been kindly provided by Astrid Hagelkruys (lab group of Christian Seiser, Mfpl).

2.3.2. Growth of bacteria:

All bacterial strains, except EL350, were grown in LB-medium or on LB-agar plates at 37°C containing 100µg/ml Ampicillin. EL350 are temperature sensitive and were grown at 32°C without adding antibiotics.

2.3.3. Freezing/thawing of bacteria:

For freezing, 200ml of glycerol and 800µl of bacterial o/n culture were mixed thoroughly and stored at -80°C. For thawing, the freezing stock was scraped with a pipette tip and the scraped material was inoculated in 5ml of LB-medium including the appropriate antibiotics o/n at 37°C on a shaker.

2.3.4. Transformation of temperature sensitive bacterial strains:

An aliquot of temperature sensitive bacteria was thawed on ice. 10μl of a ligation reaction or ~50ng of plasmid DNA was added to the bacteria. In case of a retransformation 1-2ng of plasmid DNA was used. After DNA addition, the sample was incubated for 15 minutes on ice and 1 minute at 42°C for heat shock. The sample was cooled for 2 minutes on ice and 1ml LB-medium (without antibiotics) was added. The bacteria were incubated for 1 hour at 37°C while shaking. Subsequently cells were centrifueg at 14.000rpm for 15 seconds and 2/3 of the supernatant was discarded. The pellet was resuspended with the rest of the supernatant and plated onto LB-agar plates containing the respective selective antibiotics. Incubation was carried out o/n at 37°C.

2.3.5. Bacterial expression of fusion proteins:

5ml LB-Amp have been inoculated with a bacterial clone from a LB-agar plate and incubated o/n at 37°C. The o/n culture was diluted in 200ml LB-Amp and incubated at 37°C until it reached an OD_{550} of 0.8-1. The expression of recombinant protein was induced with 1mM IPTG for 3 hours at 37°C. A small aliquot of bacterial culture was kept uninduced as negative control. Bacteria were centrifuged for 5 minutes at 5000rpm at 4°C, supernatant discarded and the pellet of uninduced bacteria was resuspended in 2ml of 25mM Tris pH8.4 (containing Aprotinin and PMSF) per OD_{550}. The pellet of induced bacteria was resuspended in an appropriate volume of 25mM Tris pH8.4 (containing Aprotinin and PMSF) according to OD_{550}. Subsequently, bacteria were lysed via sonication for 3 times 30 seconds each with ~30 seconds of incubation on ice between the sonication steps. A 60μl aliquot was taken and centrifuged for 10 minutes at 10.000rpm and 4°C. 30μl of 3xGSD was added to the supernatant and the insoluble protein fraction was resuspendend in 90μl of 1xGSD. The samples were boiled for 5 minutes at 95°C and analysed by SDS-PAGE, Western blotting and Coomassie staining. The rest of bacterial lysate was centrifuged for 30 minutes at 5000rpm and 4°C after sonication. The supernatant was stored at 4°C and the insoluble fraction at -20°C. For the expression of PTPA-His (full length), Origami, Rosetta (-) and Rosetta (+) were used in order to compare the efficiency of three different strains.

2.3.6. Transformation of BAC DNA into EL350 bacteria via Electroporation:

5ml of LB-medium were inoculated with a single clone of EL350 bacteria and incubated o/n at 32°C. 1ml of o/n culture was transferred to 20ml LB-medium and incubated at 32°C until an OD_{600} of 0.5. 10 ml of bacterial culture was used per preparation. To achieve cell competence, 10ml of bacterial culture was incubated on ice for 5 minutes and subsequently centrifuged for 5 minutes at 4000rpm and 0°C. The pellet was resuspended in 1ml of ice-cold ddH_2O and transferred to a 1.5ml eppendorf tube (pre-cooled on ice). Centrifugation was repeated for 5 minutes at 4000rpm and 0°C, and the pellet was washed again with 1ml of ice-cold ddH_2O. The third washing step was carried out with 15% ice-cold glycerol. The bacterial pellet was resuspended after the centrifugation step in 50µl of 15% ice-cold glycerol and cells were transferred to a 0.2cm electroporation cuvette, which was cooled at -20°C before. Before the electroporation could be started, the cuvettes were wiped dry with a tissue to prevent drops of liquid in the aperture. Electroporation was carried out with a Bio-Rad Gene Pulser[®] at 2.5kV, 200Ω and 25µF with three different concentrations of BAC-DNA, 200ng, 500ng and 1000ng respectively. 200ng of the pSuper-plasmid have been used as a positive control for the electroporation. Right afterwards, every sample was incubated with 1ml of LB-medium at 32°C for 1 hour, plated on LB-agar plates including selective antibiotics and incubated for 2 days at 32°C. Two different concentrations of chloramphenicol were used for selective antibiotics on LB-agar plates for BAC-DNA: 15µg/ml and 7.5µg/ml. Two clones of BAC-preparations were used: RP24339 D2#4, RP23431 H3#4

2.4. Working with DNA

2.4.1. Solutions and Media:

50x TAE: 484g Tris; 114ml acetic acid; 200ml 0.5M EDTA pH8.0; Dissolve and fill up to 2l with ddH_2O and store at RT.

1x TAE (working solution): 40mM Tris acetate; 2mM EDTA.

Lambda DNA Marker (Fermentas #SM0111): Dilute the concentrated marker to a final concentration of 0.1µg/µl, heat the solution to 65°C for 5 minutes, cool on ice and store aliquots at -20°C.

6x DNA loading dye (Fermentas #R0611)

Low molecular weight DNA Ladder (NEB #N3233L)

Gene Ruler^{TM} 1kb DNA Ladder (Fermentas #SM0311)

<u>**BAC-preparation solutions:**</u>

Solution 1: 50mM Tris pH8.0; 10mM EDTA; 100µg/ml Rnase A; Dissolved in ddH$_2$O, filter sterilized through a membrane filter with a pore size of 0.2µm and stored at 4°C.

Solution 2: 0.2N NaOH; 1%SDS; Dissolved in ddH$_2$O, filter sterilized through a membrane filter with a pore size of 0.2µm and stored at RT.

Solution 3: 3M Potassium acetate; Dissolved in ddH$_2$O, pH was adjusted to pH5.5 with glacial acetic acid, autoclaved and stored at 4°C.

RNAse A (Sigma #R-5125): 10mg/ml RNAse A were dissolved in 10mM sodium acetate pH5.2, heated up to 100°C for 15 minutes and cooled down to RT. The pH was adjusted by adding 0.1 volumes of 1M Tris-Cl pH7.4 and aliquots were stored at -20°C.

2.4.2. Plasmid Mini preparation using the QIAprep$^®$ Spin Miniprep Kit (Qiagen #27106):

The guidelines provided by the supplier´s protocol were followed.

2.4.3. Plasmid Midi preparation using PureYield^{TM} Plasmid Midiprep System (Promega #252219):

For large amounts of plasmid DNA preparation the Pure Yield^{TM} Plasmid Midiprep System kit was used. The guidelines provided by the supplier´s protocol were used.

2.4.4. DNA Isolation of BAC clones:

A sterile toothpick was used to inoculate a single isolated bacterial colony into 5ml of LB-medium containing 15µg/ml Chloramphenicol. The bacterial culture incubated o/n at 37°C while shaking. After removing the toothpicks, the o/n culture was centrifuged for 10 minutes at

3000rpm at RT. The supernatant was discarded and the pellet resuspended in 0.3ml of Solution 1. After adding 0.3ml of Solution 2, the components were mixed by gently shaking the tube. After incubation at RT for ~5 minutes, the appearance of the solution changed from turbid to almost translucent. 0.3ml of Solution 3 was added slowly during slight shaking and an incubation for at least 5 minutes on ice followed. Samples were centrifuged for 10 minutes at 10.000rpm and 4°C and the supernatant was transferred to an eppendorf tube containing 0.8ml of ice-cold isopropanol. The sample was mixed by inverting and incubated on ice for at least 5 minutes. Centrifugation carried out again for 15 minutes at 10.000rpm and 4°C. Subsequently, the supernatant was removed and 0.5ml of 70% Ethanol was added to wash the DNA pellet. After centrifuging the sample for 5 minutes at 10.000rpm and 4°C, the supernatant was removed and the pellet was air dried. When the appearance of the DNA pellet turned from white to translucent, it was resuspended in ~40µl of TE through slightly tipping at the bottom of the tube or alternatively by incubation at 37°C for 15 minutes. Isolated DNA was stored at 4°C or used immediately for further analysis.

BAC clones used for DNA Isolation were: RP23431 H3; RP24339 D2; RP23165L 19.

2.4.5. Analysis of DNA isolated from BAC clones with PCR:

To confirm the identity of the obtained BAC-clones (purchased from http://bacpac.chori.org/), whether they contain the PTPA gene, the DNA of the three clones was isolated (see 2.4.4.) and checked by PCR. PCR was carried out using the GoTag®Green Master Mix (Promega), which already includes DNA polymerase, dNTPs, $MgCl_2$ and reaction buffer. 10µl of GoTag®Green Master Mix, 9µl of nuclease free ddH_2O, 5pmol/µl of PTPA specific primers and 50-100ng of BAC-DNA were mixed on ice and placed in a preheated PCR Thermocycler.

PTPA specific primers for analysis of DNA isolated from BAC clones:

Exon 6 sense: GTCTCTGCAAGATTGGTGTACTCCG

Exon 7 antisense: GACCCCATACGCCCTGGCTGCCTG

Both primers have been ordered from Sigma-Aldrich, resuspended according to supplier´s datasheet with nuclease free ddH_2O at 37°C for 15 minutes. The primer mix used in the Polymerase chain reaction, was made by mixing 5pmol/µl of each primer-solution and 90µl of ddH_2O (5µmol).

Afterwards, PCR products were analysed on a 1.8% agarose gel (in 1xTAE), which was run at 120V for ~40 minutes.

Positive BAC clones used for Transformation of BAC DNA into EL350 bacteria via Electroporation (see 2.3.6.): **RP23431 H3 #4**; **RP24339 D2 #4**.

2.4.6. Restriction digest:

For digesting 1µg of plasmid DNA, 1 U of appropriate restriction enzyme was used and the reaction mix was prepared as suggested by the supplier. The total volume of the reaction mix was 150µl for preparative purpose. The samples were incubated o/n at 37°C. 10µl of restriction digest were mixed afterwards with 2µl of 6x DNA loading dye and analysed on a 1.5% agarose gel (in 1xTAE).

2.4.7. Elution of DNA fragments:

For isolation of DNA fragments from agarose gels, the Wizard®SV Gel and PCR Clean-Up System (Promega #A9283) was used and instructions of suppliers protocol followed. The desired DNA band was excised from the gel and placed into a 1.5ml eppendorf tube. The eluted DNA was stored at -20°C and 1-5µl of elution was checked on an agarose gel.

2.4.8. Ligation of DNA fragments:

50-100ng of plasmid DNA were mixed and DNA inserted at a molar ratio of 1:3 in a final volume of 20µl containing 2µl of T4 ligation buffer (containing 10mM ATP) and 0.5 U of T4 DNA ligase (NEB). The mixture was incubated o/n at 16°C. 10µl of ligated DNA were used to transform heat-shock competent *E.coli* (see 2.3.4.).

2.4.9. Cloning of pRetroSuper$_{Stuffer}$-CT/Mis:

pRetroSuper$_{Stuffer}$ was chosen for the infection of mammalian cells with a retroviral vector (see 2.1.10.). The final pRetroSuper$_{Stuffer}$-CT transfected into a packaging cell line expresses the viral packaging signal, the H1-shRNA expression cassette and a puromycin resistance gene.

The pSuper-CT and pSuper-Mis were cut with EcoRI and XhoI (fragment sizes of ~300bp) to obtain the DNA fragment including the H1-RNA promoter and shRNA sequence. The restriction products were electrophoretically seperated in an agarose gel, eluted from the gel and used for ligation with EcoRI and XhoI cutted, electrophoretically separated and eluted pRetroSuper$_{Stuffer}$ (fragment size of 5.3kb). After ligation of each 300bp DNA fragment with one pRetroSuper$_{Stuffer}$, the samples were used to transform heat-shock competent *E.coli*.

Positive clones of pRetroSuperStuffer-CT used for Retroviral Infection: Clone 3

Positive clones of pRetroSuperStuffer-Mis used for Retroviral Infection: Clone 2

Both vectors were sequenced at LGC genomics with primer **H1RNApro**:

5´-GAATCGCGGGCCCAGTGTCA-3´

2.5. Working with RNA

2.5.1. Solutions and Media:

Trizol®Reagent (Invitrogen): kindly provided by the lab of Christian Seiser

10x MOPS: 41.85g MOPS (morpholinopropanesulfonic acid); 6.8g sodium acetate-3H$_2$O; Dissolve in 800ml of ddH$_2$O, add 20ml of 0.5M Na$_2$EDTA and adjust pH to 7.0. Fill up to 1 litre with ddH$_2$O.

Iscript cDNA synthesis kit (BioRad)

3M sodium-acetate: Dissolve in ddH$_2$O, adjust to pH5.5, filter sterilize and store at 4°C.

Lipofectamine 2000 (Invitrogen #11668-019)

2.5.2. Isolation of RNA using Trizol®Reagent:

1×10^6 of HelaTRex-pNTOneo-CT Cl.L or Mis Cl.D cells were seeded on a p100 tissue culture dish, and induced with doxycycline (1µg/ml) for 96 hours (see 2.1.6.). Hela cells were seeded as well and used as a standard. For the first step of homogenization, cells were washed with 1xPBS, trypsinized and harvested with 1ml of Trizol®Reagent for each p100 culture dish. The sample was centrifuged for 10 minutes at 12.000rpm at 4°C and the supernatant transferred to a new eppendorf tube. For the next step, the phase separation, 0.2ml chloroform were added, the sample was shaken vigorously for ~15 seconds, incubated at RT for 3 minutes and centrifuged again for 15 minutes at 12.000rpm and 4°C. To precipitate the RNA, the upper aqueous phase was transferred to a new eppendorf tube, 0.5ml of isopropyl alcohol were added, the sample was incubated for 10 minutes at RT and centrifuged for 10 minutes at 12.000rpm and 4°C. For washing the RNA pellet, the supernatant was removed and 1ml of 75% ethanol was added. The sample was mixed and centrifuged again for 5 minutes at 7500rpm and 4°C. The supernatant was removed, the pellet air dried and finally resuspended in ~30µl of nuclease free ddH$_2$O. For the second precipitation, 3µl of 3M sodium-acetate and 75µl of 96% ethanol were added and incubated with the sample at -20°C o/n. Centrifugation was carried out for 30 minutes at 12.000rpm and 4°C, the pellet was washed again with 1ml of 75% ethanol and resuspended in 30µl of nuclease free water. The concentration of RNA was measured with a NanoDrop spectrophotometer.

To check the integrity of the RNA, 1µg of isolated RNA was mixed with 9µl of ddH$_2$O and 2µl of RNA loading buffer with ethidiumbromide, incubated at 65°C for 5 minutes and put on ice for 1 minute. 1.2g agarose, 90ml ddH2O, 10ml of 10xMOPS and 5.2ml formaldehyde were mixed, heated and poured in the appropriate gel tray. Subsequently, samples were loaded and the MOPS-gel and run at 70V for ~20 minutes.

2.5.3. cDNA-synthesis using iScript™ cDNA Synthesis Kit (BIO-RAD):

For the synthesis of cDNA, iScript™ cDNA Synthesis Kit (BIO-RAD #170-8891) was used. 1µg of RNA in a maximum of 10µl volume, 4µl of 5x iScript reaction mix, 1µl of iScript reverse transcriptase and 5µl of nuclease-free water were mixed together on ice and placed in a preheated PCR-Thermocycler. For the PCR program to reverse transcribe RNA into cDNA, the

guidelines of supplier´s protocol were followed. Afterwards, the cDNA product was filled up with 180 µl of ddH$_2$O and the efficiency of the cDNA-synthesis checked on an agarose gel.

2.5.4. Gradient RT-PCR with KAPA SYBR® FAST Bio-Rad iCycler 2x qPCR Master Mix (Kapa Biosystems):

For determining the optimal annealing temperature for the used primer sets, a gradient PCR was set up using a BIO-RAD light cycler. Both primer pairs for human PTPA, hPTPA 1 (marked in red) and hPTPA 2 (marked in blue), producing fragment sizes of 210bp and 270bp respectively, were tested. Annealing temperatures used for testing were: 65°C, 64.5°C, 63.3°C, 61.4°C, 58.9°C, 57.1°C, 55.8°C and 55.0°C.

The KAPA SYBR® FAST Bio-Rad iCycler 2x qPCR Master Mix was used, including fluorescein reference dye. Hela cDNA served as a template. Each component was thawed on ice and put on an ice-cold tray while pipetting onto the 96-well plate. A foil was placed over the surface of the plate, which was centrifuged at 1200rpm for 30 seconds. All samples were analysed in duplicates. The guidelines of supplier´s protocol were followed and the set-up of the qRT-PCR was done with the help of Anna Sawicka (lab group of Christian Seiser, Mfpl). After the reaction, samples were analysed on a 1.5% agarose gel. Although every annealing temperature gave rise to a product, the most stringent temperature working for both primerpairs was 58°C.

Human PTPA cDNA (NM_021131.4, NM_178000.2):

5´-ATGGCTGAGGGCGAGCGGCAGCCGCCGCCAGATTCTTCAGAGGAGGCCCCTCCAGCCAC TCAGAACTTCATCATTCCAAAAAAGGAGATCCACACAGTTCCAGACATGGGCAAATGGAAG CGTTCTCAGGCATACGCTGACTACATCGGATTCATCCTTACCCTCAACGAAGGTGTGAAGGG GAAGAAGCTGACCTTCGAGTACAGAGTCTCCGAGGCCATTGAGAAACTAGTCGCTCTTCTC AACACGCTGGACAGGTGGATTGATGAGACTCCTCCAGTGGACCAGCCCTCTCGGTTTGGGA ATAAGGCATACAGGACCTGGTATGCCAAACTTGATGAGGAAGCAGAAAACTTGGTGGCCAC AGTGGTCCCTACCCATCTGGCAGCTGCTGTGCCTGAGGTGGCTGTTTACCTAAAGGAGTCAG TGGGGAACTCCACGCGCATTGACTACGGCACAGGGCATGAGGCAGCCTTCGCTGCTTTCCTC TGCTGTCTCTGCAAGATTGGGGTGCTCCGGGTGGATGACCAAATAGCTATTGTCTTCAAGGT GTTCAATCGGTACCTTGAGGTTATGCGGAAACTCCAGAAAACATACAGGATGGAGCCAGCC GGCAGCCAGGGAGTGTGGGGTCTGGATGACTTCCAGTTTCTGCCCTTCATCTGGGGCAGTTC GCAGCTGATAGACCACCCATACCTGGAGCCCAGACACTTTGTGGATGAGAAGGCCGTGAAT GAGAACCACAAGGACTACATGTTCCTGGAGTGTATCCTGTTTATTACCGAGATGAAGACTG GCCCATTTGCAGAGCACTCCAACCAGCTGTGGAACATCAGCGCCGTCCCTTCCTGGTCCAAA GTGAACCAGGGTCTCATCCGCATGTATAAGGCCGAGTGCCTGGAGAAGTTCCCTGTGATCC AGCACTTCAAGTTCGGGAGCCTGCTGCCCATCCATCCTGTCACGTCGGGCTAG- 3´

hPTPA sense 1: AGTCGCTCTTCTCAACAC

hPTPA antisense 1: TGTGCCGTAGTCAATGC

hPTPA sense 2: TGTCTTCAAGGTGTTCAATCG

hPTPA antisense 2: GCTGGTTGGAGTGCTCTG

2.5.5. qRT-PCR with KAPA SYBR® FAST Bio-Rad iCycler 2x qPCR Master Mix (Kapa Biosystems):

For qPCR, the KAPA SYBR® FAST Bio-Rad iCycler 2x qPCR Master Mix was used following the guidelines of supplier´s protocol. All samples were prepared and analysed in duplicates, normalized onto a dilution series of Hela cDNA (1:1, 1:2, 1:4, 1:8, 1:16), with a starting amount of 50μg, and a gapdh primer pair as a control for a housekeeping gene. The qRT-PCR was run with a BIO-RAD light cycler at an annealing temperature of 58°C with each primer (sense and antisense) at a concentration of 10μM. After the reaction, each value of samples with hPTPA primers was normalized onto the respective value of gapdh primers. The dilution curve was necessary to control the linear range. All calculations and analysis were done with the help of Anna Sawicka and Sabine Lagger (lab group of Christian Seiser, Mfpl).

2.5.6. Transfection of mammalian cells using Lipofectamine 2000:

Different cell lines were used for transfection using Lipofectamine 2000 (Invitrogen #11668-027): Hela, HEKTREX, HelaTRex-pNTOneo-CT Cl.L and HelaTRex-pNEOneo-Mis Cl.D. All cell lines used for transient transfections were grown in DMEM + 10% FCS with appropriate selective antibiotics and medium was changed to DMEM + 10%FCS w/o antibiotics the day before transfection was performed. $5x10^5$ cells of HEKTRex cells and $4x10^5$ cells of Hela-derived cell lines were seeded on 6-well tissue culture plates on the day before transfection according to the optimization of transfection efficiency (see 2.5.7.). Prior to transfection, everything was wiped with RNase AWAY® (Fisher Scientific) and 70% ethanol. Either 25pmol, 50pmol or 100pmol of siRNA was diluted in 250μl of Opti-MEM® I Reduced-Serum Medium (1x) (#11058-021) and incubated for 5 minutes at room temperature. 8μl of Lipofectamine 2000 was diluted as well in 250μl of Opti-MEM and incubated at room temperature for 5 minutes.

Both samples were mixed carefully and incubated together at room temperature for 20 minutes. Meanwhile, cells were washed with 1xPBS and supplemented with 2ml of DMEM (Dulbecco´s modified Eagle´s medium) + 10%FCS. The transfection mix was added dropwise and removed after 5 hours. For further analysis, whole cell lysats were made (see 2.2.3.), followed by SDS-PAGE, western blotting and quantification using the Li-Cor infrared scanner.

2.5.6.1. Sequences of siRNAs:

		25pmol	50pmol	100pmol
hPTPA-CT(sense) hPTPA-CT(antisense)	5´-GUUCCCUGUGAUCCAGCAC [dT] [dT]-3´ 5´-GUGCUGGAUCACAGGGAAC[dT] [dT]-3´	333ng	666ng	1333ng
hPTPA-Mis (sense) hPTPA-Mis (antisense)	5´-GUU<u>U</u>CCUGU<u>A</u>AUCC<u>A</u>ACAC[dT] [dT]-3´ 5´-GUG<u>U</u>UGGAUU<u>U</u>ACAGG<u>A</u>AAC[dT] [dT]-3´	332ng	664ng	1328ng
SASI_Hs01_00123722 SASI_Hs01_00123722_AS	5´-CAAUCGGUACCUUGAGGUU[dT] [dT]-3´ 5´-AACCUCAAGGUACCGAUUG[dT] [dT]-3´	333ng	665ng	1330ng

The abbrevation "CT" refers to C-terminal part of human PTPA and is identical with the shPTPA sequence (see 2.1.1.2.) with the exception of uracil replacing thymine, as shPTPA is DNA in contrast to siRNAs. "Mis" is the siRNA sequence including mismatches and was used as a non-binding negative control. The siRNAs were ordered and purchased from SIGMA-Aldrich and provided as duplexes of above sequences. SASI_Hs01_00123722 sense and antisense was a prevalidated siRNA from the SIGMA-Aldrich library spanning exon 7 and 8 of human PTPA, with position 660-679 in ORF according to sequence NM_178001.2, and termed "siRNA$_{sigma}$" in further results. siRNAs were diluted with Nuclease free water according to supplier´s protocol and stored at -20°C. Nanogram calculation was made for duplex siRNAs.

2.5.7. Optimizing transfection efficiency:

For the optimization of transfection efficiency, different cell numbers of Hela and HEKTRex cells were transfected with 0.8µg of pmax GFP (provided by Matthias Artaker), followed by a flow cytometric analysis with FACS-Aria^{TM} cell sorter (BD Biosciences). Cells were seeded on a 24-well tissue culture plate the day before transfection. For the transfection, three different amounts of Lipofectamine 2000 were used: 1µl, 1.5µl and 2µl. The day after transfection, cells were washed once with 1xPBS, trypsinized, resuspended in DMEM + 10%FCS, centrifuged at 1200rpm for 5 minutes and resuspended in 0.5ml of 1xPBS. Samples were transferred to FACS-tubes and analysed.

HEKTRex (cells/well)	Lipofectamine 2000 (µl)	Hela (cells/well)	Lipofectamine 2000 (µl)
250.000	2	85.000	1.5
200.000	2	80.000	1.5
175.000	2	77.500	1.5
150.000	2	75.000	1.5
125.000	2	72.500	1.5
100.000	2	70.000	1.5
75.000	2	67.500	1.5
50.000	2	65.000	1.5
150.000	1.5	75.000	1
150.000	2	75.000	1.5
150.000	2.5	75.000	2

2.6. Working with mice and rabbits

For the production of a new antibody against PTPA, which would also work in an immunofluorescence-staining, 4 mice and 1 rabbit were immunized with full length His-tagged PTPA, antisera were tested in Western blot and immunofluorescence analyses.

2.6.1. Solutions and media:

Purified His-tagged PTPA: pB´His NP SpHI/NcOI PTPA#2

HAT Medium: 400ml DMEM (Sigma #D5671); 50ml Fetal Cl.1 (HyClone #SH30080.03); 25ml BM-Condimed H1 (LaRoche #11088947001); 5ml Penicillin/Streptomycin (P/S) (Sigma #P4333); 5ml L-Glutamine (Sigma #G2150); 5ml Na-Pyruvate (Sigma #S8636); 10ml HAT supplement (Gibco #21060)

2.6.2. Mouse Immunisation:

Four mice, originating from the strain RBF/DnJ RB(8.12)5Bnr, were immunized with 50µg of antigen. The antigen was mixed with adjuvants in a ratio of 1:1. The mix was applied subcutaneously and the final immunization (final boost) was carried out without adjuvants and injected intraperitoneally. All mice were immunized by Marko Roblek.

2.6.3. Mouse Bleeds:

The bleeds were taken from the tail vein except the final bleed, which was taken from the heart. All bleeds were taken from Marko Roblek. About 50µl of blood was taken, incubated at 37°C for 1 hour and centrifuged for 5 minutes at 14.000rpm. After o/n storage at 4°C, centrifugation was done again for 10 minutes at 14.000rpm, the serum was taken and sodium-azide (0.02%) added. The serum was stored at 4°C.

2.6.4. Mouse Immunisation schedule:

Day 0	Pre-immune bleed from tail vein 1.immunisation (sc) with ~50μg of antigen + adjuvants
Day 14	2.immunisation (sc) with ~50μg of antigen + adjuvants
Day 24	1.bleed from tail vein
Day 35	3.immunisation (sc) with ~50μg of antigen + adjuvants
Day 45	2.bleed from tail vein
Day 56	Final boost for best responder (ip) with ~50μg of antigen
Day 59	Fusion of splenocyte from best responder

2.6.3. Generation of hybridoma:

2.6.3.1. Fusion:

To create monoclonal antibodies, splenocytes of the immunised mice were fused with a certain cell number of myeloma cells. The fusion has been done by Marko Roblek (please see diploma thesis of Marko Roblek for further details, pages 61-62 and Roblek et al., 2010).

2.6.3.2. Test of hybridoma supernatant:

The supernatant of the hybridomas was tested for presence of antibodies 8-10 days after fusion by immunoblotting assay on whole cell lysates using miniblotter devices from Immunetics (#MN28).

2.6.3.3. Minimal dilution of positive hybridoma clones:

The supernatant of the respective hybridoma mixclone was taken as a control for further testings and stored at 4°C. Hybridoma mix clones were resuspended in HAT medium, the number of cells was determined using a counting chamber and dilutions of 3.6 cells/well and 1.5 cells/well were prepared on a 96 well tissue culture plate. Other positive mixed clones were frozen as well

as remaining cells of the minimally diluted clone. The minimal dilution has been done by Stefan Schüchner.

2.6.3.4. Expansion of monoclonal hybridoma and production of monoclonal antibody:

Single hybridoma clones, tested positive by Western blotting or immunofluorescence, were expanded to bigger tissue culture dishes and at least 3 vials of each clone were frozen. Before cultivating the clones in DMEM containing 10%FCS w/o selection drugs, the clones were grown in HT medium for three passages. I froze at least three vials of cells and expanded the clone onto 5-10 p150 cell culture dishes, cultivated it without change of medium until all cells were dead and harvested the supernatant, stored it at 4°C or froze it at -20°C.

2.6.4. Rabbit immunisation and bleeds:

One New Zealand White Rabbit has been immunized with a defined amount of antigen (see below) and the immunisation has been done according to the schedule shown. The antigen emulsion has been applied intradermaly at the neck. The bleeds were taken from the ear vein and up to 50ml of blood was taken. Preparation and storage has been done as described under 2.6.3. The bleeds were taken by Prof.Marcela Hermann as well as immunisations.

2.6.5. Immunisation schedule of rabbit

Day 0	Pre-immune bleed from ear vein 1.immunisation (id) with ~250µg of antigen + adjuvants
Day 14	2.immunisation (id) with ~125µg of antigen + adjuvants
Day 24	1.bleed from ear vein
Day 35	3.immunisation (id) with ~75 µg of antigen + adjuvants
Day 45	2.bleed from ear vein
Day 56, 77	Last immunisation with 75 µg of antigen + incomplete adjuvants

3. Results

Knockdown of PTPA

3.1. Knockdown of PTPA with stably transfected single clones

3.1.1. Testing of stable transfected HelaTRex-pNTOneo single clones

Previous studies revealed no effect on the phenotype of N2ATRex and HEKTRex cell lines (diploma thesis of Mitterhuber and Kugler) after downregulation of PTPA to 25-40% of wild type levels. Thus, the current project was focused on the analysis of phenotypical effects, apoptotic behaviour or effects on the biogenesis of PP2A in HelaTRex cells. Single clones of stably transfected HelaTRex-pNTOneo-CT or Mis cells (transfected and selected by Michaela Kugler during her diploma thesis) were tested for the ability of PTPA knockdown by western blotting and quantification using the LI-COR Odyssey infrared scanning system. The targeting RNAi consisted of a 21bp shRNA, expressed by the RNA Pol III dependent H1 promoter upon induction with doxycycline, and shared complete sequence identity between mouse and human. In contrast, the mismatch RNAi contained three mismatch base pairs compared to the PTPA wild type sequence at positions 14, 10 and 16, and therefore should be incapable of binding to the mRNA of PTPA.

To induce the knockdown of PTPA, 1µg/ml of doxycycline was applied every day to the cells for 96 hours. Subsequently, whole cell lysates were PTPA levels were analysed by western blotting and quantified using the LI-COR Odyssey infrared imaging system. In summary, 18 HelaTRex single clones stably transfected with the targeting construct and 9 single clones stably transfected with the missense construct were tested (for further data please see protocols of 2009 and 2010 regarding this study). Additionally, HelaTRex cells stably transfected with an empty vector construct, served as negative control.
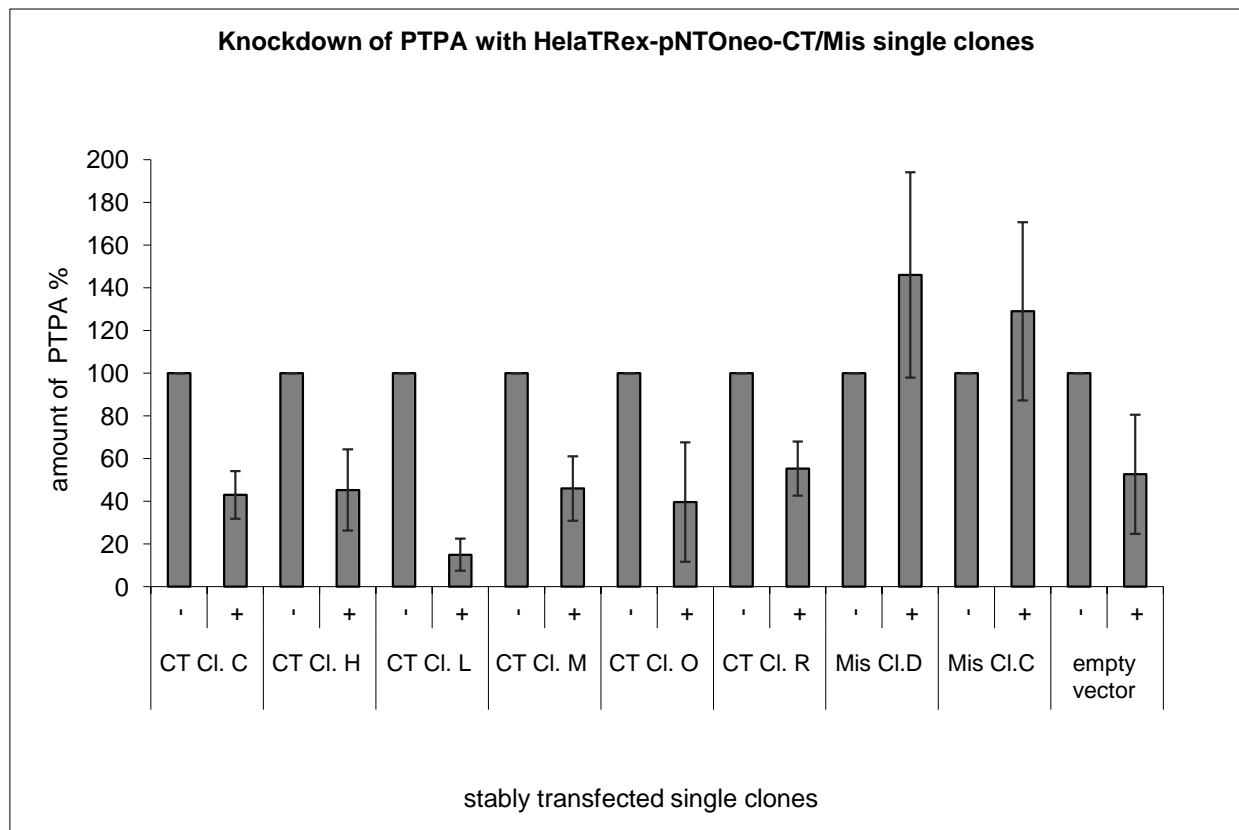
Figure 6: Summary of stably transfected HelaTRex-pNTOneo-CT/Mis single clones. HelaTRex-pNTOneo-CT and Mis cells were induced for 96 hours with 1µg/ml of doxycycline added every 24 hours and uninduced samples were taken as negative control. Whole cell lysates were prepared. 50µg were used for immunoblotting (10% SDS-PAG) with anti-gapdh (1:40.000) and anti-β-tubulin (1:10.000) antibodies, while 150µg were used for immunoblotting (10% SDS-PAG) with anti-PTPA-antibody (132/10; 1:10.000). Amounts of PTPA of induced samples (+) were normalized to the gapdh and β-tubulin levels, respectively, and uninduced samples (-) were set as 100%. Obtained results (representing a triplicate of induction) were quantified with the Li-Cor Odyssey imaging system and were included only if the quantification was in the linear range of detection. CT = shRNA against C-terminal part of PTPA, targeting construct; Mis = mismatch construct, non-targeting control; Cl. = Clone. Figure adapted from my Vertiefungsübungsprotokoll, 2010.

One single clone, expressing the targeting RNAi, HelaTRex-pNTOneo-CT Cl.L, achieved a knock down to approximately 15% of total amount of PTPA. Surprisingly, HelaTRex-pNTOneo-Mis Cl. D and HelaTRex-pNTOneo-Mis Cl. C, expressing a missense sequence upon induction with doxycycline, revealed an upregulation of PTPA rather than remaining the amount on a constant level, while the negative control, cells stable transfected with an empty vector, showed a downregulation to 52% of PTPA in comparison to uninduced cells.

Due to the efficient potential to knock down PTPA, HelaTRex-pNTOneo-CT Cl.L, a single clone expressing a PTPA targeting sequence, represented the most promising candidate for further investigations.

3.1.2. Proliferation assay with HelaTRex-pNTOneo-CT Clone L and HelaTRex-pNTOneo-Mis Clone C

Due to the fact, that a low amount of PTPA was unable to kill cells, we hypothesized that a reduction of PTPA levels could have an impact on the proliferation of mammalian cells. HelaTRex-pNTOneo-CT Clone L and Mis Clone C cells were induced with doxycycline and counted each day before lysis. Subsequently, lysates were analysed by western blotting and PTPA expression quantified with the LI-COR Odyssey imaging system. We wanted to test whether there would be a correlation between cell number and amount of PTPA level.

The cells transfected with the empty vector showed no difference in proliferation between induced and uninduced state, although a reduction to 68% of PTPA was calculated on day 5 in induced cells in comparison to uninduced cells (figure 7A and D). Furthermore, HelaTRex-pNTOneo-Mis Clone C cells revealed a slightly altered proliferation upon induction with doxycycline at days 3 and 4 in comparison to uninduced cells (figure 7C). This effect could be caused by a difference in cell number previous to the induction, as all whole cell lysates and cell counts were prepared separately for each day. Moreover, induced HelaTRex-pNTOneo-Mis Cl. C cells contained 96% of normal PTPA level.

HelaTRex cells containing the vector expressing the targeting RNAi, appeared to be hampered in proliferation on day two, but recovered quickly and showed normal proliferation and doubling time starting at day three (figure 7B). Finally, induced HelaTRex-pNTOneo-CT Cl.L cells, revealed a knock down to 8% of cellular PTPA in comparison to uninduced sample.

However, the minimum and maximum standards for the definition of the linear range for the quantification were inaccurate. Thus, the exact calculation of downregulated PTPA could vary. Furthermore, the proliferation assay was performed one time and has to be repeated at least two more times in order to have a definite result.
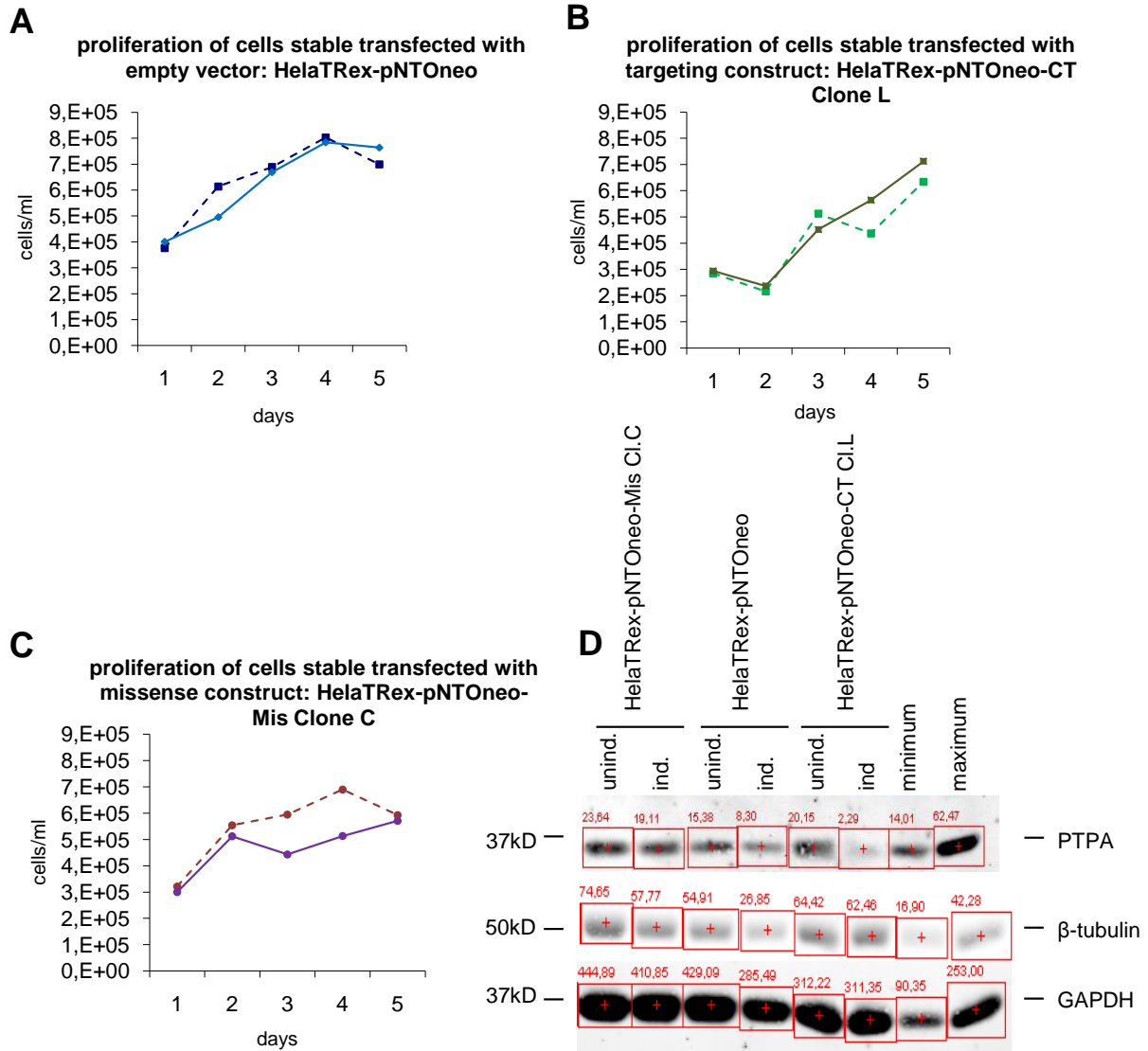
Figure 7: Proliferation growth curves. A-C) HelaTRex-pNTOneo-CT Cl.L, -**Mis Cl.C** and **cells transfected with emtpy vector** (see 2.1.7. for cell numbers) were induced for 120 hours with 1µg/ml of doxycycline added every 24 hours, uninduced cells of each clone were taken as negative control. Cells were counted every day. Dashed and solid lines represent uninduced and induced sample, respectively. **D)** Whole cell lysates of day 5 were analysed by western blotting (10%SDS-PAG). 50µg was used for immunoblotting (10% SDS-PAG) with anti-gapdh (1:40.000) and anti-β-tubulin (1:10.000) antibodies, while 150µg was used for immunoblotting (10% SDS-PAG) with anti-PTPA-antibody (132/10; 1:10.000). Amounts of PTPA of induced samples (+) were normalized to the gapdh and β-tubulin levels, respectively, and uninduced samples (-) were set as 100%. Obtained results (representing a single experiment) were quantified with the Li-Cor Odyssey imaging system. Minimum (80µg and 30µg for PTPA and for loading controls, respectively) and maximum protein standards (240µg and 90µg for PTPA and for loading controls, respectively) were used for the definition of a linear range. CT = shRNA against C-terminal part of PTPA, targeting construct; Mis = mismatch construct, non-targeting control; Cl. = Clone.

3.1.3. Nocodazole assay with HelaTRex-pNTOneo-CT Clone L

RRDΔ mutants were demonstrated to be hypersensitive to nocodazole and reveal inappropriate mitotic spindle formation, without showing a G2 arrest. Thus, a function in mitotic spindle formation was proposed [Van Hoof et al., 2001].

Nocodazole is a drug interfering with the polymerization of microtubules and prevents cells to form metaphase spindles [Nüsse et al., 1984]. As microtubules cannot attach to kinetochores, the spindle checkpoint gets activated and cells arrest in prometaphase. Furthermore, synchronized cells can be analysed via flow cytometer. The Nocodazole assay was performed, to investigate whether a reduced amount of PTPA would affect the spindle assembly checkpoint arrest.

1×10^6 HelaTRex-pNTOneo-CT Cl.L cells were seeded and induced for 96 hours with 1µg/ml of doxycycline. After 75 hours of doxycycline induction, 0.5µg/ml of Nocodazole was used to arrest the cells for 20 hours [Yeong et al., 2003]. After 20 hours of Nocodazole arrest, cells were divided into two fractions: Whereas one fraction was taken for the preparation of whole cell lysates, the second fraction was stained with propidium iodide, which intercalates in the DNA, and subsequently analysed by flow cytometry. Two gates were defined for the analysis of Hela-TRex-pNTOneo-CT Cl.L cells with flow cytometry (data not shown). The first gate was set as single cell gate, to exclude debris and aggregates. The second gate served to avoid doublets, which occur when two cells stuck together and cross the path of the laser beam at the same time.

No significant difference in the DNA histogram was observed between doxycycline induced and uninduced cells without treatment of Nocodazole (see figure 8.1.C and A, respectively). The cells residing in the logarithmic phase were proliferating, with most of the cells resided in G1 phase, represented by a clear G1 peak, followed by cells in S phase, doubling their DNA content, and finally, cells were observed to be in G2 phase, containing a double amount of DNA, indicated by the G2 peak.

Doxycycline induced and uninduced HelaTRex-pNTOneo-CT Cl.L cells treated with Nocodazole, respectively, revealed similar DNA histograms (figure 8.1.D and B, respectively). Obviously, the cell-arrest in the transition of G2/M phase was successful, as reflected by a higher number of cells residing in G2 phase. However, there was an increase of a small population of cells with DNA content below 2n, a sub G1 population, which can be characteristic for apoptotic cells or cells that pass over the spindle assembly checkpoint (figure 8.1.D). The additional peak prior to a value of 2n DNA content (FL2-A) occurred in cells treated with Nocodazole and

doxycycline (figure 8.1.D, peak indicated by red arrow). Finally, immunoblotting of whole cell lysates of the samples used in this assay (figure 8.1.E) showed a knock down of PTPA in cells induced for the expression of RNAi.

The 20 hour treatment of HelaTRex-pNTOneo-CT Cl.L cells was repeated without containing an sub G1 population. However, a major amount of cells of doxycycline induced cells was observed to reside in G1 phase (figure 8.2.B) in comparison to doxycycline uninduced cells (figure 8.2.A). Surprisingly, this effect turned out to be similar in doxycycline induced cells treated with Nocodazole for 30 hours (8.2.D) in comparison to doxycycline uninduced cells (figure 8.2.C).

In summary, it is still unclear, if cells with a reduced amount of PTPA succeed to emerge a spindle assembly checkpoint and start to proliferate again.
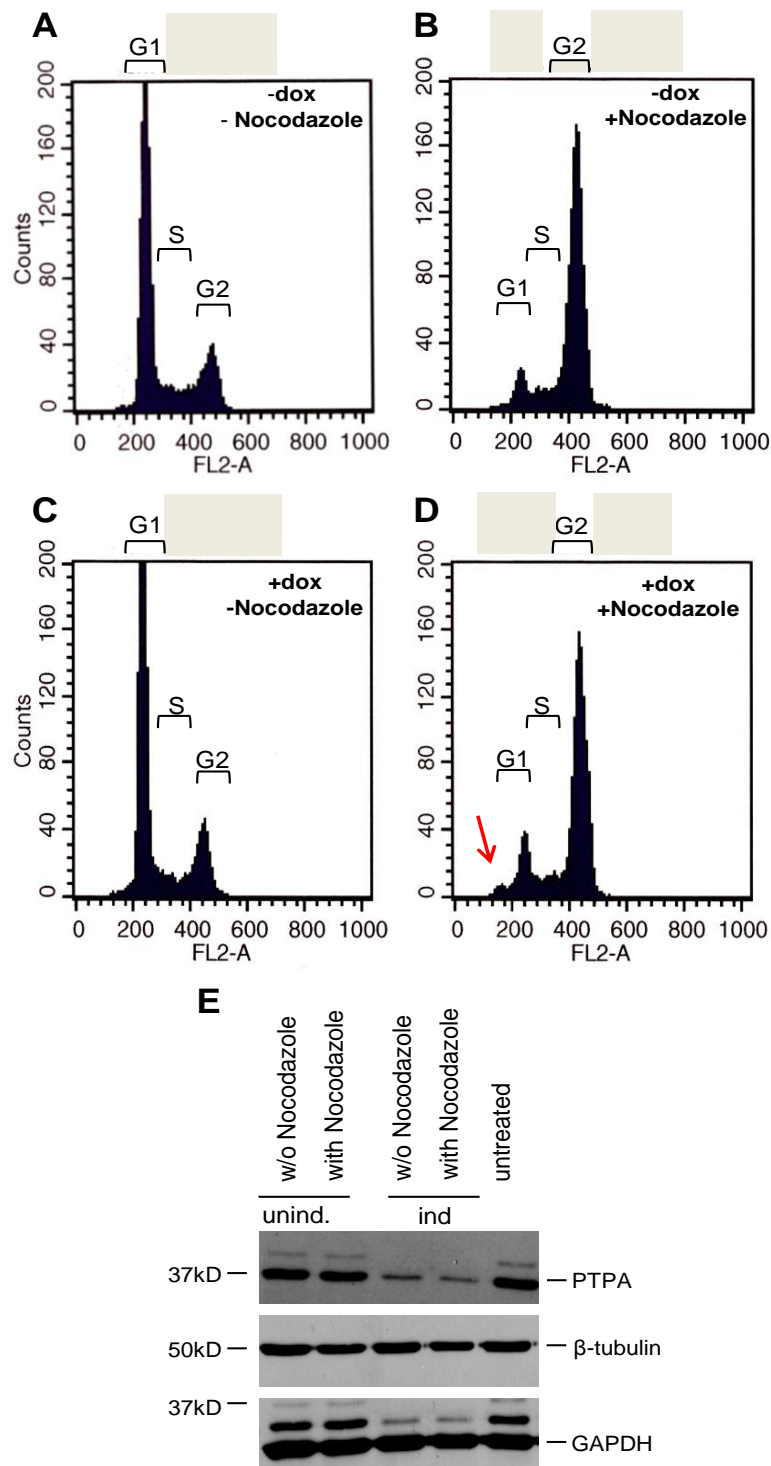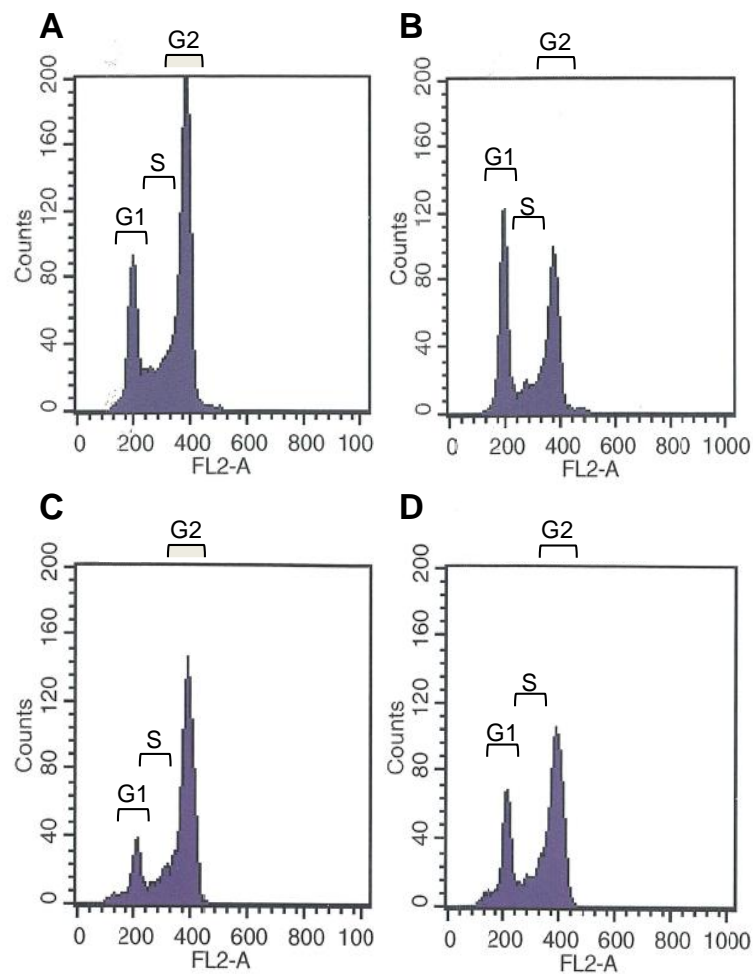
Figure 8.1.: Nocodazole treatment with induced and uninduced HelaTRex-pNTOneo-CT Cl.L. Cells were induced for 96 hours with 1µg/ml of doxycycline, added every 24 hours. Nocodazole treatment was performed with 0.5µg/ml for 20 hours, cells were stained with propidium iodide and analysis was performed with FACS Calibur[TM]. Untreated and uninduced HelaTRex-pNTOneo-CT Cl.L cells were utilized for gating and furthermore, cells were divided due to their size and granularity. 10.000 cells were analysed for each profile. PI labeling was detected in FL-2 channel. **A) – D)** represent DNA histograms of HelaTRex-pNTOneo-CT Cl. L cells without doxycycline and w/o and with Nocodazole, respectively (A, B)

and DNA histograms of doxycycline induced cells w/o and with Nocodazole, respectively (C, D). Red arrow depicts additional peak (D). **E)** Whole protein lysates were tested by western blot analysis (10%SDS-PAG). 30µg were used for immunoblotting with anti-gapdh (1:40.000), anti-β-tubulin (1:10.000) antibodies and anti-PTPA-antibody (1:1.000; 5G3). "Untreated" relates to a lysate of HelaTRex-pNTOneo-CT Cl.L without doxycycline or Nocodazole treatment and was taken as negative control. un-ind. = uninduced with doxycyline; ind. = induced with doxycyline.

Figure 8.2.: Nocodazole treatment with induced and uninduced HelaTRex-pNTOneo-CT Cl.L. Cells were induced for 96 hours with 1µg/ml of doxycycline, added every 24 hours. Nocodazole treatment was performed with 0.5µg/ml for 20 hours or 30 hours, **A-B** and **C-D** respectively. Cells were stained with propidium iodide and analysis was performed with FACS Calibur[TM]. Untreated and uninduced HelaTRex-pNTOneo-CT Cl.L cells were utilized for gating and furthermore, cells were divided due to their size and granularity. 10.000 cells were analysed for each profile. PI labeling was detected in FL-2 channel. **A) and B)** represent DNA histograms of doxycycline uninduced (A) and induced (B) HelaTRex-pNTOneo-CT Cl. L cells, respectively, with 20 hours treatment of Nocodazole. **C) and D)** represent DNA histograms of doxycycline uninduced (C) and induced (D) HelaTRex-pNTOneo-CT Cl. L cells, respectively, with 30 hours treatment of Nocodazole.

3.1.4. Evaluation of the stable knockdown of PTPA by qRT-PCR

The knockdown of cellular PTPA with stably transfected HelaTRex-pNTOneo-CT/Mis cells has been quantified on protein level by using the LI-COR Odyssey imaging scanner. A knock down to a minimum of 15% +/- 7.5% of cellular PTPA was achieved in the clone HelaTRex-pNTOneo-CT Cl. L expressing a targeting RNAi (see above). Due to the fact, that such a low level of PTPA did not cause phenotypical effects in terms of proliferation or spindle assembly checkpoint (see above), a qRT-PCR was set up, to allow additional quantification on the mRNA level. By this approach we aimed to address two questions: The determination of the effect of the targeting shRNA on downregulation of the mRNA for PTPA isoforms and the correlation of downregulated protein and mRNA amounts to check the knock down efficiency. We speculated about the presence of a compensating mechanism, by which a PTPA isoform that might not have been affected by the chosen shRNA targeting sequence could have taken over the role of the mainly expressed isoform, PTPAα. The shRNA targets exon 10 in the conserved C-terminal part of PTPA mRNA and would affect most of the published PTPA isoforms. Janssens and co-workers showed the presence of 7 main isoforms with 2 of them lacking exon 3 and all of them containing exons 5 to 8. However, 27 protein coding isoforms were published on ensembl.org with 15 PTPA isoforms lacking exons 3 and 4 and only 14 PTPA isoforms containing exon 5. Therefore, two primerpairs for human PTPA were designed (Beacon Designer^{TM} program) spanning exon 3 to exon 4 (primerpair 1), leading to a product of 210bp, and exon 5 to exon 8 (primerpair 2), leading to a product of 270bp.

Prior to analysis of the PTPA mRNA isolated from the doxycycline induced samples, a gradient PCR was carried out with temperatures ranging from 55°C to 65°C, in order to find the optimal temperature for both primers regarding their specificity (please see section 2.5.4. for details), which turned out to be at 58°C. HelaTRex cells, taken as negative control, and HelaTRex-pNTOneo-CT Cl.L cells, were induced for 96hours with 1µg/ml of doxycycline. Subsequently, RNA was isolated and reverse transcribed into cDNA (see 2.5.2. and 2.5.3.). Furthermore, a dilution series with RNA isolated from Hela cells was prepared (see 2.5.5.) in order to obtain a standard curve defining the linear range. Values of the samples were extrapolated from the standard curve. To ensure accurate results, every sample was analysed twice and normalized to the PCR product of human GAPDH. Relative differences of mRNA abundance are presented in figure 9.
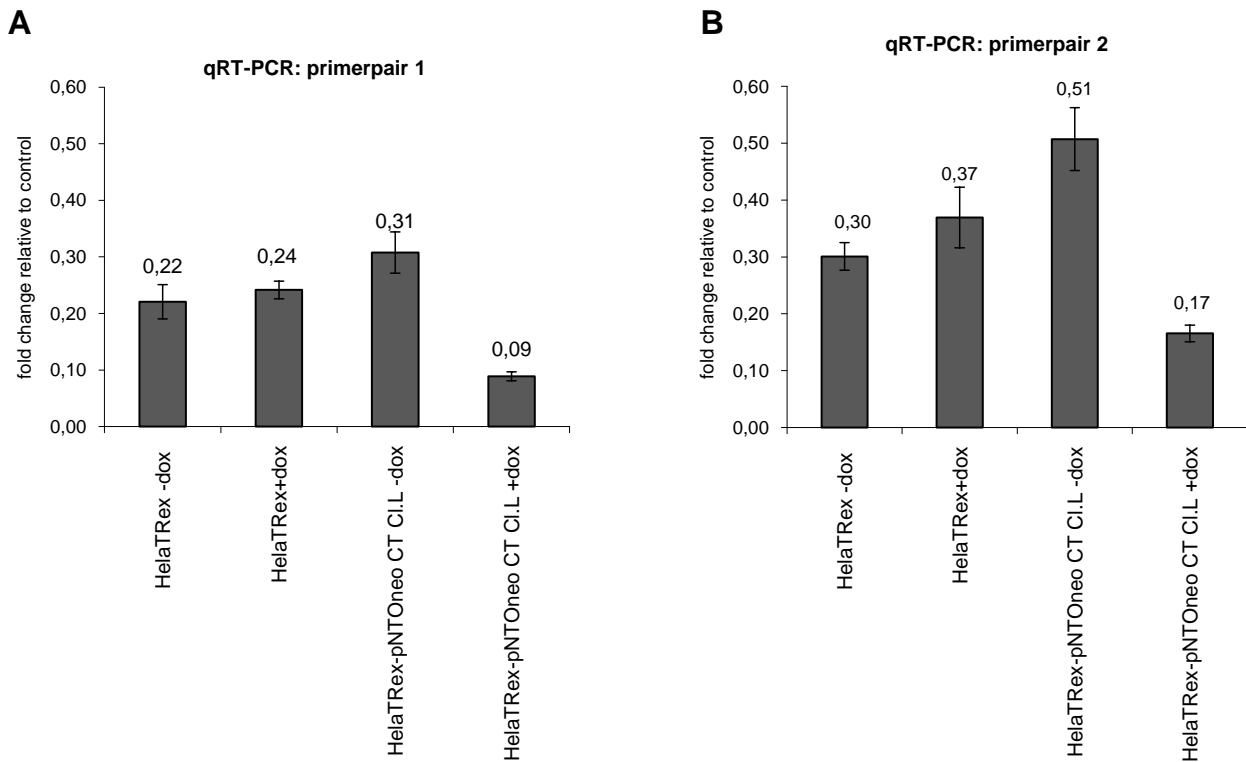
Figure 9: qRT-PCR of stably transfected single clones with two primerpairs. Cells were induced for 96 hours with 1μg/ml of doxycycline, added every 24 hours, and analysed via qRT-PCR. 50μg of Hela cDNA served as standard for a dilution series (1:1, 1:2, 1:4, 1:8, 1:16) to construct the standard curve. Results represent samples normalized onto GAPDH as housekeeping gene control and were calculated as fold change relative to control. Standard deviation reveals double measurements of one experiment. **A)** and **B)** represent primerpair1 and 2. CT = C-terminal; Mis = missense construct; -/+ dox = uninduced and induced cells, respectively.

qPCR results obtained from mRNA of HelaTRex cells revealed no significant difference between doxycycline induced and non-induced samples. In contrast, the amount of PTPA mRNA (calculated as fold change relative to uninduced negative control) of doxycycline induced cells expressing the targeting RNAi, represented 29% with primerpair 1 in comparison to uninduced sample (figure 9 A). Further, doxycycline induced sample amplified with primerpair 2 revealed a downregulation to 40.9% in comparison to the respective uninduced sample (figure 9B). Remarkably, primerpair 2 spanning exon 5 to exon 8, generally led to a higher amount of mRNA when comparing the relative values.

To summarize, PTPA mRNA of knock down cells was still present. Although values gained with qRT-PCR describe relative rather than absolute levels of PTPA mRNA, a reduction to either 29% or 40.9%, depending on the primerpair, represented a higher amount, in comparison to

the PTPA protein values quantified with the LI-COR Odyssey scanning system. Second, qRT-PCR with primerpair 2, targeting the conserved C-terminal part of PTPA mRNA, resulted in higher values of PTPA mRNA in comparison to primerpair 1.

3.2. Knockdown of PTPA with siRNAs

Based on previous experiments, where a suppression of PTPA protein down to 15% did not cause phenotypic effects, we decided to further test the knock down of PTPA with siRNAs. Short hairpin RNAs and small interfering RNAs are intrinsically different molecules [Rao et al., 2009] and their mechanisms, off-target effects and interference pathways vary. Thus, we decided to design and evaluate the knockdown of PTPA using siRNA constructs in order to analyse whether this system would have a more striking effect, regarding PTPA levels.

To design siRNAs, we followed the guidelines summarized by Tuschl and coworkers [Tuschl et al., 2004]. The sequences of the siRNAs termed "siRNA-CT" and "siRNA-Mis", were identical with the previously used shRNAs, targeting the C-terminal part of PTPA and including three mismatches at position 4, 10 and 16, respectively. Furthermore, a second siRNA, named "siRNA-sigma", targeted exon 7 and 8 of human PTPA (see 2.5.6.1. for further details). Both siRNAs had a length of 21 nucleotides including two thymidines at the 3´end, and a GC content of approximately 50%. Possible off-target effects were checked in a homology BLAST with the help of an algorithm developed at Whitehead institute (http://jura.wi.mit.edu/bioc/siRNAext/) without identifying additonal targets.

3.2.1. Optimizing the transfection efficiency

In order to avoid problems with specificity due to the use of inappropriate amounts of transfection reagent or cell count, the transfection efficiency was optimized by adjusting cell number and concentration of transfection reagent.

Different amounts of Hela and HEKTRex cells were seeded on 24-well tissue culture plates and transfected with 0.8μg of pmax-GFP, a vector encoding the green fluorescent protein. 1μl, 1.5μl, 2μl and 2.5μl of transfection reagent, Lipofectamine 2000, were used. The day after transfection, cells were prepared for flow cytometric analysis with the FACS-Aria[TM] cell sorter (please see table of 2.5.7. for exact cell counts analysed).

99% of transfection efficiency was accomplished for the HEKTRex cell line, using 100.000 cells/well, 2μl Lipofectamine 2000 and 0.8μg plasmid on a 24-well tissue culture plate. Up to 60% of transfection efficiency was obtained with Hela cells at a density of 80.000 cells/well with either 1.5μl or 2μl Lipofectamine 2000 and 0.8μg plasmid. The parameters including cell density, transfection reagent and amount of plasmid for cotransfection were applied for all further transfections unless stated differently.

3.2.2. Evaluation of different amounts of siRNAs

Unlike shRNA, siRNA is delivered into the cytoplasm and rather unstable. Further, siRNA is more susceptible to degradation in the cytoplasm and high doses are required to achieve a knockdown of mRNA. Moreover, high amounts of siRNAs were correlated to cytotoxic and non-specific off-target effects. The application of low doses of potent siRNAs has been reported to efficiently reduce side-effects [Zhen Li et al., 2008]. Thus, evaluation of a suitable amount of siRNA for transfections represents a crucial part of any siRNA experiment.

As first transfections using 25pmol of siRNAs (data not shown) revealed an insufficient down-regulation of PTPA, 50pmol and 100pmol of siRNAs were applied (please see 2.5.6.1. for the amount of ng corresponding to pmol).

Hela and HEKTRex cells were seeded according to optimized transfection conditions (see 3.2.2.) and transfected transiently with either 50pmol/100pmol of siRNA-Mis, the mismatch control, 50pmol/100pmol of siRNA-CT, targeting the C-terminal part of PTPA, or 50pmol/100pmol of siRNA-sigma, targeting exon 7-8. Samples were analysed by western blotting, 48 hours post transfection, and PTPA levels were quantified with the LI-COR Odyssey system.
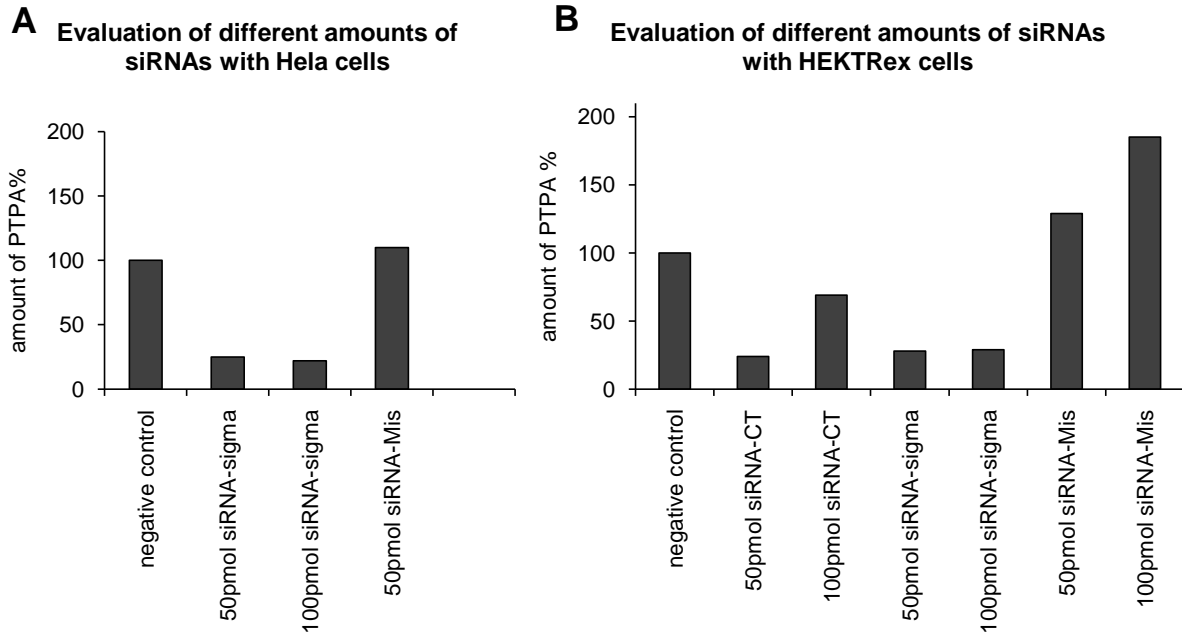
Figure 10: Evaluation of different amounts of siRNAs with Hela and HEKTRex cells. Hela and HEKTRex cells were transfected transiently for 48 hours with either 50pmol or 100pmol of different siR-NAs. Whole cell lysates were analysed by western blotting (10%SDS-PAG). 30µg of whole cell lysates was used for immunoblotting (10% SDS-PAG) with anti-gapdh (1:40.000), anti-β-tubulin (1:10.000) anti-bodies and anti-PTPA-antibody (132/10; 1:10.000). Amounts of PTPA were normalized onto gapdh and β-tubulin taken as loading controls and the negative control taken as 100%. Obtained results (representing single experiments) were quantified with the Li-COR Odyssey imaging system. Minimum (10µg) and maximum (60µg) protein standards were used for the definition of a linear range. CT = siRNA against C-terminal part of PTPA, targeting construct; Mis = mismatch siRNA, non-targeting control; Cl. = Clone; negative control = cells transfected solely with mastermix.

Transfection of 50pmol of siRNA-CT was most successful for a knock down of PTPA in HEK-TRex cells, as western blot analyses revealed a downregulation to one fourth of the PTPA levels in the control cells. 100pmol of siRNA-CT resulted in a knock down to approximately 75% of PTPA. No significant difference was observed between 50 and 100pmol of siRNA-sigma, as both were sufficient to knock down PTPA to 30%. Interestingly, an upregulation to either 125% or ~180% of PTPA was observed when using 50pmol or 100pmol of siRNA-Mis, respectively (see figure 10B). As 50pmol of siRNA-Mis implied less increase of PTPA, this amount was applied for further investigations. In contrast to the result of HEKTRex cells, both amounts of siRNA-sigma, 50pmol and 100pmol, efficiently reduced PTPA to 30% of its levels in Hela cells (figure 10A).

To summarize, 50pmol of siRNA-CT was used in further studies as a standard amount. Additionally, none of the transient transfections did cause killing of cells.

3.2.3. Evaluation of the knockdown of PTPA with siRNAs by qRT-PCR

Again, the knock down was evaluated using the complementary approach of quantifying the PTPA mRNA using qRT-PCR.

40.000 Hela cells were seeded in each well of a 6-well tissue culture plate and transfected with different amounts of siRNAs: 50pmol of siRNA-CT, 50pmol of siRNA-Mis, 50pmol of siRNA-sigma and a mixture of 25pmol of siRNA-CT and 25pmol of siRNA-sigma. 48 hours post transfection, RNA was isolated and reverse transcribed into cDNA. In this case, solely primerpair 2, spanning exon 5 to 8, was applied for amplification of mRNA. Again (see above), a dilution series with RNA isolated from Hela cells was prepared (see 2.5.5.) in order to obtain a standard curve defining the linear range. Values of the samples were extrapolated from the standard curve. Once more, every sample was analysed twice and normalized to the PCR product of human GAPDH, to ensure accurate results. Relative differences of mRNA abundance, correlated to each other, are presented in figure 11.

First of all, the quantification of PTPA mRNA in the negative control was affected by a large standard deviation, rendering the reliability of the results uncertain (figure 11). Nevertheless, amounts of mRNA were calculated as fold change relative to non-transfected negative control. Transfection with 50pmol of siRNA-CT or siRNA-sigma, showed a knock down to approximately one third of PTPA mRNA, while 50pmol of siRNA-Mis revealed a slight decrease to 80% of PTPA mRNA level. Finally, a combination of both targeting siRNAs, siRNA-CT and siRNA-sigma, sufficiently induced the degradation of PTPA mRNA down to 23% of the original amount.

To sum up, the levels quantified by the LI-COR Odyssey system on protein level and qRT-PCR on RNA level turned out to be similar.
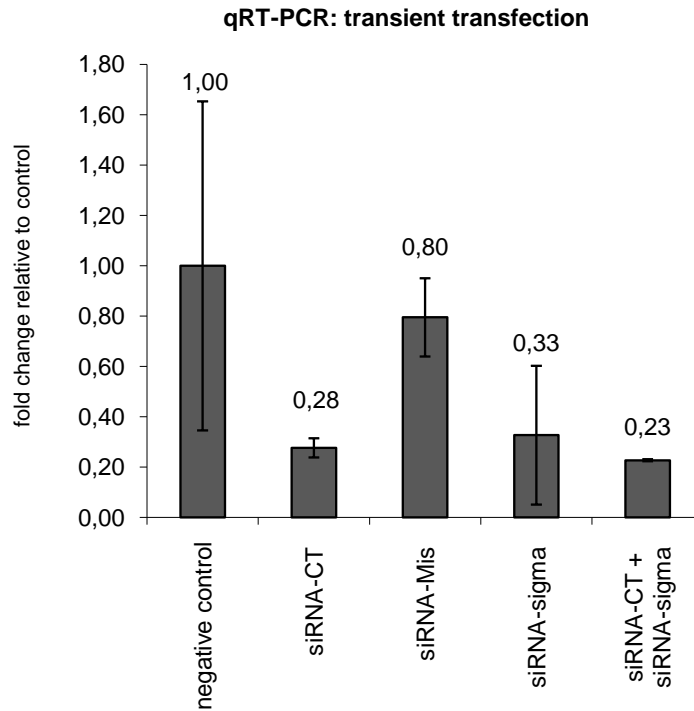
qRT-PCR: transient transfection

Figure 11: qRT-PCR of transient transfection. Hela cells were transfected for 48 hours with four different amounts of siRNAs: 50pmol siRNA-CT, 50pmol siRNA-Mis, 50pmol siRNA-sigma, 25pmol siRNA-CT + 25pmol siRNA-sigma. Mastermix of transfection served as negative control. Samples were analysed by qRT-PCR. 50µg of Hela cDNA served as standard for a dilution series (1:1, 1:2, 1:4, 1:8, 1:16) to construct the standard curve. Results represent samples normalized onto GAPDH as housekeeping gene control and were calculated as fold change relative to control. Standard deviation reveals double measurements of one experiment. CT = C-terminal; Mis = missense construct; sigma = prevalidated siRNA.

3.3. Combination of siRNA snd shRNA to suppress PTPA in Hela cells

Suppression of PTPA to 15%, achieved either by shRNA or siRNA, did not have obvious effects on cell proliferation or survival. Therefore, we hypothesized that a combination of both methods might further decrease PTPA levels. Thus, HelaTRex-pNTOneo-CT Cl.L and HEK-TRex-pNTOneo-CT Cl.8 cells were analysed for the capability to knock down PTPA to an even lower level than achieved by each method alone (see diploma thesis of Michaela Kugler for description of HEKTRex-pNTOneo-CT Cl.8).

1×10^6 HelaTRex-pNTOneo-CT Cl.L cells and HEKTRex-pNTOneo-CT Cl.8 cells (described and validated in diploma thesis of Michaela Kugler) were seeded and induced with 1µg/ml of doxycycline for 96 hours. After 96 hours, cells were transfected (for details see 2.5.6.) with dif-

ferent amounts of siRNAs: 50pmol of siRNA-CT, siRNA-sigma, siRNA-Mis and a combination of 25pmol of siRNA-CT and siRNA-sigma, respectively. After 48 hours, whole cell lysates were prepared and analysed.

HEKTRex-pNTOneo-CT Cl.8 cells, induced with doxycycline, revealed a knockdown to 72% of PTPA, if transiently transfected with siRNA-CT. A downregulation to 41% of PTPA protein was achieved, if transfected with siRNA-sigma. An upregulation to 180% of PTPA protein was obtained with siRNA-Mis, the missense control. Finally, a knockdown to 20% of total amount of PTPA was achieved, if transiently transfected with a combination of both siRNAs (figure 12A). These results were obtained after normalization of values to the PTPA level of transfection control cells. If normalized to the PTPA levels in doxycycline uninduced cells (negative control), doxycycline induced HEKTRex-pNTOneo-CT Cl.8 cells revealed a downregulation to 22% of PTPA protein if transfected with siRNA-CT, 16% with siRNA-sigma, 39% with siRNA-Mis and 9% if transfected with a combination of siRNA-CT and siRNA-sigma.

Due to a mistake, it was not possible to normalize values of HelaTRex-pNTOneo-CT Cl.L cells to an uninduced negative control. So, reduced amounts of PTPA were normalized to the transfection control only, represented by the value of a doxycycline induced sample incubated with transfection reagents. Doxycycline induced HelaTRex-pNTOneo-CT Cl.L cells exhibited a knockdown to 35% of PTPA protein with siRNA-CT, 40% with siRNA-sigma, 127% with siRNA-Mis and 40% with the combination of both targeting siRNAs (figure 12 B).
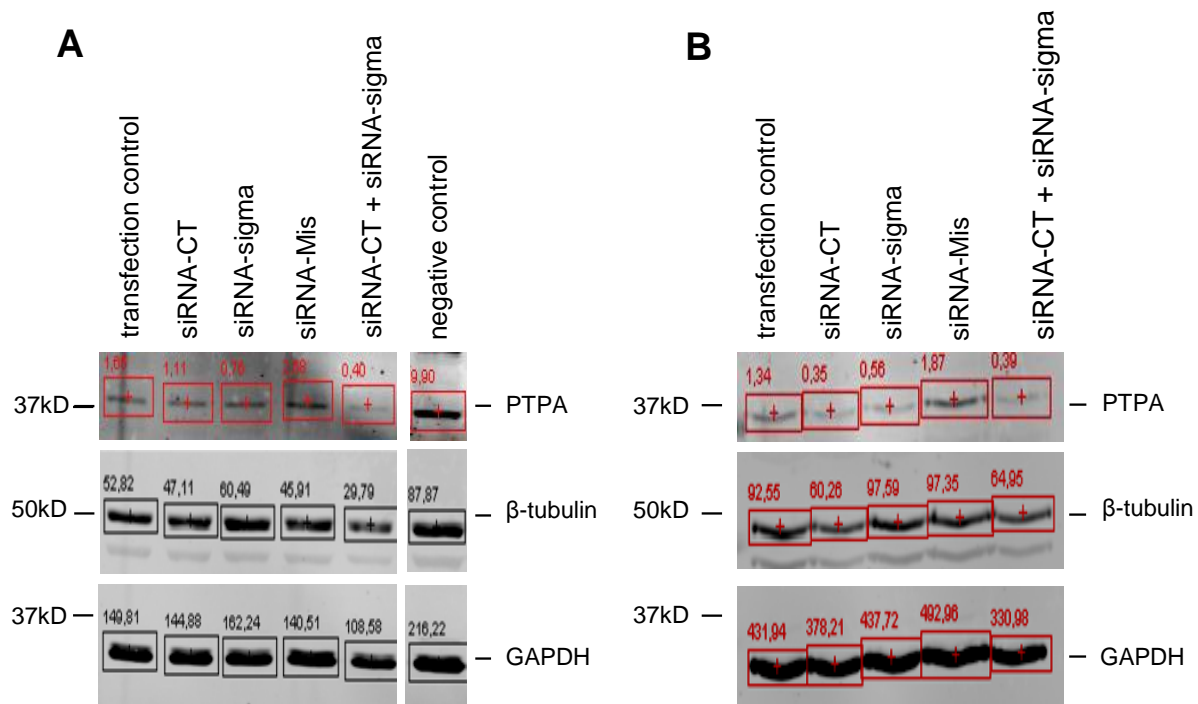
Figure 12: Combination of siRNA and shRNA suppression of PTPA in HelaTRex-pNTOneo-CT Cl.L and HEKTRex-pNTOneo-CT Cl.8 cells. Cells were induced for 96 hours with 1µg/ml of doxycycline, added every 24 hours, transiently transfected and incubated for another 48 hours without additional induction of doxycycline. Whole cell lysates were prepared and tested by western blot analysis (10% SDS-PAG). PTPA levels were quantified with a LI-COR Odyssey imaging system. 30µg were taken for immunoblotting with anti-gapdh (1:40.000), anti-β-tubulin (1:10.000) and anti-PTPA antibod (5G3, 1:1000). **A) Induced HEKTRex-pNTOneo-CT Cl.8 cells.** Amounts of PTPA were first normalized onto GAPDH and β-tubulin as loading controls. Then, values were normalized to the "negative control", related to the PTPA amount in negative control cells, or to the transfection control. **B) Induced HelaTRex-pNTOneo-CT Cl.L cells.** Amounts of PTPA were first normalized onto GAPDH, β-tubulin as loading controls. Then, values were normalized to the "transfection control", representing a cell lysate of induced sample transfected with mastermix solely. CT = RNAi sequence against C-terminal part of PTPA; Mis = mismatch construct; sigma = prevalidated siRNA; Cl. = Clone; transfection control = induced sample transfected with mastermix.

Although the application of siRNA-CT in HelaTRex-pNTOneo-CT Cl.L cells revealed a knockdown to 35%, the residing amount of protein was representative for already reduced protein levels due to the lack of a negative control for normalization. Thus, a significant interpretation of these data was not possible. Furthermore, a combination of both targeting siRNAs turned out to be most effective in terms of knocking down PTPA in induced HEKTRex cells, with a reduction to 9% in comparison to uninduced cells. Regardless of the use of RNAi, there was still an

amount of at least 9% of PTPA protein present. That low amount did not affect cell viability so far.

3.4. Knockdown of PTPA by retroviral infection

So far, the combination of shRNA and siRNA against PTPA suppressed PTPA levels to 9% in comparison to untreated samples. As this low level seemed to be sufficient for the function of PTPA, I speculated whether the long half-life of PTPA [Donehower et al., 1992] or a low threshold level could be responsible for rendering cellular functions intact. Therefore, we hypothesized, that a retroviral vector, pRetroSuper$_{Stuffer}$, constitutively expressing a RNAi targeting sequence for the mRNA of PTPA, could downregulate PTPA more efficiently below an amount of 9%. The RNAi expression of pRetroSuper$_{Stuffer}$ was under control of a polymerase III dependent H1-promoter and the shRNA sequence was identical to "siRNA-CT". Additionally, a puromycin resistance gene served as a marker for selection of infected cells and a specially designed 3′LTR with a deletion of the LTR promoter facilitated the inactivation the LTR mediated transcription upon integration. Finally, an ampicillin resistance allowed propagation of the plasmid in *E. coli*.

Further, pRetroSuper$_{Stuffer}$-CT Clone 3 and pRetroSuper$_{Stuffer}$-Mis Clone 2 were chosen for the production of retroviral contamining supernatants, which were used for subsequent infections of NIH3T3 cells. NIH3T3 cells were selected with 5μg/ml puromycin, to avoid untransfected cells. Finally, samples were analysed by western blotting three days in a row post infection.
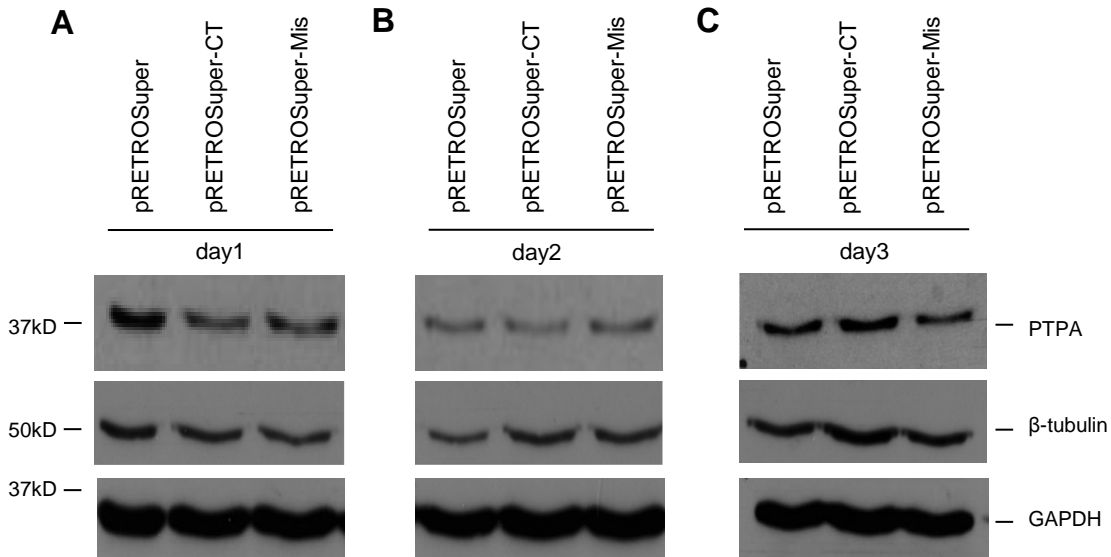
Figure 13: Retroviral Infection of mouse fibroblast cells for 3 days. NIH3T3 cells were selected with 5µg/ml puromycin for infection with either pRetroSuper$_{Stuffer}$-CT, containing a targeting shRNA against mRNA of PTPA, pRetroSuper$_{Stuffer}$-Mis, containing a shRNA uncapable of binding to the mRNA, or emtpy vector control, pRetroSuper$_{Stuffer}$. 30µg of whole cell lysates were analysed by immunoblotting (10%SDS-PAG) with anti-PTPA-antibody (5G3, 1:1000), anti- β-tubulin (1:10.000) and anti-gapdh (1:40.000). **A), B)** and **C)**, refer to **day 1**, **day 2** and **day 3** post infections, respectively. CT = shRNA against C-terminal part of PTPA, targeting construct; Mis = mismatch construct, non-targeting control.

Although a slight reduction of PTPA could be observed at day 1 post infection with pRetroSuper$_{Stuffer}$-CT (figure 13A), no significant knock down of PTPA could be visualized at day 2 or 3 post infections (figure 13B and C). Therefore, the infection with retroviral contaming supernatant of NIH3T3 cells was repeated but did not reveal an effect on the level of PTPA again (data not shown). The RNAi sequence is fully complementary between mouse and human. Thus, the infection was repeated with Hela cells stably transfected with the pWZL vector, constitutively expressing an ecotropic murine retroviral receptor and furthermore allowing for an infection with murine specific retroviruses (data not shown). A significant knock down of PTPA was achieved neither in NIH3T3 cells nor in Hela-pWZL cells. Hence, a vector backbone mutation could be held responsible, as the shRNA sequences of the vector were verified through sequencing.

3.5. First steps of cloning a conditional knock-out vector targeting PTPA

RRD1/RRD2, the PTPA homologues in yeast, were shown to fulfill essential functions in yeast. In this study, the results of knockdown experiments revealed, that ~10% of PTPA were sufficient for PTPAs function. In order to find out about PTPAs function, we aimed to delete the PTPA gene in a loss-of-function approach and started the design of a conditional knock-out vector targeting PTPA in mouse in collaboration with Arabella Meixner ("Stem Cell Centre – Mouse Gene Targeting", IMBA, Vienna). A conditional knock-out vector can be used to generate both, null and conditional alleles of a gene, using the Cre/LoxP and Flp/FRT recombinase system [Adams and Weyden, 2008]. As such, a vector could inactivate PTPA in the germline or in certain tissues, it represents an elegant model to elucidate PTPA´s function.

First, the length of homology arms, critically affecting targeting frequency [Hasty et al 1991], and selection of targeted exon was the matter of debate. Due to the fact, that all isoforms related to PTPA are expressed from the same promoter [Janssens 1999], we decided to target N-terminal exon 2 and exon 3 and thereupon inhibit the production of all isoforms. Furthermore, site-specific recombinase target sites including Flp/FRT and Cre/loxP were planned to flank the DNA sequence. The target would then be cre- excisable and the resistance marker gene, used for selection of ES cells, could be removed.

3.5.1. Verifying BAC-clones

In order to construct the targeting vector, a bacterial artificial chromosome (BAC), containing the PTPA gene, had to be used. Three such clones were obtained and had to be checked by PCR for the presence of the PTPA gene: RP23431 H3, RP24339 D2 and RP23165L 19.

The DNA of two BAC-type clones was isolated and checked by PCR (for further details please see 2.4.4. and 2.4.5.). The correct PCR product, containing 676bp, was determined for two BAC-clones, RP23431 H3 #4 and RP24339 D2 #4 (figure 14, positive samples are marked in red). Subsequently, both were used for electroporation into EL350 bacteria.
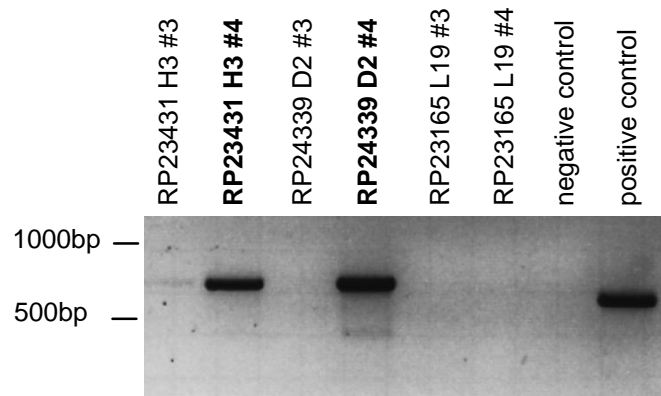
Figure 14: Verifying BAC-clones. DNA of three BAC-clones, RP23431 H3, RP24339 D2 and RP23165L 19, was isolated and checked by PCR to confirm the identity whether they contain the PTPA gene. Samples were analysed on a 1.8% agarose gel which was run for 40 minutes. The positive control gave a product with a size of ~700bp. Samples positive for PTPA gene are marked in red. Negative control = PCR mastermix without template; positive control = Rosa 26 (kindly provided by Stefan Schüchner)

3.5.2. Electroporation of BAC-clone and EL350

After identifying the BAC-clone containing the PTPA gene, I tried to electroporate the BAC-clone into EL350 bacteria, which are capable of Red homologous recombination and Cre/loxP mediated recombination due to a temperature shift up to 37°C [Lee at al., 2001].

Different amounts of BAC-DNA were chosen for the electroporation. I used 100ng/500ng/1000ng or 200ng/500ng/1000ng of DNA preparation of BAC-clone RP24339 D2 #4 and selected with 15µg/ml or 7.5µg/ml of Chloramphenicol after electroporation, repspectively. Furthermore, I used 200ng/500ng/1000ng of DNA preparation of BAC-clone RP23431 H3 #4 and selected again with either 15µg/ml or 7.5µg/ml of Chloramphenicol (for details please see 2.3.6.). 100ng or 200ng of pSuper vector served as electroporation control. The electroporation was carried out three times with a Bio-Rad Gene Pulser® at 2.5kV, 200Ω and 25µF and freshly prepared competent cells (see 2.3.6.). However, none of the attempts including BAC-DNA turned out to be successful, although the electroporation with pSuper vector control worked out each time.

3.6. Subcellular localization of PTPA

So far, knockdown experiments with siRNA or shRNA revealed a PTPA level of 10% without hampered proliferation or affected cell viability. Michaela Kugler found signs of apoptosis in transiently transfected Hela, U2OS, SW480 and N2A cells due to the knockdown of PTPA (see diploma thesis of Michaela Kugler for details), no precise conclusions could be drawn, as a PTPA specific antibody, which would work in immunofluorescence, was missing. Therefore, we aimed to identify the PTPA levels in Hela cells transiently transfected with shRNA and determine whether low amounts of PTPA would correlate with apoptosis induction.

Additionally, Azam and coworkers proposed a mainly nuclear localization of PTPA [Azam et al., 2007]. These authors overexpressed a PTPA-GFP fusion protein in HCT116 cells and primarily found a nuclear distribution. They assumed the cytoplasmic occurrence to be a consequence of the overexpression. As this study was based solely on overexpression, we aimed to identify the subcellular localization of PTPA with the advantage of a new antibody specific for PTPA.

3.6.1. Subcellular localization of PTPA via fractionation

As a second method to determine the subcellular localization of PTPA, we applied subcellular fractionation, which works with a separation of nucleus and cytoplasm [Roblek et al., 2010, Rosner and Hengstschläger, 2008] (for details see 2.2.12.).
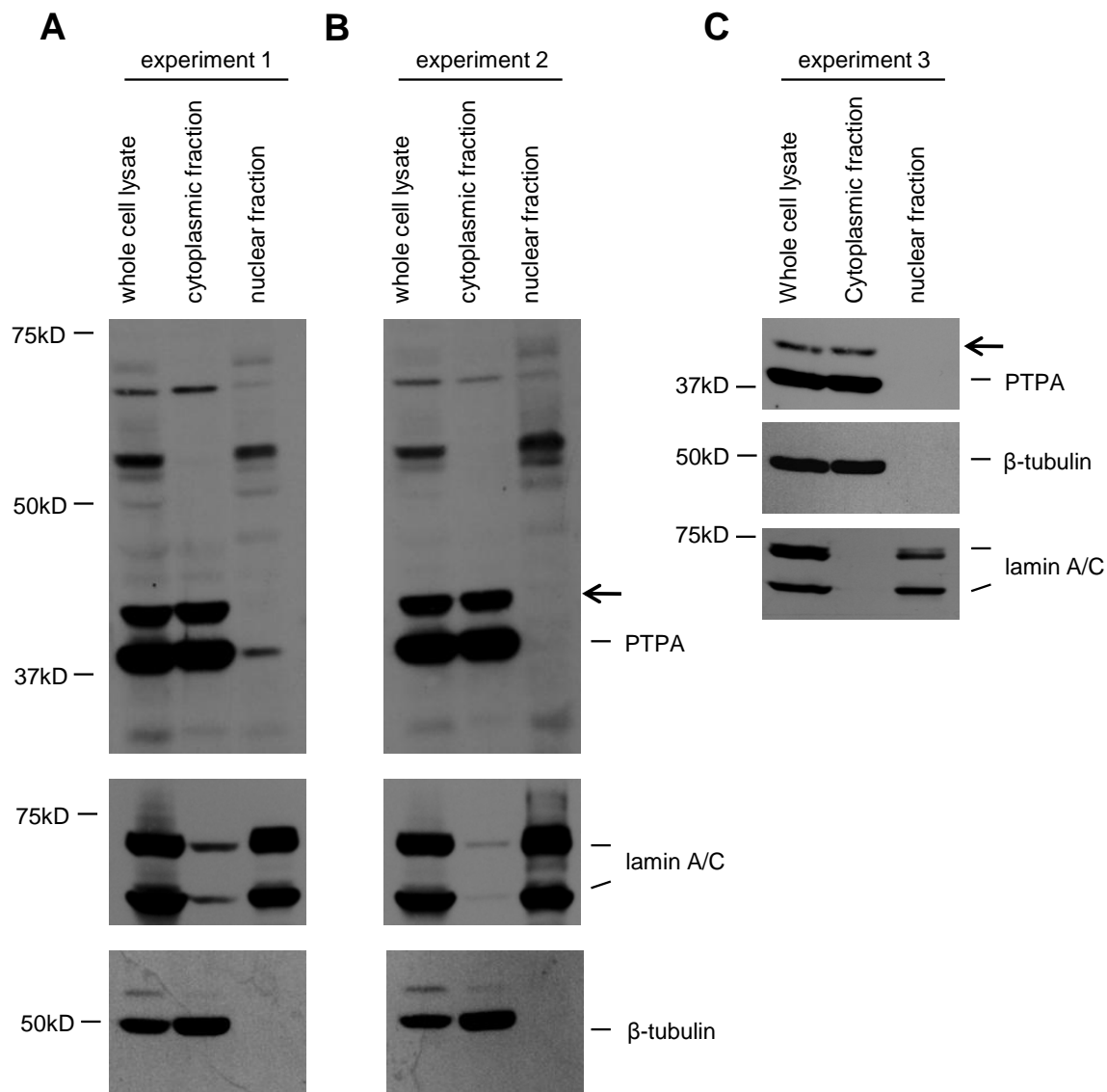
Figure 15: Subcellular localization of PTPA in Hela cells. Hela cells were fractionated into a cytoplasmic and nuclear fraction by centrifugation. Subsequently, lysates of each fraction were tested by western blot analysis (10% SDS-PAG) with each lane containing the lysates from 100.000 cells. Immunoblotting was performed with anti-lamin A/C (4C11; 1:1000) and anti-β-tubulin (1:10.000), with Lamin A/C and β-tubulin serving as nuclear and cytoplasmic marker, respectively. PTPA was detected with anti-PTPA antibody (5G3; 1:1000). All panels, **A)**, **B) and C)** represent independent fractionation experiments. Arrows indicats an additional band above PTPA.

Hela cell lysates were subdivided into three fractions: whole cell lysate, cytoplasmic and nuclear fraction and analysed by immunoblotting with monoclonal anti-PTPA antibody (5G3) and monoclonal anti-β-tubulin and anti-lamin A/C antibodies, as markers for cytoplasm and nucleus, respectively [Roblek et al., 2010, Thyberg and Moskalewski, 1985].

Immunoblotting with anti-lamin A/C antibody revealed two strong bands occurring at 69kDa and 62kDa, representing Lamin A and C (figure 15A-C). Furthermore, anti-β-tubulin antibody recognized β-tubulin in the cytoplasmic fractions (figure 15A and B, lower part of both panels). PTPA was detectable mainly in the cytoplasmic fraction of Hela cells with a molecluar weight of approximately 38kDa (figure 15A-c). A weak signal was detectable in the nuclear fraction once (figure 15A). Since a signal of anti-lamin A/C antibody was detectable as well in the cytoplasmic fraction, the fractionation seemed not to be as pure as intended. Therefore, the subcellular fractionation was repeated and revealed a specific signal for PTPA occurring in the cytoplasmic fraction (figure 15C). In this case, a clear distinction was obvious, with signals of anti-lamin A/C and anti-β-tubulin antibody referring to the nuclear fraction and cytoplasmic fraction solely. However, the exposure times of immunoblots shown in figure 15 varied. The results of experiments 1 and 2 represent an exposure time of 20 minutes in case of incubation with anti-lamin A/C antibody, while the result of incubation with anti-lamin A/C antibody of experiment 3 depicts a 5 minute exposure.

Interestingly, additional bands with a molecular weight of 42kDa occurred above the signal of PTPA (figure 15, additional band indicated by red arrow). To investigate, if the additional band could represent a phosphorylated species of PTPA, further experiments were necessary (see below).

3.6.2. Identification of potential phosphorylation of PTPA

To determine, if the additional band migrating above the PTPA specific signal in SDS-PAG (see above) could represent a phosphorylated species of PTPA, further analyses were carried out. Calf Intestinal Alkaline Phosphatase (CIP) was used for the removal of potential phosphorylation [e.g. Wang et al., 1993]. To further investigate the possibility of the occurrence of additional bands in further cell lines, NIH3T3, HEKTRex, HelaTRex and Hela cells were included in the assay. Finally, anti-EAPP (E2F associated phospho protein) antibody (kindly provided by Peter Andorfer) served as positive control for the phosphatase treatment, since EAPP was shown to shift in migration behaviour upon treatment with CIP due to the removal of phosphorylation [Novy et al., 2005].

100μg of whole cell lysates of the indicated cell lines were incubated with 5000 Units of CIP and analysed by western blot and immunoblotting with anti-PTPA antibody (5G3), anti-EAPP antibody and anti-β-tubulin and anti-GAPDH antibody as loading controls.

First of all, the signal referring to EAPP, appearing at ~36kDa, represented a double band in samples untreated with the phosphatase. Upon CIP treatment the upper EAPP band disappeared (figure 16A). Interestingly, the additional band above PTPA (figure 16A, indicated by red arrow) occurred in all samples, with and without incubation of CIP, except NIH3T3 lysates. Moreover, the amount of slower migrating species is less in HEKTRex cells compared to Hela cells. Further controls, whole cell lysates of Hela cells with and without buffer, were included in the second experiment and did not exhibit any difference between control samples (figure 16B).
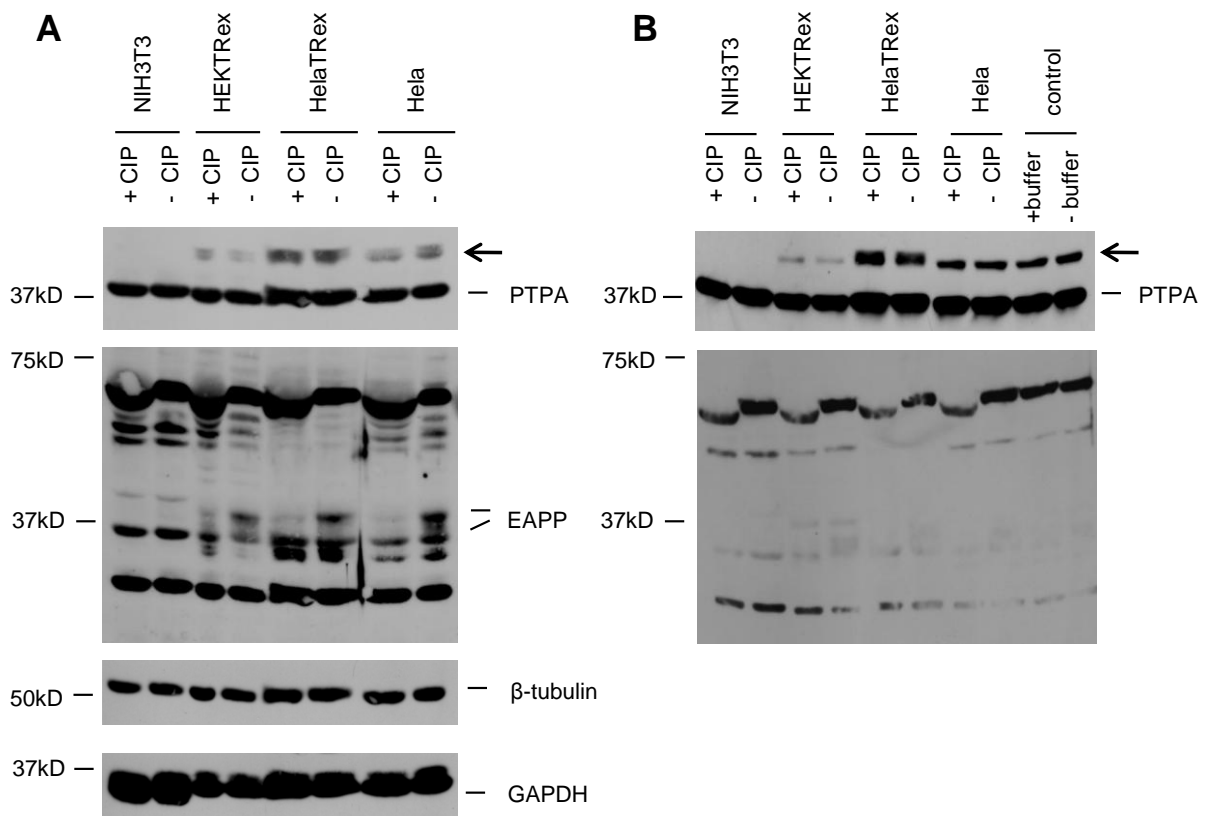
Figure 16: Phosphatase treatment of cell lysates. A) and **B)** represent independent experiments: 100μg of whole cell lysates of different cell lines was incubated with 5000 U of CIP and NEBuffer 3 (see 2.2.13. for details). Moreover, samples were analysed by immunoblotting (10% SDS-PAG) with anti-PTPA (5G3, 1:1000), anti-β-tubulin (1:10.000), anti-GAPDH (1:40.000) and anti-EAPP antibody (1:5.000). Samples without CIP incubation (-CIP) and without NEBuffer 3 (control in **B**) served as negative controls. Arrows point out the additional band of PTPA. Two bands are indicated referring to EAPP. +CIP = incubation with CIP; control = Hela lysate with or w/o buffer (-/+ buffer)

Further research in the ensembl-database (www.ensembl.org), revealed the existence of two isoforms specific for human PTPA with molecular weights of 40.6 kDa, representing the β-isoform of PTPA [Janssens et al, 2000], and 42.15 kDa, while no isoform with molecular weights more than 36.7 kDa was predicted for mouse PTPA. To sum up, an additional isoform exists for human PTPA, which could be identified by immunoblotting and did not reduce its signal intensity upon incubation with CIP. Further, the PTPA specific isoform could be suppressed by shRNA/siRNA.

3.7. Production of a new antibody against PTPA

Recently used PTPA specific antibodies did not work in immunofluorescence, as a reduction of signal intensity was missing in cells with suppressed PTPA levels (as shown in western blot analyses, please see "Wahlbeispiel-protocol" for further details). Thus, we aimed to produce a new one that might work for immunofluorescence analysis, to identify altered protein levels. Second, subcellular fractionation experiments demonstrated a distribution of the protein mainly to the cytoplasm (see above). Therefore, a new antibody specific for the application in immunofluorescence could confirm these results.

Initially, the polyclonal anti-rabbit PTPA antibody (171.1), which was applied for quantitative detection of PTPA in previous results, was affinity purified by covalent coupling on a SulfoLink antigen-column in order to improve signal intensity and specificity (for details please see 2.2.14.1.). However, even after this purification procedure various unspecific background bands were recognized in the immnunoblot analysis (data not shown). Hence, full length His-tagged PTPA was recombinantly expressed and purified on Ni-agarose beads. This purified PTPA was subsequently used for immunisation of four mice and one rabbit (in collaboration with Marko Roblek and Stefan Schüchner).

3.7.1. Recombinant expression of full length PTPA and His purification

To evaluate the most efficient bacterial strain in terms of expressing the antigen, full length His-tagged PTPA (pB´His NP SpHI/NcOI PTPA#2) was recombinantly expressed in three different bacterial strains, Origami, Rosetta (+) and Rosetta (-). Rosetta (-), the strain with the highest amounts of expressed antigen, was chosen for expressing large quantities of His-tagged PTPA.

Following the IPTG induced expression of His-tagged PTPA (please see 2.3.5. for details), soluble and insoluble fractions of cell lysates were analysed by western blotting (data not shown) and Coomassie staining, to check whether PTPA was expressed in soluble or insoluble fraction. Subsequently, samples were His-purified with NI-NTA beads (see 2.2.2.) and tested by western blotting (data not shown) and Coomassie staining. Eluted fractions, termed elution 1 and 2, NI-NTA beads, to check the amount of antigen still bound and samples uninduced for the expression of PTPA, serving as negative controls, were tested. Finally, a dilution series of re-combinantly expressed and His-purified antigen was compared with BSA-standards by Coomassie analysis to estimate protein amounts.
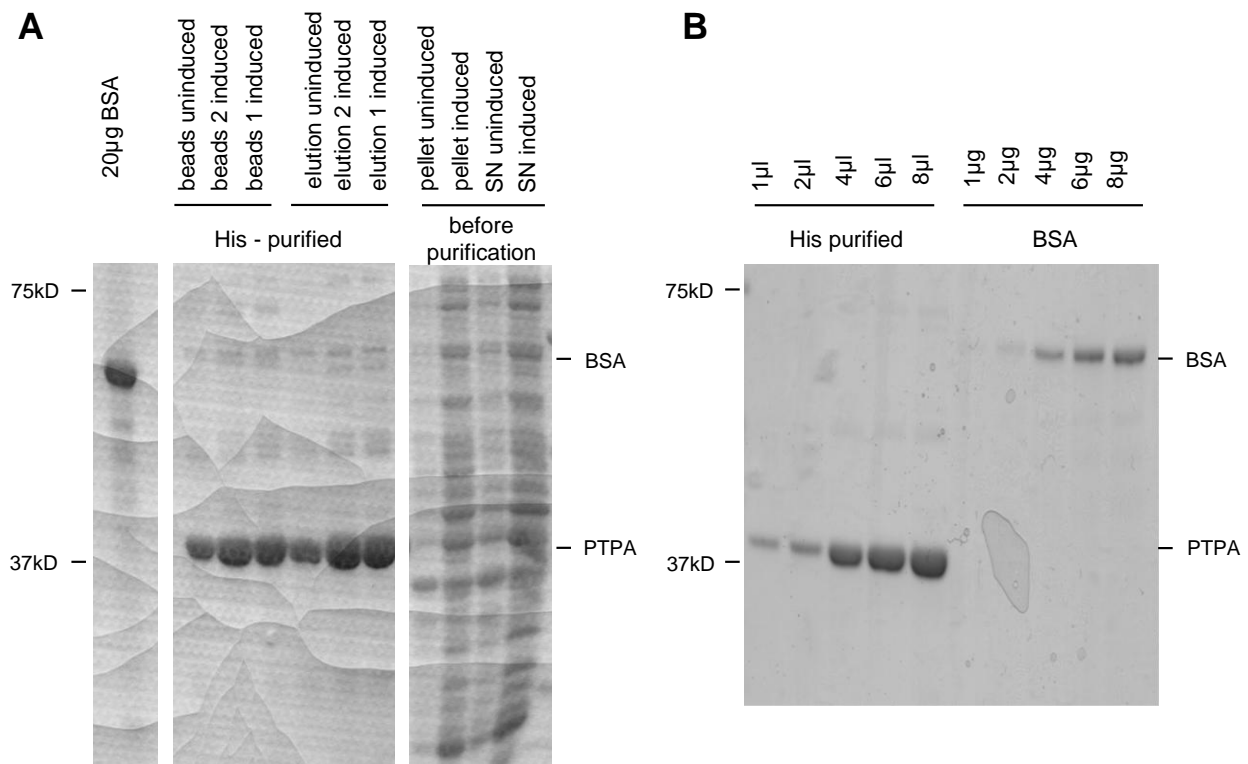
Figure 17: His – purification of recombinantly expressed PTPA. A) PTPA was recombinantly expressed in Rosetta (-) followed by His-tag purification, SDS-PAG analysis (10%) and Coomassie staining. Soluble and insoluble fractions of bacteria induced and uninduced with IPTG (0.75% and 1.5% of total volumes, of soluble and insoluble fractions) are shown in right panel (before purification). His-purified samples of induced and uninduced soluble fractions are shown in the left panel (3% of total volume). **B)** The concentration of His-tag purified samples was determined by SDS-PAG analysis (10%) and Coomassie staining. PTPA and BSA, containing molecular weights of 42kDa and 66kDa, respectively, are indicated with bars aside of each figue. pellet = insoluble fraction; SN = supernatant, soluble fraction; beads = Ni-NTA beads.

A higher amount of full length His-tagged PTPA was present in the IPTG induced soluble fraction compared to induced insoluble fraction (figure 17A, right panel). However, even without IPTG induction, there was around one fourth of the amount in comparison to induced samples. Furthermore, I purified His-tagged protein from the soluble fractions, eluted with imidazol (see 2.2.2. for further details) and tested the eluted samples with western blotting (data not shown) and Coomassie staining. Induced eluted fractions 1 and 2 contained at least more than twice as much antigen in comparison to uninduced eluted fraction (figure 17A, middle panel). As some antigen was still bound to the Ni-agarose beads, the elution with imidazol could be repeated. Finally, His-purified PTPA was compared to BSA standards in a dilution series (see above). Approximately 2µl of His-purified protein was found equivalent to 6µg of BSA standard (figure 17B). To sum up, the efficiency of the His-purification was sufficient for the production of antigen in order to immunise mice and rabbit, but the NI-NTA beads could be reused for purification once again.

3.7.2. New antibodies specific for PTPA

Following the heterologous protein expression and purification, 4 mice originating from the strain RBF/DnJ RB(8.12)5Bnr and 1 New Zealand White rabbit were immunised with full length PTPA (please see 2.6. for further details) and subsequently tested for their immunresponse. Preimmune sera and final bleeds were tested for signal specificity and intensity in the immunofluorescence and immunoblotting analyses.

The polyclonal rabbit anti-PTPA antibody recognized PTPA in the immunoblot of Hela cell lysates but also many other proteins with similar intensities (figure 18.C). Therefore, sera were stored at 4°C without further evaluation. Next, preimmune sera and sera from fourth bleeds of mouse 1 and 4, respectively, were tested in immunofluorescence (figure 19, 1-3). Fourth bleeds of mouse 1 and 4, revealed a prominent cytoplasmic signal (figure 19, 2 and 3) in comparison to anti-PTPA antibody 5G3, which showed a predominantly nuclear staining (figure 19, 4). Additionally, preimmune serum of mouse 1 stained rather diffusely (figure 19, 1). Based on a more homogenous signal arising from incubation of Hela cells with fourth bleed of mouse 4 in comparison to mouse 1 (figure 19, 2), we decided to fuse splenocytes of mouse 4 with X63.Ag8.653 cells.

Subsequently, splenocytes of mouse 4 were fused with X63.Ag8.653 cells and seeded onto 4x96 well plates and 4x12 well plates (fusion was performed by Marko Roblek). Hybridoma supernatants were tested for the presence of PTPA specific antibodies by immunoblotting 8 days after fusion. In the first testing round, pools of supernatants from 8 wells (for 96 well plate) and pools of 2 wells (for 12 well plates) were checked for the presence of antibodies specific for PTPA (data not shown). 10 pools of supernatants, positive for PTPA, were retested individually, in order to detect hybridoma clones responsible for the production of the antibody (figure 18.B).
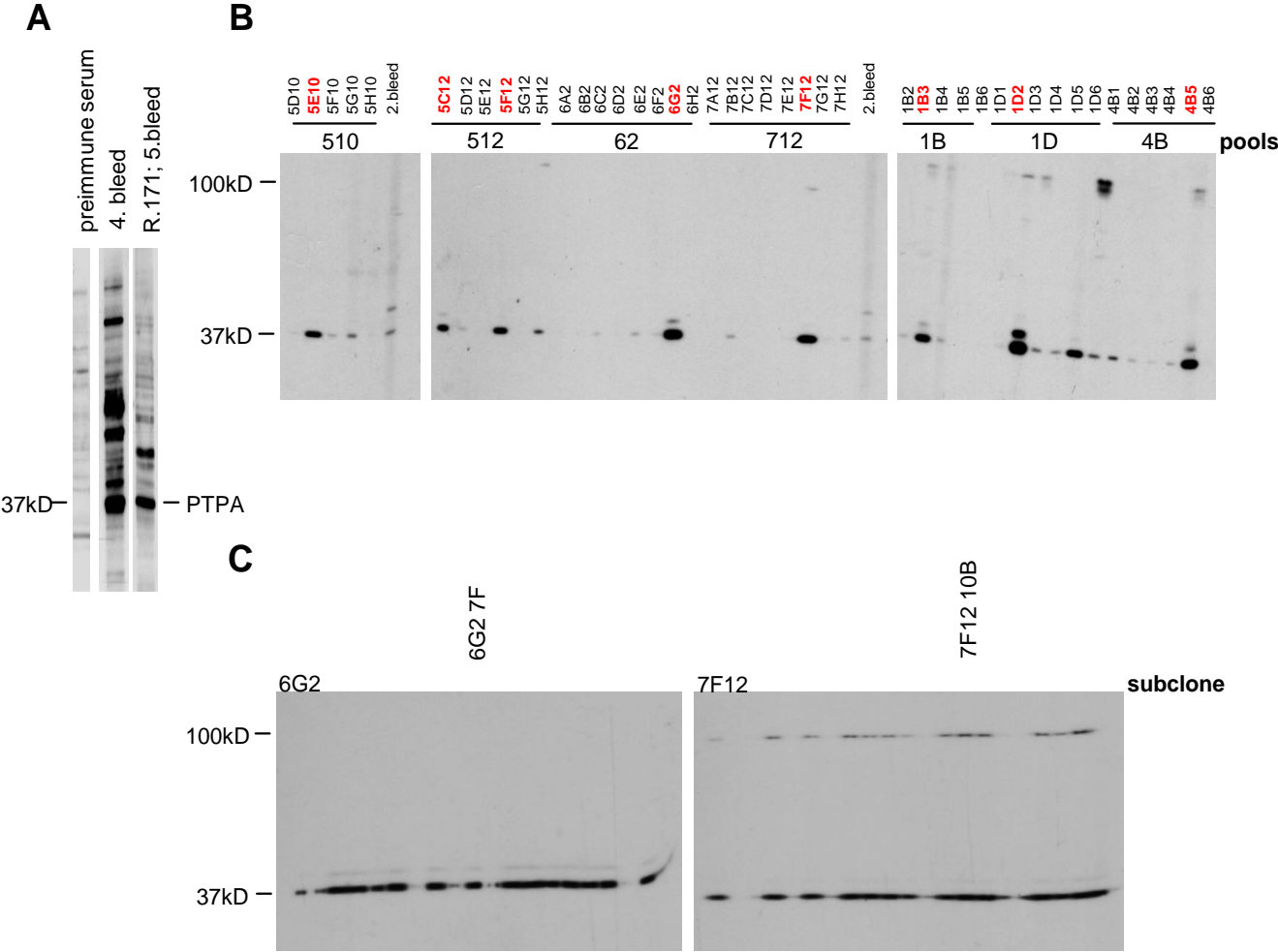
Figure 18: Test of hybridoma supernatants and polyclonal rabbit antibody. A) Final bleed of immunized rabbit was tested for PTPA specificity in a western blot analysis (10% SDS-PAG) of Hela cell lysates. Preimmune serum of rabbit 132 (1:100 with 0.5%NFDM) and 4.bleed (final bleed, 1:100 with 0.5%NFDM) were tested. Anti-rabbit polyclonal antibody against PTPA (R171.1) was used as positive control (1:10.000 with 0.5%NFDM). **B)** Hybridoma supernatans were tested for the presence of antibodies after fusion of splenocytes with X63.Ag8.653 cells in pools of supernatants (data not shown). Next, 50µl supernatant of individual wells from each positive pool of hybridoma cells was retested in western blot analysis (10% SDS-PAG) of Hela cell lysates. 2.bleed of mouse 4 (1:100 with 0.5%NFDM) served as

control. Among the PTPA positive hybridoma supernatants, the following (highlighted in red) were tested in the immunofluorescence application: 5E10, 5C12, 5F12, 6G2, 7F12, 1B3, 1D2, 1D5 and 4B5. **C)** 50µl of supernatant of minimal diluted mixed clones, 6G2 and 7F12, were analysed by western blotting (10% SDS-PAG) of Hela cell lysates. Two PTPA specific single clones, 6G2 7F and 7F12 10B, were chosen for further analysis in immunofluorescence.

Pools of hybridoma supernatant, containing PTPA specific antibodies (data not shown), were seperated into to individual supernatant of each well and the following hybridoma mix clones were chosen: 1B3, 1D2, 5E10, 6G2 and 7F12 (figure 18.B, highlighted in red). They exhibited slightly different appearances in immunoblot analyses in terms of signal strength and specificity. Additionally, each hybridoma subclone was tested in immunofluorescence. Mix clones 1D2 and 5E10 showed similar staining patterns except of intensity and clones 6G2 and 7F12 represented differential patterns to each other (figure 20, 1-5). Mixed hybridoma subclone 6G2 localized PTPA mainly in cytoplasmic regions, while 7F12 showed a detection of the antigen in the nucleus (figure 20, 4 and 5). Thus, both mixed clones were chosen for minimal dilution on 96 well plates with cell densities of 1.6 clones/well and 3.6 clones/well (please see 2.6.3. for further details).

Following minimal dilution, supernatants were analysed by western blotting in pools of 12 wells and retested for the identification of single clones producing PTPA-specific antibodies (figure 18.C). Interestingly, all single clones of minimal diluted hybridoma subclone 7F12 detected an additional band around 100kDa in the immunoblot analysis (figure 18.C, right panel), while all single clones originating from subclone 6G2, showed a similar pattern in comparison to anti-PTPA antibody, 5G3 (figure 18.C, left panel).

Furthermore, subclone 6G2 10B, which contained 1 clone/well after minimal dilution, and subclone 7F12 10B, which contained 4 clones/well after minimal dilution, were tested again in immunofluorescence (figure 21, 1-4). Single hybridoma clone 6G2 10B clearly lost the cytoplasmic staining after minimal dilution and represented a specific staining in the nucleus (figure 21, 1). In contrast, mixed subclone 6G2 still exhibited cytoplasmic staining (figure 21, 2). Although it was unclear, if the cytoplasmic staining of mixed hybridoma clone 6G2 would be due to PTPA specific binding, the supernatant was chosen for further investigations, as previous analyses of subcellular fractionated Hela cells checked by immunoblotting revealed a mainly cytoplasmic distribution of PTPA in Hela cells (see above). Finally, minimal diluted hybridoma subclone 7F12 10B allowed an improved signal intensity and its nuclear staining remained (figure 21, 3).

In order to further identify the knock down of PTPA via immunofluorescence, mixed clone 6G2 and single clone 7F12 10B, localizing PTPA in the cytoplasm and nucleus, respectively, were chosen. Therefore, both hybridoma clones were expanded to at least 10x100 diameter tissue culture plates.
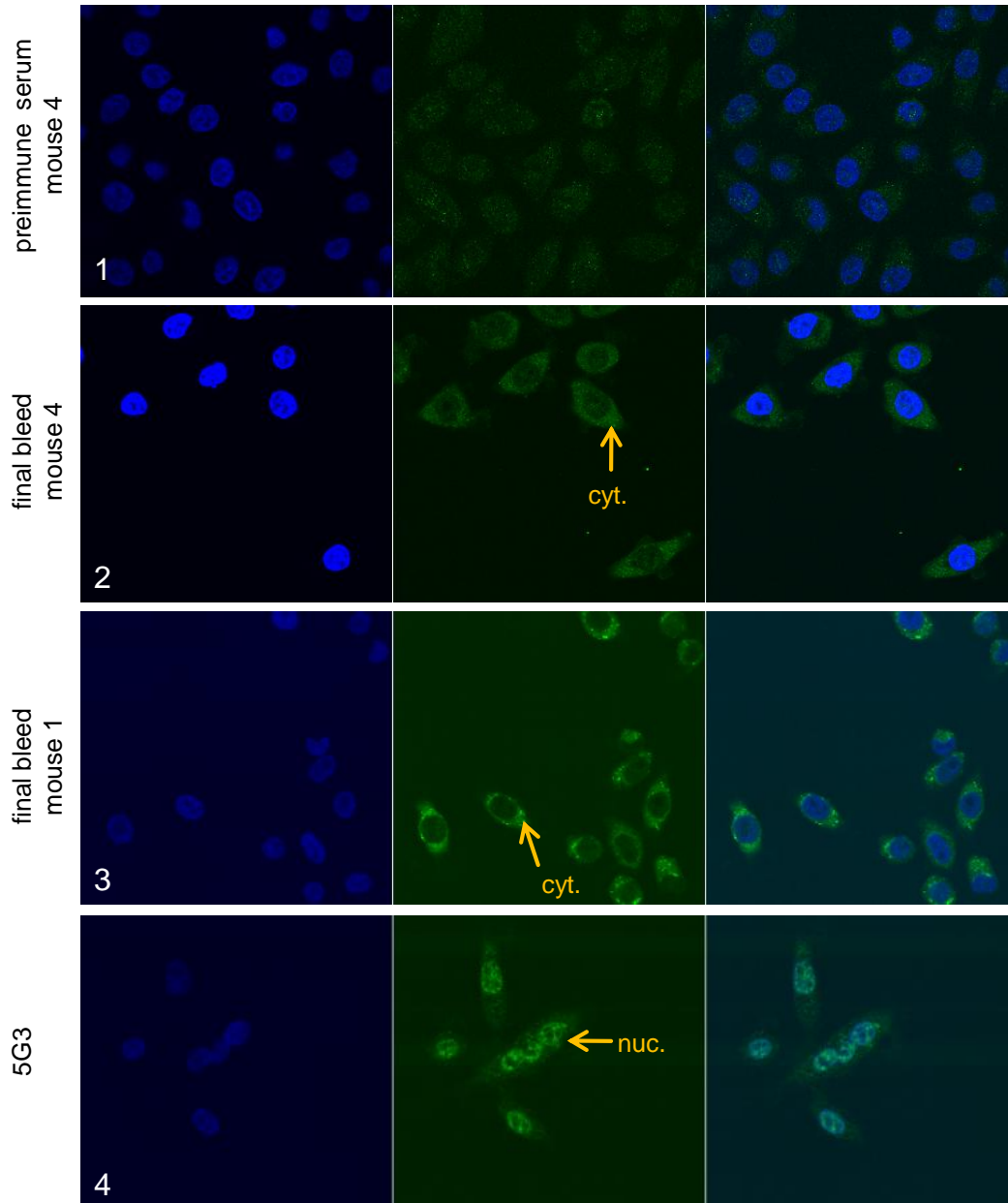
Figure 19: Test of preimmune sera and immune sera. 5×10^4 Hela cells were prepared according to the description in 2.2.10. Preimmune serum (1) and immune sera of final bleeds of mouse 4 and 1 (2 and 3), diluted 1:100 in 1%BSA/PBS, and anti-PTPA antibody 5G3 (4), diluted 1:10, were incubated o/n at 4°C. Signals appearing in green (middle panel) refer to an incubation with secondary antibody Alexa 488 (1:500 in 1%BSA/PBS). Cells were counterstained with Hoechst 33342 (left panel). Right panel represents merged pictures. Yellow arrows depict either nuclear (nuc.) or cytoplasmic (cyt.) staining. Pictures were taken with a Zeiss LSM 510 Meta confocal microscope (63x objective) using the corresponding LSM 510 Meta software.
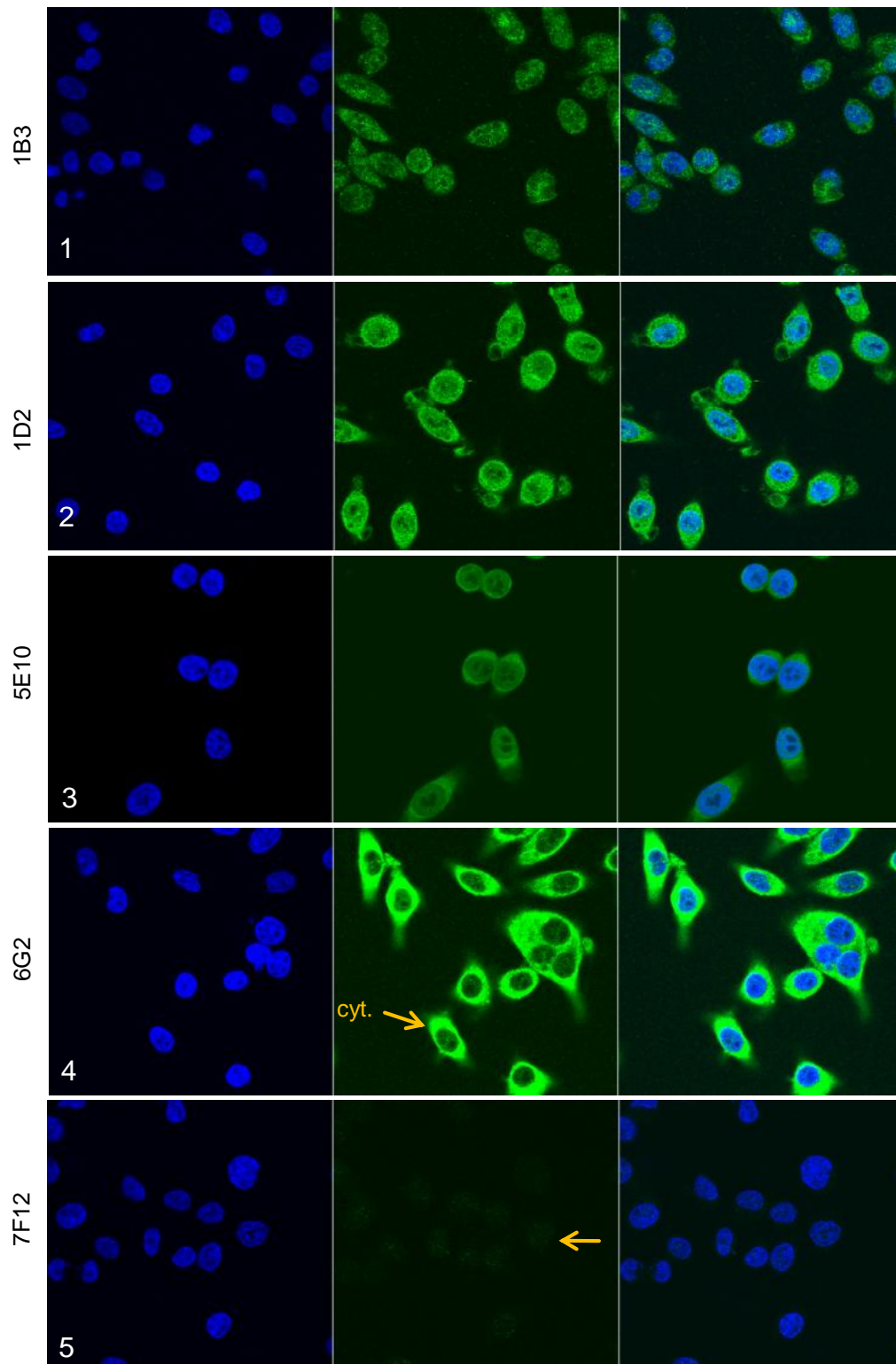
Figure 20: Test of mixed hybridoma clones. 5×10^4 Hela cells were prepared according to the description in 2.2.10. Supernatants of mixed hybridoma clone 1B3 (1), 1D2 (2), 5E10 (3), 6G2 (4) and 7F12 (5) were diluted 1:100 in 1%BSA/PBS and incubated o/n at 4°C. Signals appearing in green (middle panel) refer to an incubation with secondary antibody Alexa 488 (1:500 in 1%BSA/PBS). Cells were counterstained with Hoechst 33342 (left panel). Right panel represents merged pictures. Yellow arrows depict either nuclear (nuc.) or cytoplasmic (cyt.) staining. Pictures were taken with a Zeiss LSM 510 Meta confocal microscope (63x objective) using the corresponding LSM 510 Meta software.
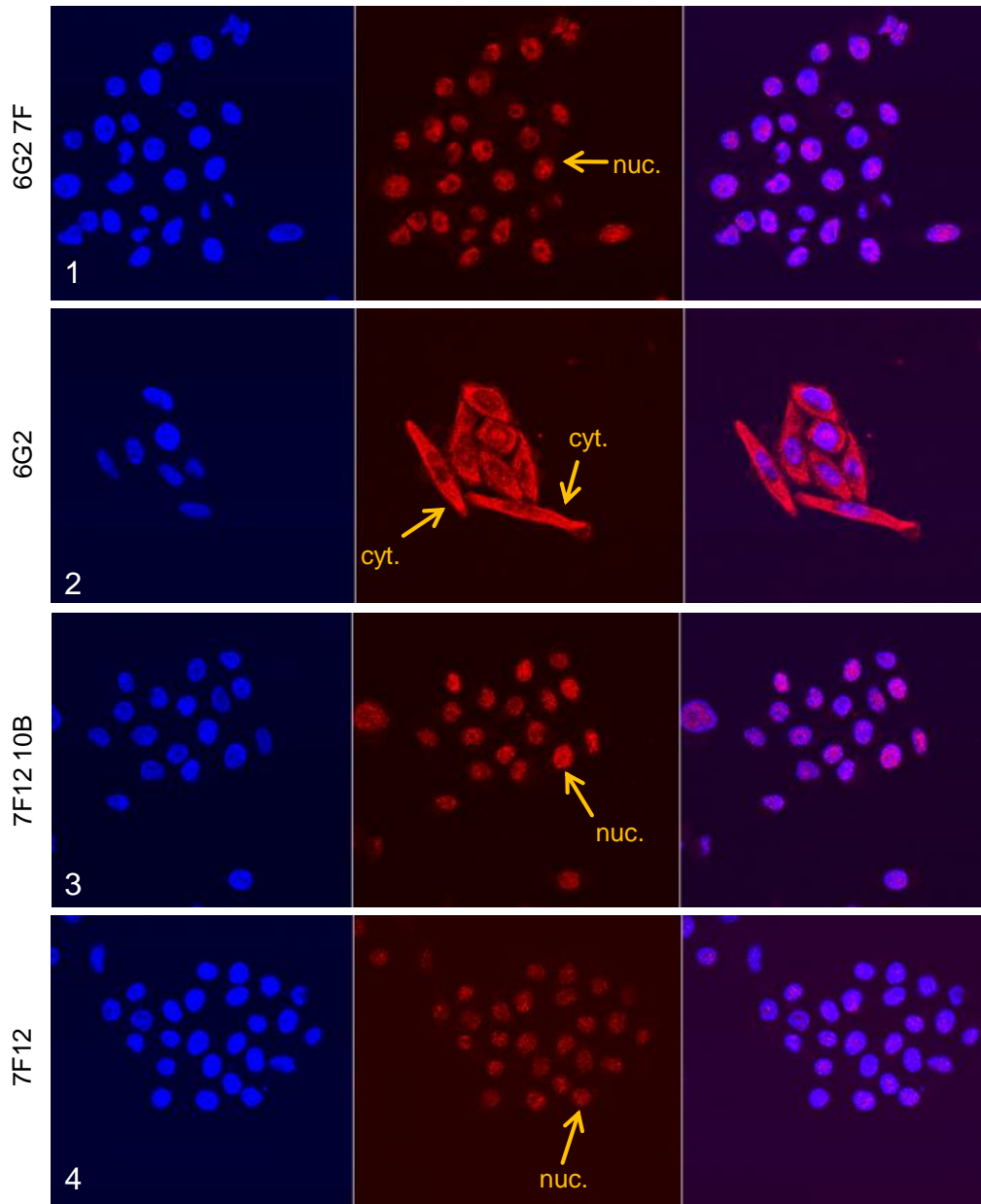
Figure 21: Test of minimally diluted hybridoma clones. 5×10^4 Hela cells were prepared according to the description in 2.2.10. Undiluted supernatants of minimally diluted hybridoma clones 6G2 7F (1) and 7F12 10B (2) were incubated o/n at 4°C. Undiluted supernatants of mixed hybridoma clones 6G2 (2) and 7F12 (4) were incubated o/n at 4°C. Signals appearing in red (middle panel) refer to an incubation with secondary antibody Alexa 594 (1:500 in 1%BSA/PBS). Cells were counterstained with Hoechst 33342 (left panel). Right panel represents merged pictures. Yellow arrows depict either nuclear (nuc.) or cytoplasmic (cyt.) staining. Pictures were taken with a Zeiss LSM 510 Meta confocal microscope (63x objective) using the corresponding LSM 510 Meta software.

3.7.3. Purification of mouse anti-PTPA subclones 6G2, 7F12 10B and rabbit anti-PTPA polyclonal serum 132/10

Immunofluorescences with mixed hybridoma clone 6G2 7F and supernatant of monoclonal 7F12 10B (figure 21), indicated, that PTPA would occur mainly in the nucleus. In contrast, the hybridoma mix clone, 6G2, displayed a predominantly cytoplasmatic staining. To further improve specificity by reducing the background and to concentrate the antibodies, supernatant of mixed subclone 6G2, single subclone 7F12 10B and polyclonal rabbit anti-PTPA serum (132/10), were affinity purified. Therefore, 1ml of each supernatant was incubated with His-tagged PTPA blotted on a nitrocellulose membrane (for details please see 2.2.14.2.). Subsequent washing and elution of antibodies completed the purification procedure.
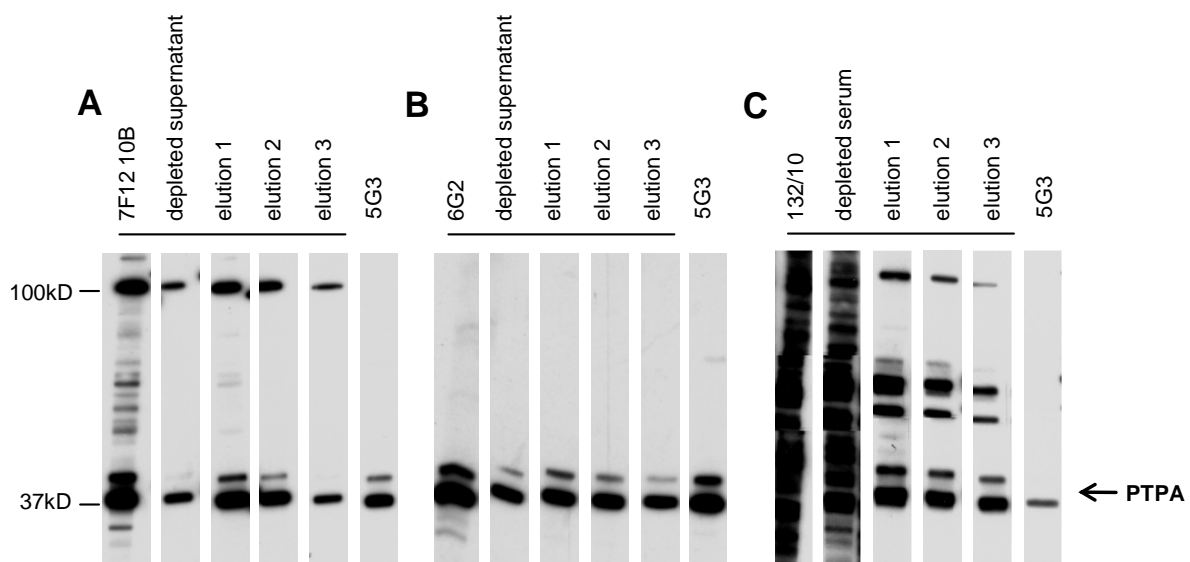
Figure 22: Purification of antibodies. Antibodies were affinity purified from supernatants or antiserum of mixed clone 6G2, subclone 7F12 10B and 132/10 were tested by western blotting analyses of whole cell Hela lysates (10%SDS-PAG). Lanes indicated as 7F12 10B (**A**), 6G2 (**B**) and 312/10 (**C**) (1:20), were incubated with supernatants before purification (1:20). Lanes of "depleted supernatant/serum" (1:200) were incubated with supernatants after incubation of the nitrocellulose bound antigen. Eluates 1-3 were incubated with purified antibodies of eluted fractions (1:200). Monoclonal anti-PTPA antibody 5G3 (1:1000) represents the positive control. Arrow is indicating PTPA for A, B and C and molecular weights are indicated as well for A, B and C.

In case of subclone 7F12 10B (figure 22 A), eluted fractions 1 and 2 showed less off target signals in comparison to the immunoblot incubated with raw supernatant of 7F12 10B. Interestingly, all immunoblots with 7F12 10B supernatants demonstrated an additional band at 100kDa.

Finally, eluted fraction 1 and 2 were pooled for further analysis without including eluted fraction 3, as it showed reduced signal intensity. Second, only slight differences in signal intensities were recognized in immunoblots with mixed hybridoma subclone 6G2 (figure 22 B). Each fraction revealed clear PTPA-specific signals occurring at 37kDa and 42kDa, representing two main human isoforms, respectively. Thus, all eluted fractions were pooled for further use. Finally, purified rabbit serum 132/10 showed improved specificity in all eluates and eluted fractions one to three were pooled (figure 22 C).

Although the purification turned out to be successful, due to a reduction of unspecific background bands and an increase of PTPA specific signal, some PTPA specific antibody was still bound to the nitrocellulose membrane (figure 22, depleted supernatant/serum). Moreover, raw supernatants were incubated with the nitrocellulose membrane at a dilution of 1:20, while the result of eluates represented a dilution of 1:200. Thus, it is difficult to compare the samples directly.

3.7.4. Evaluation of downregulated PTPA via immunofluorescence

To determine the degree of PTPA knock down using the purified antibodies, HelaTRex-pNTOneo CT Cl.L and HelaTRex-pNTOneo-Mis Cl.D cells were induced for the expression of RNAi (see above for details) and analysed by western blotting and immunofluorescence.

Cells induced with doxycycline for 96 hours and uninduced cells were permeabilized and fixed with 3.7% formaldehyde, and incubated with purified or raw hybridoma supernatant. Finally, samples were analysed by confocal laser scanning microscopy and western blotting, to visualise remaining PTPA and to determine the degree of PTPA knock down, respectively.

First, knock down of PTPA was confirmed by immunoblotting with the purified 7F12 10B supernatant (figure 23). The monoclonal anti-PTPA antibody 5G3 as well as the novel hybridoma supernatant 7F12 10B detected the decrease of PTPA levels. Upon shRNA induced downregulation of PTPA, the 100kDa protein, detected by 7F12 10B, was not reduced suggesting that it was not a PTPA specific protein. So, the novel monoclonal 7F12 10B antibody detected specific PTPA.
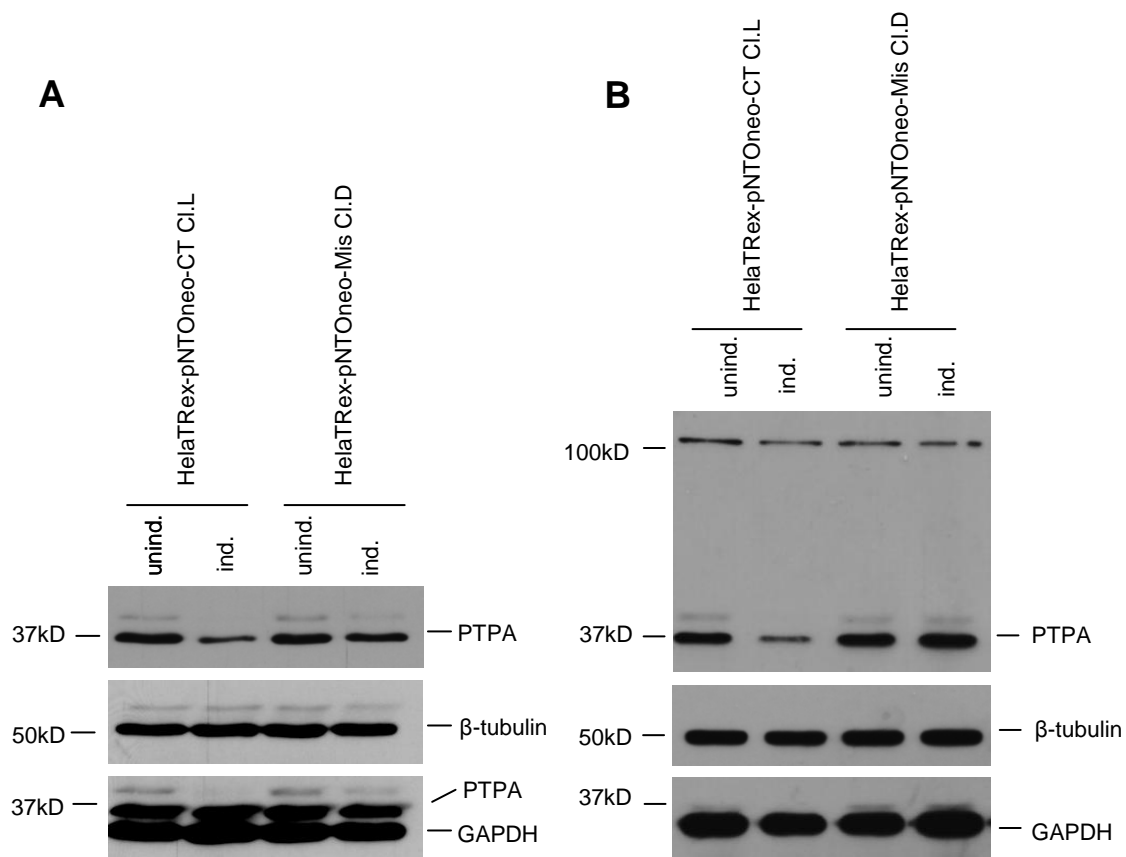
Figure 23: Evaluation of downregulated PTPA by immunoblot analyses with different antibodies.
HelaTRex-pNTOneo-CT Cl.L and HelaTRex-pNTOneo-Mis Cl.D cells were induced for 96 hours with 1µg/ml of doxycycline added everey 24 hours and uninduced samples were taken as negative control. Whole cell lysates were prepared and analysed by 10% SDS-PAG. Immunoblotting was performed with anti-PTPA antibody 5G3 (1:1000), **A)**, raw supernatant of monoclonal 7F12 10B (1:20), **B)**, β-tubulin (1:10.000) and GAPDH (1:40.000). unind. = uninduced sample without doxycycline; ind. = sample induced with doxycycline.

Furthermore, we expected that the downregulation of PTPA would be also detected in immunofluorescence analysis. Raw supernatants of 7F12 10B, exhibiting nuclear staining, did not show any differences in signal intensity between induced and uninduced sample (figure 24 A, 3 and 4). Surprisingly, purified supernatant of 7F12 10B, previously exhibiting nuclear staining, showed a cytoplasmic accompanied by an intense staining surrounding the nucleus.
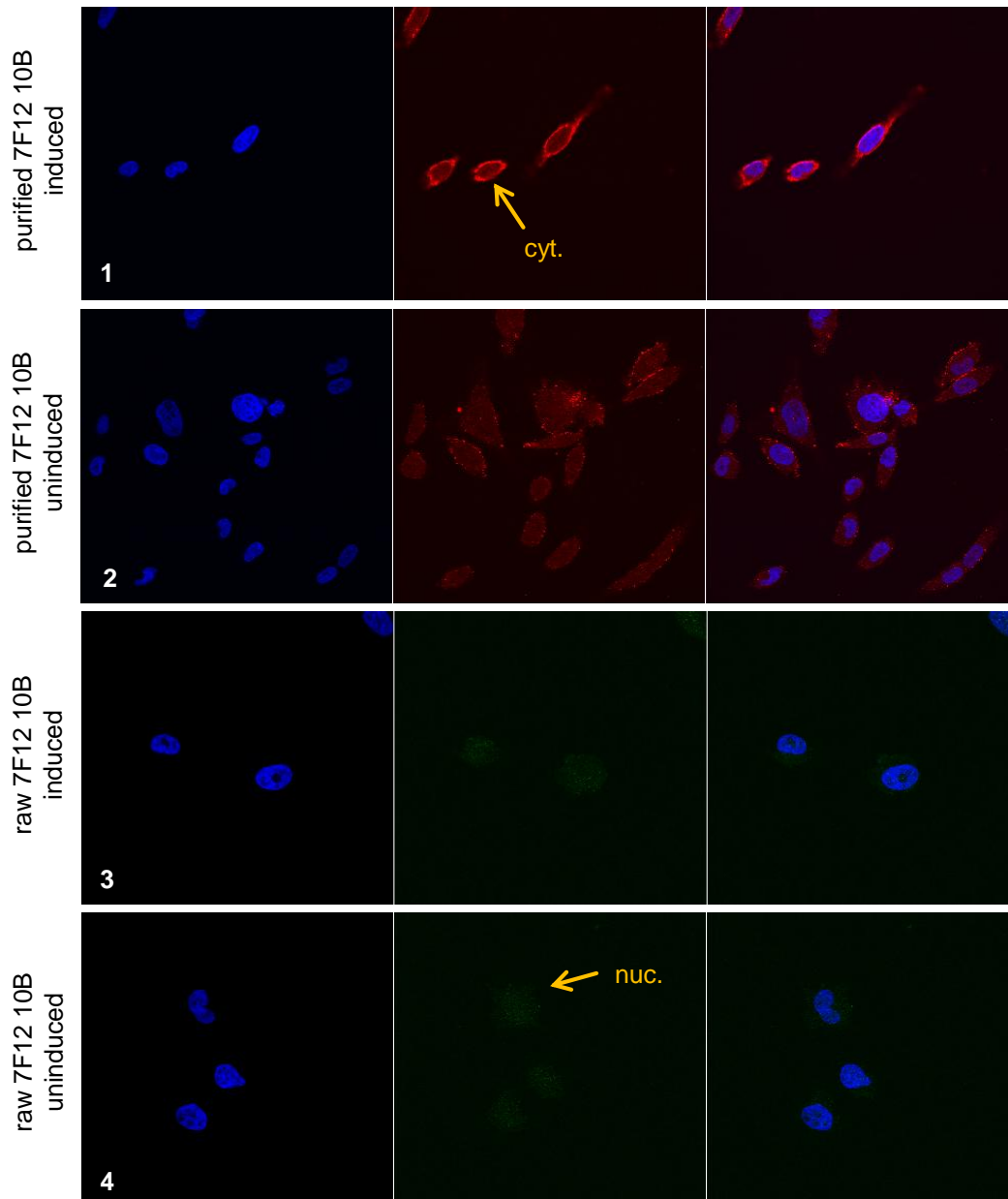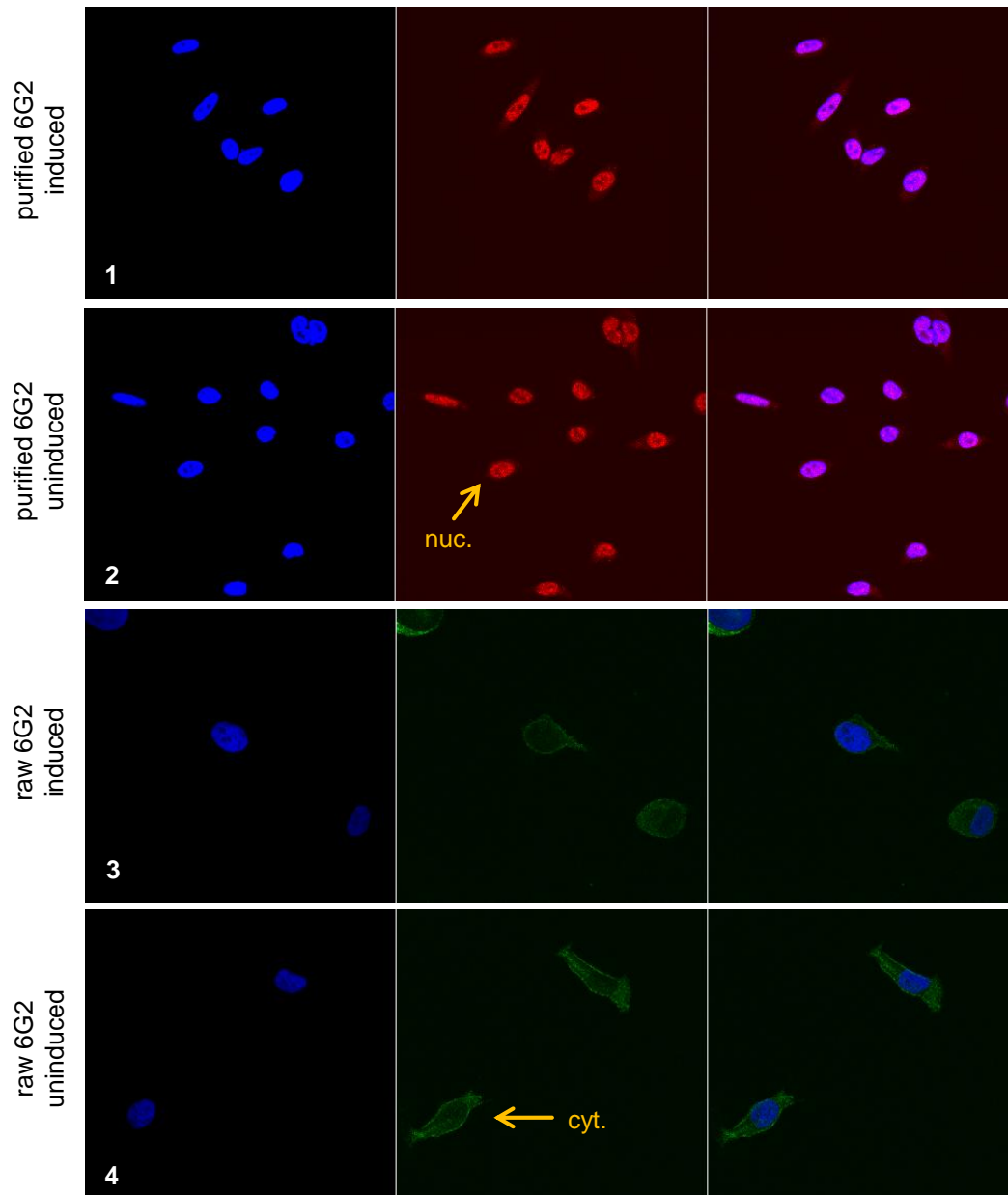
Figure 24: Detection of PTPA in cells with purified/raw 7F12 10B. HelaTRex-pNTOneo-CT Cl.L cells were induced for 96 hours with 1µg/ml of doxycycline added every 24 hours, seeded on 6-well tissue culture plates, permeabilized and fixed with 3.7% formaldehyde (see 2.2.10). Undiluted affinity purified supernatant of 7F12 10B, with doxycycline induced (1) and uninduced (2) cells, and undiluted raw supernatant, with doxycycline induced (3) and uninduced (4) cells, were incubated o/n at 4°C. Signals appearing in red and green (middle panel) refer to incubation with secondary antibodies Alexa 594/488 (1:500 in 1%BSA/PBS). Cells were counterstained with Hoechst 33342 (left panel). Right panel represents merged pictures. Yellow arrows depict either nuclear (nuc.) or cytoplasmic (cyt.) staining. Pictures were taken with a Zeiss LSM 510 Meta confocal microscope (63x objective) using the corresponding LSM 510 Meta software.

Figure 25: Detection of PTPA in cells with purified/raw 6G2. HelaTRex-pNTOneo-CT Cl.L cells were induced for 96 hours with 1µg/ml of doxycycline added every 24 hours, seeded on 6-well tissue culture plates, permeabilized and fixed with 3.7% formaldehyde (see 2.2.10). Undiluted affinity purified superna- tant of mixed hybridoma clone 6G2, with doxycycline induced (1) and uninduced (2) cells, and undiluted raw supernatant of mixed clone 6G2, with doxycycline induced (3) and uninduced (4) cells, were incu- bated o/n at 4°C. Signals appearing in red and green (middle panel) refer to incubation with secondary antibodies Alexa 594/488 (1:500 in 1%BSA/PBS). Cells were counterstained with Hoechst 33342 (left panel). Right panel represents merged pictures. Yellow arrows depict either nuclear (nuc.) or cytoplasmic (cyt.) staining. Pictures were taken with a Zeiss LSM 510 Meta confocal microscope (63x objective) using the corresponding LSM 510 Meta software.

Moreover, application of the supernatant of hybridoma mix clone 6G2, which mostly detected PTPA in the cytoplasm (as shown in figures 20 and 21), revealed similar characteristics as the monoclonal anti-PTPA antibody, 5G3, if purified (figure 25, 1 and 2). The immunofluorescence of raw supernatant of mixed clone 6G2 displayed weaker signal intensity in comparison to purified supernatant (figure 25). However, we did not observe any differences in intensities of immunofluorescence signals between doxycycline induced and uninduced samples of HelaTRex-pNTOneo CT Cl.L cells (figures 24 and 25). Due to affinity purification, one species of antibody specific for PTPA was enriched. Thus, the result was similar to the outcome using minimal diluted clones in immunofluorescence, as the monoclonal hybridoma supernatant of 6G2 7F exhibited same staining characteristics as purified mixed clone 6G2 mixed. Furthermore, hybridoma mix clone 6G2 could contain other species specific for PTPA strongly staining the cytoplasm in immunofluorescence.

Finally, no significant signs of signal reduction could be ascertained in immunofluorescence, neither by using purified polyclonal rabbit anti-PTPA antibody nor by using monoclonal anti-PTPA antibody 5G3 (data not shown). One consistent effect emerged: All monoclonal supernatants, 6G2 7F, 7F12 10B and purified mixed clone 6G2, predominantly displayed a nuclear staining together with weak cytoplasmic staining (figures 21, 24, 25). On the other hand, hybridoma mix clones 6G2, 5E10, 1B2 and 1D3, displayed differential staining patterns.

3.7.5. Subcellular localization of PTPA by using 6G2 and 7F12 10B in subcellular fractionation

Previously, evidence was found for the nuclear distribution of PTPA, as overexpressed GFP-tagged PTPA was found to occur predominantly in the nucleus [Azam et al., 2007].

Furthermore, my own experiment (figure 15), using subcellular fractionation, revealed that PTPA was detected most abundantly in the cytoplasmic fraction. To confirm this result, we generated new antibodies specific for PTPA and tested them in immunofluorescence application. Surprisingly, PTPA could not be localized exclusively to one cellular compartment but rather appeared to occur in both albeit not to a similar extend. Therefore, the subcellular fractionation was repeated and immunoblots were performed with raw supernatant of hybridoma subclone 6G2 and raw supernatant of monoclonal 7F12 10B.
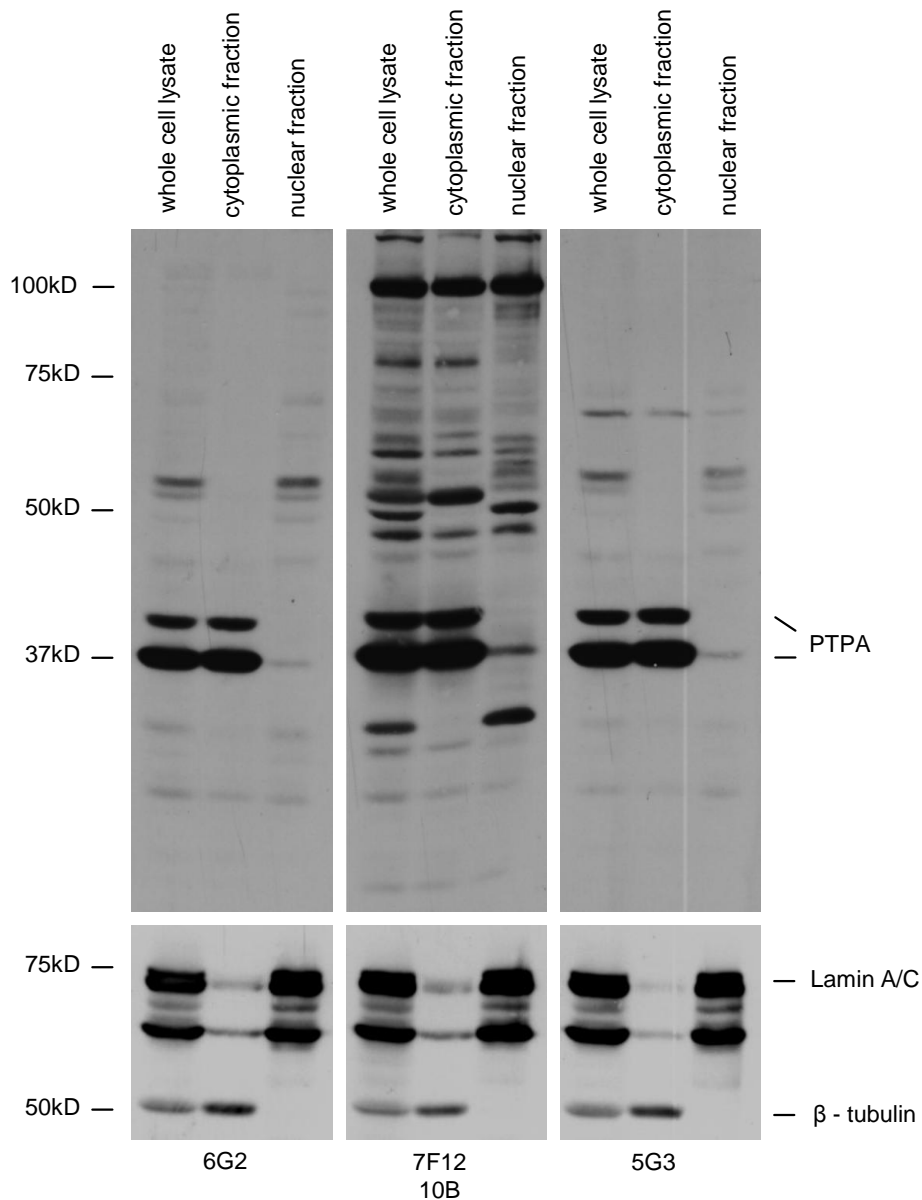
Figure 26: Detection of subcellular localization of PTPA with 6G2 and 7F12 10B. Hela cells were fractionated into a cytoplasmic and nuclear fraction by centrifugation. Subsequently, lysates of each fraction were tested by western blot analysis (10% SDS-PAG) with each lane containing the lysates from 100.000 cells. Immunoblotting was performed with hybridoma mix clone 6G2 (1:20), hybridoma single clone 7F12 10B (1:20), anti-PTPA antibody 5G3 (1:1000), anti-lamin A/C (4C11; 1:1000) and anti-β-tubulin (1:10.000). Lamin A/C and β-tubulin constitute marker for nucleus and cytoplasm, respectively.

First, immunoblotting with anti-lamin A/C antibody, revealed, that this nucleus specific protein was also detected in the cytoplasmic fraction, indicating that, for technical reasons, the cytoplasmic fraction was slightly contaminated with nuclear proteins (lowest panel in figure 26). However, immunoblotting with β-tubulin, the cytoplasmic marker, showed a clear distinction between both cellular compartments and allowed further interpretation of results. To be able to

compare all antibodies, the exposure time of 35 minutes (figure 26) was the same for each incubation.

All three antibodies recognized the double band of PTPA occuring at 37kDa and 42kDa with the majority of PTPA residing in the cytoplasmic fraction and only a minor fraction found in the nucleus. So, the main difference between these antibodies was in the pattern of background bands. Hybridoma mix clone 6G2 and monoclonal anti-PTPA antibody 5G3 detected mostly identical background bands with an additional band occurring around 55kDa in whole cell lysates and nuclear fractions. But, only hybridoma mix clone 6G2 demonstrated a dominant cytoplasmic staining in immunofluorescence analyses, whereas anti-PTPA antibody 5G3 predominantly showed a nuclear staining. Hybridoma subclone 7F12 10B recognized a huge number of unspecific background bands, possibly due to the fact, that the supernatant still included 3 clones after minimal dilution. However, 7F12 10B detected PTPA as well mainly in the cytoplasmic fraction and a prominent additional band around 100kDa, featuring similar intensities in all fractions.

To sum up, the subcellular fractionation experiment revealed a clear predominant presence of PTPA in the cytoplasm rather than the nucleus. This result is partly in contrast to immunofluorescence analyses with same antibodies.

4. Discussion

Protein phosphorylation and dephosphorylation, catalysed by kinases and phosphatases, respectively, represent highly conserved mechanisms responsible for activation and deactivation of protein functions. One of the most abundant serine/threonin phosphatases, PP2A, makes up to 0.1% of the total cellular protein content and distinct forms PP2A holoenzymes to regulate cellular development and important pathways inhibiting cancer or apoptotis [Gallego and Virshup, 2005]. PP2A exhibits a multisubunit architecture, with a fully active and specific heterotrimer assembled through a catalytic, a structural and one of a large number of regulatory subunits. Due to its various roles in cellular processes, PP2A needs to be tightly regulated, facilitated through posttranslational modifications such as phosphorylation and methylation. Moreover, PTPA, the highly conserved phosphatase two A phosphatase activator, was shown to be involved in the de novo activation of PP2A [Fellner et al., 2003, Longin et al., 2004, Van Hoof et al., 2005]. Deletion of both PTPA homologues in yeast, *RRD1* and *RRD2*, affects substrate specificity, protein stability and metal dependence of PP2A [Fellner et al., 2003]. Highly conserved between yeast and human, the importance of PTPA is further emphasised through apoptotic conditions emerging upon transient PTPA knock down with RNAi or overexpression in mammalian cells [Fellner et al., 2003, Azam et al., 2007].

Primarily, the project aimed to investigate the potential involvement of PTPA in Alzheimer´s disease, as decrease of active PP2A holoenzymes was demonstrated to be a critical factor for this neurodegenerative disorder [Sontag et al., 2010]. Therefore, a neuroblastoma cell line, N2ATRex, was stably transfected with a vector system expressing RNAi towards PTPA upon induction with doxycycline. Due to the fact, that PP2A activity and cell proliferation were unaffected upon a reduction of PTPA to 50%, another mammalian cell line, HEKTRex, was analysed in the same way. However, again neither PP2A activity nor cell proliferation were affected by a knock down of PTPA to ~20% of its wild type level [Mitterhuber, 2008, Kugler, 2009]. Based on previous transient knock down experiments in Hela cells, in which suppression of PTPA caused apoptosis, we wanted to unravel the effects of downregulated PTPA on cell survival and proliferation in HelaTRex cells.

Knockdown of PTPA

4.1. Knockdown of mammalian PTPA with shRNA

First, stably transfected single clones of HelaTRex cells were analysed for possible knockdown of PTPA upon doxycycline induced expression of shRNA. In HelaTRex-pNTOneo-CT Clone L cells, we could efficiently downregulate PTPA protein to approximately 15% of its wild type level. The proliferation behaviour of cells with reduced PTPA levels was monitored and cells were treated with Nocodazole in order to check the integrity of the spindle assembly checkpoint. However, although proliferation of HelaTRex-pNTOneo-CT Clone L cells seemed to be hampered once at day 2 of knock down, the cells recovered quickly. It is very likely, that the observed variations in cell counts of HelaTRex cells, could arise from differences in cell numbers seeded prior to the induction with doxycycline. In conclusion, a downregulation to approximately 15% of cellular PTPA did not result in a detectable effect on proliferation.

However, HelaTRex-pNTOneo-CT Cl.L cells showed a sub G1 peak upon a 20 hours treatment with Nocodazole. In a repetition and as well in a 30 hours treatment with Nocodazole, doxycycline treated cells contained a major amount of cells in the G1 phase. If cells with a reduced amount of PTPA protein succeed to emerge a spindle assembly checkpoint is still unclear. Though, further experiments will be necessary to allow a specific statement.

Different issues could be hold responsible for the lack of a significant phenotype upon knock down of the protein. First of all, I speculated about high protein stability and long half-life time [Janssens et al., 2000] rendering enough protein present in order to maintain a functional level. However, the quantification of PTPA with the LI-COR Odyssey infrared scanning system revealed a knock down to 15% of original amount. This successful knock down demonstrated that a calculated half-life time of 24 hours cannot be the reason for a missing phenotype. Moreover, PTPA probably works as an enzyme and thus, 15% of its amount could be sufficient to fulfill its function. Third, HelaTRex and HEKTRex represent transformed cell lines, possibly containing compensatory mutations for a low PTPA level. Furthermore, those cell lines could possess upregulated PTPA levels as normal amounts, rendering them less affected by a downregulation of PTPA protein. In addition, a balance, defined by a certain level of PTPA protein, could be feasible for viable cells after downregulation. Previously, Schönthal and coworkers demon-

strated an autoregulatory control adjusting the amount of PP2A C subunit to constant levels, exerted at the translational level [Schönthal et al., 1998].

However, it could as well be possible, that another PTPA specific isoform would complement the knockdown of PTPA. In this study, an isoform with a molecular weight of 42kDa, which was identified as such (see 3.6.2.), demonstrated a reduction of signal intensity upon knock down of PTPA. Although this isoform cannot be responsible to compensate the loss of PTPA, it is tempting to speculate that others would be functionally redundant and exert this function. Human PTPA is defined by different isoforms with α and β isoforms mainly expressed in some tissues [Janssens et al., 2000]. The shRNA/siRNA used in this study, targeting exon 10 of conserved C-terminal part of PTPA, would affect most of the published isoforms, as almost every protein coding isoform contains exons of the conserved part. Although Janssens and coworkers showed the presence of 7 main isoforms of PTPA, 2 of them lacking exon 3 and all of them containing the C-terminal part of mRNA, 27 protein coding isoforms are published on ensembl.org, with only 14 PTPA isoforms containing the first exon of the conserved C-terminal part.

To reveal the existence of an isoform, potentially increased in its amount upon knock down, we aimed to determine the downregulation of PTPA with a second method, reverse transcription quantitative real-time PCR. Before that, PTPA knock down was analysed on protein level by using the LI-COR Odyssey scanning system, measuring chemiluminescence of fluorescent labelled secondary antibodies, and presenting a semi-quantitative method [www.licor.com]. In order to detect mRNA at different positions, two primerpairs were applied. Primerpair 1 targeted exon 3 and 4, and primerpair 2, was leading to a product ranging from exon 5 to 8, spanning the conserved C-terminal part of mRNA. Due to the fact, that some isoforms are lacking exon 3 or 4, we expected to observe a difference in PCR products.

The qRT-PCR product of the doxycycline induced sample correlated well with the amount of downregulated protein, determined as described above. PTPA mRNA of doxycycline induced HelaTRex-pNTOneo-CT Clone L cells was reduced to 29% or 40.9% in comparison to uninduced cells, if checked with primerpair 1 or primerpair 2, respectively. Generally, a higher amount of PTPA mRNA was detectable with primerpair 2, possibly due to the fact, that most of the isoforms contain exons 5 to 8. However, 29% of PTPA mRNA, if checked with qRT-PCR and a primerpair targeting exon 3 and 4, was higher in comparison to 15% of PTPA protein, quantified with immunoblotting and the LI-COR Odyssey scanning system. Hence, a compensa-

tory mechanism could exist, increasing the level of transcription upon knock down and thus, affirming the essential function of PTPA.

An additional observation accompanied the analysis of PTPA knock down with stably transfected single clones: HelaTRex-pNTOneo-Mis Clone D and C exhibited elevated amounts of PTPA protein upon expression of mismatch shRNA in comparison to uninduced samples. This was an exclusive effect of the non-binding RNAi construct and could not be observed in HelaTRex cells stable transfected with an empty vector. Although the sequence was checked *in silico* for possible off-target effects, no reasons for this result could be identified so far. Nevertheless, it is unclear, if an off-target effect can be hold responsible for the observation of increased PTPA levels in HelaTRex-pNTOneo-Mis Clone C/D cells.

Following, we wanted to suppress the PTPA levles in shRNA induced cells even further. Therefore, we aimed to use small interfering RNAs for the knock down of PTPA mRNA. The use of different amounts of siRNAs could facilitate the achievement of variable knock down degrees, thereby enabling the determination of a hypothetical PTPA threshold level. In addition, it could be investigated, if the upregulation of PTPA, observed in stable transfected single clones expressing mismatch RNAi, would occur as well in the application of siRNA.

4.1.2. Knockdown of PTPA with siRNAs

Primarily, conditions for transient transfections of siRNAs in Hela and HEKTRex cells were optimized and yielded up to 60% and approximately 99% of efficiency, respectively. Transient transfections were performed with two targeting siRNAs, one exhibiting the same sequence as previously used "CT" shRNA and a second, targeting exon 7 and 8 of human PTPA, together with a mismatch siRNA, with an identical sequence to shRNA-Mis. 50pmol or 100pmol of siRNAs were delivered to Hela and HEKTRex cells.

Surprisingly, a reduction to approximately 30% of PTPA was achieved with 50pmol of siRNA targeting exon 7 and 8 in both cell lines. On the contrary, the application of 50pmol of siRNA, featuring an identical sequence to shRNA-CT, accomplished a knock down to one fourth of PTPA in comparison to its normal amount. Once again, the success of the downregulation via transient transfections was quantified by real-time PCR and showed a reduction to one third of mRNA with each targeting siRNA. McAnuff and coworkers demonstrated, that the assimilation of shRNA into the endogenous miRNA pathway results in a significantly higher efficiency in

comparison to siRNA [McAnuff et al., 2007]. Furthermore, siRNAs were described to suffer from high degradation and turnover and additionally require a higher dose to fulfil knock down, contributing to a higher extend of off-target effects [Rao et al., 2009]. Our results were consistent with these findings, as the shRNA expression system seemed to work more efficiently and could provide a higher degree of PTPA knock down in comparison to transient transfected Hela or HEKTRex cells.

Most interestingly, the effect of upregulated PTPA on protein level upon expression of mismatch RNAi was recurring. Transient transfections with 50pmol or 100pmol of mismatch RNAi induced an increase of 125% or 180% of PTPA on protein level. As the real-time PCR revealed a constant level of PTPA mRNA after transfection with missense siRNA, the off-target effect is detectable solely by immunoblotting with specific antibodies. Similar findings were demonstrated by Stout Delgado and coworkers [Stout-Delgado et al., 2007] without mentioning possible reasons. Recently, Ge Shan proposed, that targeting siRNAs and negative or positive controls should be used at the same dosage and outlined, that non-binding control RNAs would not utilize the RNAi pathway [Ge Shan, 2010]. So, possibly the use of another cellular pathway could account for an upregulation of PTPA protein. Although short interfering and small hairpin RNAs are intrinsically different molecules, this unwanted off-target effect was inherent to both methods. Interestingly, it has been shown, that siRNA and shRNA constructs with complementary sequences can produce same off-target effects across cell lines and independently of delivery method [Jackson et al., 2006]. However, the cause for the upregulation of PTPA when expressing or transfecting mismatch constructs is still unclear. To further avoid off-target effects, chemical modifications of riboses were found to increase stability and specificity of siRNA without affecting the potency [Jackson et al., 2006, Federov et al., 2006].

To sum up, shRNA demonstrated a higher knock down efficiency, down regulating PTPA to 15% of its normal amount in comparison to transiently applied siRNAs, which represented a downregulation to appoximately 30%. Remarkably, this downregulation seems to exceed standard knock down efficiencies, as previously summarized by Ge Shan [Ge Shan, 2010]. As an effect on cell survival was still missing, the same explanations as made for shRNA mediated suppression of PTPA are possible: A very low treshold level of PTPA needed to maintain its functional role in mammalian cells or a compensatory mechanism, as for instance functional redundancy of isoforms.

4.1.3. Additional methods and future prospective

To downregulate the mRNA of PTPA further below its potential critical threshold level, a combination of doxycycline induced stable transfected single clones and transient transfection of siRNAs was made. After a 96 hour induction with doxycycline in HelaTRex-pNTOneo-CT Clone L, cells were transiently transfected with targeting siRNAs. Disappointingly, PTPA still seemed to be present, despite this harsh knockdown treatment. The lowest level of PTPA in doxycycline induced HEKTRex-pNTOneo-CT Clone 8 and HelaTRex-pNTOneo-CT Clone L cells was achieved with a combination of of siRNA-CT and siRNA-sigma and yielded a knock down to 20% and 40%, respectively. The reason for the fact, that stably transfected single clones alone were more successful in terms of PTPA downregulation upon shRNA induction as the combination of stably transfected clones and transient siRNA transfections remains elusive.

Furthermore, a retroviral infection using pRetroSuper$_{Stuffer}$ constitutively expressing a targeting shRNA, representing the same C-terminal sequence as previously used, was carried out in mouse fibroblast cells, NIH3T3. However, a significant reduction of PTPA could not be demonstrated. Since the shRNA sequence was correct as determined by sequencing, a putative vector backbone mutation could be hold responsible.

In summary, the methods to downregulate PTPA below a critical threshold level failed. Therefore, we started to design a conditional knock-out vector for the generation of PTPA knock-out mice in cooperation with Arabella Meixner. The vector was decided to target exons 2 and 3, becuase targets near the highly conserved C-terminal end could again facilitate the production of N-terminal domains of PTPA. Subsequently, bacterial artificial chromosomes with the respective partial PTPA gene sequence were ordered. Unfortunately, I failed to electroporate these BACs into EL350 bacteria, which express the cre-recombinase upon heat shift, represented a hurdle which could not be cleared.

To sum up, using a conditional knock-out mouse model will presumably facilitate the elucidation of the function of PTPA in future investigations. So, *in vivo* studies of complete loss of PTPA could complement previous analyses in yeast, clear up the mystery of how the phosphatase two A activator works in mammalian cells and which factors possibly stimulate its performance.

Subcellular localization of PTPA

Previously, Azam and coworkers showed that overexpressed GFP-tagged PTPA occurred in the nucleus [Azam et al., 2007]. As this result was based solely on microscopy analysis, we aimed to determine the localization by two different methods: subcellular fractionation and immunofluorescence analyses. First, Hela cells were subdivided into nucleus and cytoplasm, according to recently published protocols [Hengstschläger and Rosner, 2008], and analysed by immunoblotting. Second, new monoclonal antibodies specific for PTPA were generated, tested by immunoblottiung with subcellular fractionated samples and applied in immunofluorescence analyses using Hela cells.

Initially, we found human PTPA in our cellular fractionation experiments mainly localized in the cytoplasm, with some also detectable in the nuclear compartment. For the determination of PTPA localization, we aimed to apply a second method. Therefore, the production of a new monoclonal antibody specific for PTPA was initiated. The evaluation of hybridoma subclones, arising from fusion of mouse 4 splenocytes with X63 cells, resulted in the decision for one minimally diluted hybridoma clone, 7F12 10B, and a hybdridoma mix clone, 6G2 to be included in further experiments. The decision for hybridoma clones was based on immunofluorescence analyses of Hela cells with antigen containing supernatant. Hybridoma clone 7F12 10B showed a predominantly nuclear staining, while hybridoma mix clone 6G2 revealed an intense cytoplasmic together with a minor nuclear staining. To further improve specificity by reducing the background bands in immunoblotting and possibly increase the staining intensity, supernatants of mixed subclone 6G2 and single subclone 7F12 10B were affinity purified by incubation with His-tagged PTPA blotted on a nitrocellulose membrane. Purified supernatant of hybridoma mix clone 6G2 revealed similar characteristics in immunofluorescence analysis as monoclonal anti-PTPA antibody 5G3, as it showed mainly nuclear staining. As mentioned above, affinity purification can enrich one species of antibodies out of supernatant containing different antibodies. The application of purifed 7F12 10B supernatant exhibited cytoplasmic staining accompanied by an intense staining surrounding the nucleus. One effect was striking: All monoclonal anti-PTPA antibodies displayed a mainly nuclear staining together with weak cytoplasmic occurrence.

Furthermore, purified and raw supernatants of 7F12 10B and mix clone 6G2 were applied in immunofluorescences of HelaTRex-pNTOneo-CT Clone L cells induced with doxycycline for

the expression of shRNA. None of the new produced antibodies was able to ascertain a significant signal reduction in immunofluorescence analyses of the PTPA protein, which was shown to be reduced to 15% of its wild type level.

Finally, supernatants of hybridoma clone 7F12 10B and hybridoma mix clone 6G2 were applied in immunoblotting with subcellular fractionated samples and demonstrated a mainly cytoplasmic distribution of PTPA. Interestingly, additional bands seemed to belong to particular compartments, especially regarding the nuclear fraction. Most obvious, immunoblotting with 7F12 10B antibody, showed a prominent band at 100kDa without reducing the signal intensity upon knock down of PTPA in both cellular compartments.

Due to diverging results obtained with subcellular fraction of cellular compartments and immunofluorescences with novel antibodies against PTPA, the exact localization of PTPA is still a matter of debate. Interestingly, Bollen and Beullens recently pointed out that protein phosphatases shuttle between cytoplasm and nucleus which enables them to act as signal transducers [Bollen and Beullens, 2002]. PP2A was found to occur as well in the nucleoplasma [Turowski et al., 1995] and therefore, indicating a possible explanation for the differential localization of PTPA. PTPA could shuttle to fulfil its versatile functions.

Concluding, PTPA possibly plays a multifactorial role in cellular mechanisms. Fellner and coworkers proposed a chaperone function of PTPA, facilitating the incorporation of divalent cations to the PP2A active site, which was accompanied by recent findings of Sablina and coworkers, who demonstrated PTPA to regulate methylation of PP2A C subunit [Fellner et al., 2003, Sablina et al., 2010]. Further observations implicated a role as tumor suppressor for PTPA, as overexpression induced apoptosis in colon carcinoma cells [Azam et al., 2007].

Further studies are needed to illuminate PTPAs function and to shed light upon the interaction with PP2A and other targets.

5. References

Adams DJ, van der Weyden L. (2008) "Contemporary approaches for modifying the mouse genome." Physiol Genomics **34**(3):225-38.

Alonso A, Sasin J, Bottini N, Friedberg I, Friedberg I, Osterman A, Godzik A, Hunter T, Dixon J, Mustelin T. (2004) "Protein tyrosine phosphatases in the human genome." Cell. **117**(6):699-711.

Arino J, Woon CW, Brautigan DL, Miller TB Jr, Johnson GL. (1988) "Human liver phosphatase 2A: cDNA and amino acid sequence of two catalytic subunit isotypes." Proc Natl Acad Sci USA**. 85**(12):4252-6.

Austin S, Ziese M, Sternberg N. (1981) "A novel role for site-specific recombination in maintenance of bacterial replicons." Cell. **25**(3):729-36.

Azam S, Drobetsky E, Ramotar D. (2007) "Overexpression of the cis/trans isomerase PTPA triggers caspase 3-dependent apoptosis." Apoptosis. **12**(7):1243-55.

Baharians Z, Schönthal AH. (1998) "Autoregulation of protein phosphatase type 2A expression." J Biol Chem. **273**(30):19019-24.

Begum N, Ragolia L. (1996) "cAMP counter-regulates insulin-mediated protein phosphatase-2A inactivation in rat skeletal muscle cells." J Biol Chem. **271**(49):31166-71.

Begum N, Ragolia L. (1999) "Role of janus kinase-2 in insulin-mediated phosphorylation and inactivation of protein phosphatase-2A and its impact on upstream insulin signalling components." Biochem J. **344**(3):895-901

Bollen M, Beullens M. (2002) "Signaling by protein phosphatases in the nucleus." Trends Cell Biol. **12**(3):138-45.

Cayla X, Goris J, Hermann J, Hendrix P, Ozon R, Merlevede W. (1990) "Isolation and characterization of a tyrosyl phosphatase activator from rabbit skeletal muscle and Xenopus laevis oocytes." Biochemistry. **29**(3):658-67.

Cayla X, Van Hoof C, Bosch M, Waelkens E, Vandekerckhove J, Peeters B, Merlevede W, Goris J. (1994) "Molecular cloning, expression, and characterization of PTPA, a protein that activates the tyrosyl phosphatase activity of protein phosphatase 2A." J Biol Chem. **269**(22):15668-75.

Chan LY, Amon A. (2009) "The protein phosphatase 2A functions in the spindle position checkpoint by regulating the checkpoint kinase Kin4." Genes Dev. **23**(14):1639-49.

Chao Y, Xing Y, Chen Y, Xu Y, Lin Z, Li Z, Jeffrey PD, Stock JB, Shi Y. (2006) "Structure and mechanism of the phosphotyrosyl phosphatase activator." Mol Cell. **23**(4):535-46.

Chen J, Martin BL, Brautigan DL. (1992) „Regulation of protein serine-threonine phosphatase type-2A by tyrosine phosphorylation." Science. **257**(5074):1261-4.

Chen J, Parsons S, Brautigan DL. (1994) "Tyrosine phosphorylation of protein phosphatase 2A in response to growth stimulation and v-src transformation of fibroblasts." J Biol Chem. **269**(11):7957-62.

Cho DH, Choi YJ, Jo SA, Ryou J, Kim JY, Chung J, Jo I. (2006) "Troglitazone acutely inhibits protein synthesis in endothelial cells via a novel mechanism involving protein phosphatase 2A-dependent p70 S6 kinase inhibition." Physiol Cell Physiol. **291**(2):C317-26.

Cho US, Xu W. (2007) "Crystal structure of protein phosphatse 2A hetrotrimeric holoenzyme." Nature. **445**(7123):53-7

De Baere I, Derua R, Janssens V, Van Hoof C, Waelkens E, Merlevede W, Goris J. (1999) "Purification of porcine brain protein phosphatase 2A leucine carboxyl methyltransferase and cloning of the human homologue." Biochemistry. **38**(50):16539-47.

Di Como CJ, Arndt KT. 1996 "Nutrients, via the Tor proteins, stimulate the association of Tap42 with type 2A phosphatases." Genes Dev. **10**(15):1904-16.

Donehower LA, Harvey M, Slagle BL, McArthur MJ, Montgomery CA Jr, Butel JS, Bradley A. (1992) "Mice deficient for p53 are developmentally normal but susceptible to spontaneous tumours." Nature. **356**(6366):215-21.

Drewes G, Mandelkow EM, Baumann K, Goris J, Merlevede W, Mandelkow E. (1993) " Dephosphorylation of tau protein and Alzheimer paired helical filaments by calcineurin and phosphatase-2A." FEBS Lett. **336**(3):425-32.

Elbashir SM, Harborth J, Lendeckel W, Yalcin A, Weber K, Tuschl T. (2001) "Duplexes of 21-nucleotide RNAs mediate RNA interference in cultured mammalian cells." Nature. **411**(6836):494-8.

Fedorov Y, Anderson EM, Birmingham A, Reynolds A, Karpilow J, Robinson K. (2006) "Off-target effects by siRNA can induce toxic phenotype." RNA. **12**(7):1188–96.

Fellner T, Lackner DH, Hombauer H, Piribauer P, Mudrak I, Zaragoza K, Juno C, Ogris E. (2003) "A novel and essential mechanism determining specificity and activity of protein phosphatase 2A (PP2A) in vivo." Genes Dev. **17**(17): 2138-50.

Gallego M, Virshup DM. (2005) "Protein serine/threonine phosphatases: life, death, and sleeping." Curr Opin Cell Biol.**17**(2):197-202.

Gong CX, Grundke-Iqbal I, Iqbal K. (1994) "Dephosphorylation of Alzheimer's disease abnormally phosphorylated tau by protein phosphatase-2A." Neuroscience. **61**(4):765-72.

Götz J, Probst A, Ehler E, Hemmings B, Kues W. (1998) "Delayed embryonic lethality in mice lacking protein phosphatase 2A catalytic subunit Calpha." Proc Natl Acad Sci U S A. **95**(21):12370-5.

Green DD, Yang SI, Mumby MC. (1987) "Molecular cloning and sequence analysis of the catalytic subunit of bovine type 2A protein phosphatase." Proc Natl Acad Sci U S A. **84**(14):4880-4.

Guy GR, Philp R, Tan YH. (1995) "Activation of protein kinases and the inactivation of protein phosphatase 2A in tumour necrosis factor and interleukin-1 signal-transduction pathways." Eur J Biochem. **229**(2):503-11

Hasty P, Rivera-Pérez J, Bradley A. (1991) "The length of homology required for gene targeting in embryonic stem cells." Mol Cell Biol. **11**(11):5586-91.

Healy AM, Zolnierowicz S, Stapleton AE, Goebl M, DePaoli-Roach AA, Pringle JR. (1991) "CDC55, a Saccharomyces cerevisiae gene involved in cellular morphogenesis: identification, characterization, and homology to the B subunit of mammalian type 2A protein phosphatase." Mol Cell Biol. **11**(11):5767-80.

Hemmings BA, A.-P. C., Maurer F, Müller P, Goris J, Merlevede W, Hofsteenge J, Stone SR. (1990) "alpha- and beta-forms of the 65-kDa subunit of protein phosphatase 2A have a similar 39 amino acid repeating structure." Biochemistry. **29**(13):3166-3173

Hombauer H, Weismann D, Mudrak I, Stanzel C, Fellner T, Lackner DH, Ogris E. (2007) "Generation of active protein phosphatase 2A is coupled to holoenzyme assembly." PLoS Biol. **5**(6):e155.

Honkanen RE, Golden T. (2002) "Regulators of serine/threonine protein phosphatases at the dawn of a clinical era?" Curr Med Chem. 9(**22**):2055-75.

Ikehara T, Ikehara S, Imamura S, Shinjo F, Yasumoto T. (2007) "Methylation of the C-terminal leucine residue of the PP2A catalytic subunit is unnecessary for the catalytic activity and the binding of regulatory subunit (PR55/B)." Biochem Biophys Res Commun. **354**(4):1052-7.

Ingebritsen TS, Cohen P. (1983) "Protein phosphatases: properties and role in cellular regulation." Science. **221**(4608):331-8.

Jackson AL, Burchard J, Leake D, Reynolds A, Schelter J, Guo J, Johnson JM, Lim L, Karpilow J, Nichols K, Marshall W, Khvorova A, Linsley PS.(2006) "Position-specific chemical modification of siRNAs reduces "off-target" transcript silencing." RNA. **12**(7):1197-205.

Janssens V, V. H. C., De Baere I, Merlevede W, Goris J. (1999) "Functional analysis of the promoter region of the human phosphotyrosine phosphatase activator gene: Yin Yang 1 is essential for core promoter activity." Biochem J. **344** (Pt 3):755-763

Janssens V, v. H. C., Martens E, de Baere I, Merlevede W, Goris J. (2000) "Identification and characterization of alternative splice products encoded by the human phosphotyrosyl phosphatase activator gene." Eur J Biochem. **267**(14):4406-4413

Janssens, V. and J. Goris (2001). "Protein phosphatase 2A: a highly regulated family of serine/threonine phosphatases implicated in cell growth and signalling." Biochem J **353**(Pt 3): 417-39.

Jiang Y, Broach JR. (1999) "Tor proteins and protein phosphatase 2A reciprocally regulate Tap42 in controlling cell growth in yeast." EMBO J. **18**(10):2782-92.

Johnson SA, Hunter T. 2005 "Kinomics: methods for deciphering the kinome." Nat Methods. **2**(1):17-25.

Jordens J, J. V., Longin S, Stevens I, Martens E, Bultynck G, Engelborghs Y, Lescrinier E, Waelkens E, Goris J, Van Hoof C. (2006) "The protein phosphatase 2A phosphatase activator is a novel peptidyl-prolyl cis/trans-isomerase." J Biol Chem. **281**(10): 6349-6357

Khew-Goodall Y, Mayer RE, Maurer F, Stone SR, Hemmings BA. (1991) "Structure and transcriptional regulation of protein phosphatase 2A catalytic subunit genes." Biochemistry. **30**(1):89-97.

Khew-Goodall, Y., Hemmings B.A. (1988) "Tissue-specific expression of mRNAs encoding alpha- and beta-catalytic subunits of protein phosphatase 2A." FEBS Lett. **238**(2):265-8.

Kins, S., Crameri A., Evans D.R., Hemmings B.A., Nitsch R.M., Gotz J. (2001) "Reduced protein phosphatase 2A activity induces hyperphosphorylation and altered compartmentalization of tau in transgenic mice." J Biol Chem. **276**(41):38193-200.

Kitajima TS, Sakuno T, Ishiguro K, Iemura S, Natsume T, Kawashima SA, Watanabe Y. (2006) "Shugoshin collaborates with protein phosphatase 2A to protect cohesin." Nature. **441**(7089):46-52

Kugler Michaela (2010) "Biochemical studies of PTPA and PP2A biogenesis in mammalian cells."

Lee J, Chen Y, Tolstykh T, Stock J. (1996) "A specific protein carboxyl methylesterase that demethylates phospho-protein phosphatase 2A in bovine brain." Proc Natl Acad Sci U S A. **93**(12):6043-7.

Lee J, Stock J. (1993) "Protein phosphatase 2A catalytic subunit is methyl-esterified at its carboxyl terminus by a novel methyltransferase." J Biol Chem. **268**(26):19192–19195

Lee T, Kim SJ, Sumpio BE. (2003) "Role of PP2A in the regulation of p38 MAPK activation in bovine aortic endothelial cells exposed to cyclic strain." J Cell Physiol. **194**(3):349-55.

Zhen Li, Yves Fortin, and Shi-Hsiang Shen. (2009) "Forward and robust selection of the most potent and noncellular toxic siRNAs from RNAi libraries" Nucleic Acids Res. **37**(1): e8.

Liu F, Grundke-Iqbal I, Iqbal K, Gong CX. (2005) "Contributions of protein phosphatases PP1, PP2A, PP2B and PP5 to the regulation of tau phosphorylation." Eur J Neurosci. **22**(8):1942-50.

Longin S, Jordens J, Martens E, Stevens I, Janssens V, Rondelez E, De Baere I, Derua R, Waelkens E, Goris J, Van Hoof C. (2004) "An inactive protein phosphatase 2A population is associated with methylesterase and can be reactivated by the phosphotyrosyl phosphatase activator." Biochem J. **380**(Pt 1):111-9.

Magnusdottir A, S. P., Flodin S, Nyman T, Hammarström M, Ehn M, Bakali, Berglund H, Nordlund P. (2006) "The crystal structure of a human PP2A phosphatase activator reveals a novel fold and highly conserved cleft implicated in protein-protein interactions." J Biol Chem. **281**(32): 22434-22438

McAnuff MA, Rettig GR, Rice KG. (2007) "Potency of siRNA versus shRNA mediated knockdown in vivo." J Pharm Sci. **96**(11):2922-30.

McLeod M, Craft S, Broach JR. (1986) "Identification of the crossover site during FLP-mediated recombination in the Saccharomyces cerevisiae plasmid 2 microns circle." Mol Cell Biol. **6**(10):3357-67.

Mitterhuber Martina (2008) "The role of PP2A Phosphatase Activator in the biogenesis of PP2A in mammalian cells."

Mumby M. (2001) "A new role for protein methylation: switching partners at the phosphatase ball." Sci STKE. (79):pe1.

Mumby M. (2007) "The 3D structure of protein phosphatase 2A: new insights into a ubiquitous regulator of cell signaling." ACS Chem Biol. **2**(2):99-103.

Novy M, Pohn R, Andorfer P, Novy-Weiland T, Galos B, Schwarzmayr L, Rotheneder H. (2005) "EAPP, a novel E2F binding protein that modulates E2F-dependent transcription." Mol Biol Cell. **16**(5):2181-90.

Nüsse M, Egner HJ. (1984) "Can nocodazole, an inhibitor of microtubule formation, be used to synchronize mammalian cells? Accumulation of cells in mitosis studied by two parametric flow cytometry using acridine orange and by DNA distribution analysis." Cell Tissue Kinet. **17**(1):13-23.

Ogris E, Du X, Nelson KC, Mak EK, Yu XX, Lane WS, Pallas DC. (1999) "A protein phosphatase methylesterase (PME-1) is one of several novel proteins stably associating with two inactive mutants of protein phosphatase 2A." J Biol Chem. **274**(20):14382-91.

Ogris E, Gibson DM, Pallas DC. (1997) "Protein phosphatase 2A subunit assembly: the catalytic subunit carboxy terminus is important for binding cellular B subunit but not polyomavirus middle tumor antigen." Oncogene. **15**(8):911-7.

Queralt E, Uhlmann F. (2008) "Separase cooperates with Zds1 and Zds2 to activate Cdc14 phosphatase in early anaphase." J Cell Biol. **182**(5): 873–883.

Ramotar D, Belanger E, Brodeur I, Masson JY, Drobetsky EA. (1998) "A yeast homologue of the human phosphotyrosyl phosphatase activator PTPA is implicated in protection against oxidative DNA damage induced by the model carcinogen 4-nitroquinoline 1-oxide." J Biol Chem. **273**(34):21489-96.

Rao DD, Vorhies JS, Senzer N, Nemunaitis J. (2009) "siRNA vs. shRNA: similarities and differences." Adv Drug Deliv Rev. **61**(9):746-59.

Rempola B, Kaniak A, Migdalski A, Rytka J, Slonimski PP, di Rago JP. (2000) "Functional analysis of RRD1 (YIL153w) and RRD2 (YPL152w), which encode two putative activators of the phosphotyrosyl phosphatase activity of PP2A in Saccharomyces cerevisiae." Mol Gen Genet. **262**(6):1081-92.

Riedel CG, Katis VL, Katou Y, Mori S, Itoh T, Helmhart W, Gálová M, Petronczki M, Gregan J, Cetin B, Mudrak I, Ogris E, Mechtler K, Pelletier L, Buchholz F, Shirahige K, Nasmyth K. (2006) "Protein phosphatase 2A protects centromeric sister chromatid cohesion during meiosis I." Nature. **441**(7089):53-61.

Roblek M, Schüchner S, Huber V, Ollram K, Vlcek-Vesely S, Foisner R, Wehnert M, Ogris E. (2010) "Monoclonal antibodies specific for disease-associated point-mutants: lamin A/C R453W and R482W." PLoS One. **5**(5):e10604.

Rodriguez-Lebron E, Paulson HL. (2006) "Allele-specific RNA interference for neurological disease." Gene Ther.**13**(6):576-81.

Ronne, H., Carlberg M., Hu G.Z., Nehlin J.O. (1991) "Protein phosphatase 2A in Saccharomyces cerevisiae: effects on cell growth and bud morphogenesis." Mol Cell Biol. **11**(10):4876-84.

Rosner M, Hengstschläger M. (2008) "Cytoplasmic and nuclear distribution of the protein complexes mTORC1 and mTORC2: rapamycin triggers dephosphorylation and delocalization of the mTORC2 components rictor and sin1." Hum Mol Genet. **17**(19):2934-48.

Ruediger R, Pham HT, Walter G. (2001) "Alterations in protein phosphatase 2A subunit interaction in human carcinomas of the lung and colon with mutations in the A beta subunit gene." Oncogene. **20**(15):1892-9.

Sablina AA, Chen W, Arroyo JD, Corral L, Hector M, Bulmer SE, DeCaprio JA, Hahn WC. (2007) "The tumor suppressor PP2A Abeta regulates the RalA GTPase." Cell. **129**(5):969-82.

Sablina AA, Hector M, Colpaert N, Hahn WC. (2010) "Identification of PP2A complexes and pathways involved in cell transformation." Cancer Res. **70**(24):10474-84.

Schnütgen F, Doerflinger N, Calléja C, Wendling O, Chambon P, Ghyselinck NB. (2003) "A directional strategy for monitoring Cre-mediated recombination at the cellular level in the mouse." Nat Biotechnol. **21**(5):562-5.

Shan G. (2010) "RNA interference as a gene knockdown technique." Int J Biochem Cell Biol. **42**(8):1243-51.

Shi Y.(2009) "Serine/threonine phosphatases: mechanism through structure." Cell. **139**(3):468-84.

Shu Y, Yang H, Hallberg E, Hallberg R. (1997) "Molecular genetic analysis of Rts1p, a B' regulatory subunit of Saccharomyces cerevisiae protein phosphatase 2A." Mol Cell Biol. **17**(6):3242-53.

Sneddon AA, Cohen PT, Stark MJ. (1990) "Saccharomyces cerevisiae protein phosphatase 2A performs an essential cellular function and is encoded by two genes." EMBO J. **9**(13):4339-46.

Sontag E, Fedorov S, Kamibayashi C, Robbins D, Cobb M, Mumby M. (1993) "The interaction of SV40 small tumor antigen with protein phosphatase 2A stimulates the map kinase pathway and induces cell proliferation." Cell. **75**(5):887-97.

Sontag JM, Nunbhakdi-Craig V, Mitterhuber M, Ogris E, Sontag E. (2010) "Regulation of protein phosphatase 2A methylation by LCMT1 and PME-1 plays a critical role in differentiation of neuroblastoma cells." J Neurochem. **115**(6):1455-65.

Sontag, E., Luangpirom A., Hladik C., Mudrak I., Ogris E., Speciale S., White C.L. (2004) "Altered expression levels of the protein phosphatase 2A ABalphaC enzyme are associated with Alzheimer disease pathology." J Neuropathol Exp Neurol. **63**(4):287-301.

Sontag, E., V. Nunbhakdi Craig, et al. (1996) "Regulation of the phosphorylation state and microtubule-binding activity of Tau by protein phosphatase 2A." Neuron **17**(6): 1201-7.

Sontag, E., V. Nunbhakdi Craig, et al. (1999) "Molecular interactions among protein phosphatase 2A, tau, and microtubules. Implications for the regulation of tau phosphorylation and the development of tauopathies." J Biol Chem **274**(36): 25490-8.

Srinivasan M, Begum N. (1994) "Regulation of protein phosphatase 1 and 2A activities by insulin during myogenesis in rat skeletal muscle cells in culture." J Biol Chem. **269**(17):12514-20.

Stone SR, Mayer R, Wernet W, Maurer F, Hofsteenge J, Hemmings BA. (1988) "The nucleotide sequence of the cDNA encoding the human lung protein phosphatase 2A alpha catalytic subunit." Nucleic Acids Res. **16**(23):11365.

Stout-Delgado HW, Getachew Y, Rogers TE, Miller BC, Thiele DL. (2007) "The role of serpinb9/serine protease inhibitor 6 in preventing granzyme B-dependent hepatotoxicity." Hepatology. **46**(5):1530-40.

Strack S, Cribbs JT, Gomez L. (2004) "Critical role for protein phosphatase 2A heterotrimers in mammalian cell survival." J Biol Chem. **279**(46):47732-9.

Tang X, Wang Y. (2006) "Pds1/Esp1-dependent and -independent sister chromatid separation in mutants defective for protein phosphatase 2A." Proc Natl Acad Sci U S A. **103**(44):16290-5.

Thyberg J, Moskalewski S. (1985) "Microtubules and the organization of the Golgi complex." Exp Cell Res. **159**(1):1-16.

Tolstykh T, Lee J, Vafai S, Stock JB. (2000) "Carboxyl methylation regulates phosphoprotein phosphatase 2A by controlling the association of regulatory B subunits." EMBO J. **19**(21):5682-91.

Tom Tuschl, Sayda Elbashir, Jens Harborth, and Klaus WeberThe siRNA user guide (2004) "The siRNA user guide: Selection of siRNA duplexes from the target mRNA sequence" http://www.rockefeller.edu/labheads/tuschl/sirna.html

Turowski P, Fernandez A, Favre B, Lamb NJ, Hemmings BA. (1995) "Differential methylation and altered conformation of cytoplasmic and nuclear forms of protein phosphatase 2A during cell cycle progression." J Cell Biol. **129**(2):397-410.

Usui H, Inoue R, Tanabe O, Nishito Y, Shimizu M, Hayashi H, Kagamiyama H, Takeda M. (1998) "Activation of protein phosphatase 2A by cAMP-dependent protein kinase-catalyzed phosphorylation of the 74-kDa B" (delta) regulatory subunit in vitro and identification of the phosphorylation sites." FEBS Lett. **430**(3):312-6.

Van Hoof C, Cayla X, Bosch M, Merlevede W, Goris J. (1994) "The phosphotyrosyl phosphatase activator of protein phosphatase 2A. A novel purification method, immunological and enzymic characterization." Eur J Biochem. **226**(3):899-907.

Van Hoof C, Cayla X, Bosch M, Merlevede W, Goris J. (1994) "The phosphotyrosyl phosphatase activator of protein phosphatase 2A. A novel purification method, immunological and enzymic characterization." Eur J Biochem. **226**(3):899-907.

Van Hoof C, Ingels F, Cayla X, Stevens I, Merlevede W, Goris J. (1995) "Molecular cloning and developmental regulation of expression of two isoforms of the catalytic subunit of protein phosphatase 2A from Xenopus laevis." Biochem Biophys Res Commun. **215**(2):666-73.

Van Hoof C, Janssens V, De Baere I, Stark MJ, de Winde JH, Winderickx J, Thevelein JM, Merlevede W, Goris J. (2001) "The Saccharomyces cerevisiae phosphotyrosyl phosphatase activator proteins are required for a subset of the functions disrupted by protein phosphatase 2A mutations." Exp Cell Res. **264**(2):372-87.

Van Hoof C, Janssens V, Dinishiotu A, Merlevede W, Goris J. (1998) "Functional analysis of conserved domains in the phosphotyrosyl phosphatase activator. Molecular cloning of the homologues from Drosophila melanogaster and Saccharomyces cerevisiae." Biochemistry. **37**(37):12899-908.

Van Hoof C, Martens E, Longin S, Jordens J, Stevens I, Janssens V, Goris J. (2005) "Specific interactions of PP2A and PP2A-like phosphatases with the yeast PTPA homologues, Ypa1 and Ypa2." Biochem J. **386**(Pt 1):93-102.

van Zyl, W., N. Wills, et al. (1989) "A general screen for mutant of Saccharomyces cerevisiae deficient in tRNA biosynthesis." Genetics 123.

Virshup, D. M. (2000). "Protein phosphatase 2A: a panoply of enzymes." Curr Opin Cell Biol **12**(2): 180-5.

Wang EH, Bhattacharyya S, Prives C. (1993) "The replication functions of polyomavirus large tumor antigen are regulated by phosphorylation." J Virol. **67**(11):6788-96.

Wang SS, Esplin ED, Li JL, Huang L, Gazdar A, Minna J, Evans GA. (1998) "Alterations of the PPP2R1B gene in human lung and colon cancer." Science. **282**(5387):284-7.

Wu J, Tolstykh T, Lee J, Boyd K, Stock JB, Broach JR. (2000) "Carboxyl methylation of the phosphoprotein phosphatase 2A catalytic subunit promotes its functional association with regulatory subunits in vivo." EMBO J. **19**(21):5672-81.

Xing Y, Xu Y, Chen Y, Jeffrey PD, Chao Y, Lin Z, Li Z, Strack S, Stock JB, Shi Y. (2006) "Structure of protein phosphatase 2A core enzyme bound to tumor-inducing toxins." Cell. **127**(2):341-53.

Xu Y, Chen Y, Zhang P, Jeffrey PD, Shi Y. (2008) "Structure of a protein phosphatase 2A holoenzyme: insights into B55-mediated Tau dephosphorylation." Mol Cell. 31(6):873-85.

Xu Z, Williams BR. (2000) "The B56alpha regulatory subunit of protein phosphatase 2A is a target for regulation by double-stranded RNA-dependent protein kinase PKR." Mol Cell Biol. **20**(14):5285-99.

Yeong FM, Hombauer H, Wendt KS, Hirota T, Mudrak I, Mechtler K, Loregger T, Marchler-Bauer A, Tanaka K, Peters JM, Ogris E. (2003) "Identification of a subunit of a novel Kleisin-beta/SMC complex as a potential substrate of protein phosphatase 2A." Curr Biol. **13**(23):2058-64.

Zhang H, Kolb FA, Brondani V, Billy E, Filipowicz W. (2002) "Human Dicer preferentially cleaves dsRNAs at their termini without a requirement for ATP." EMBO J. **21**(21):5875-85.
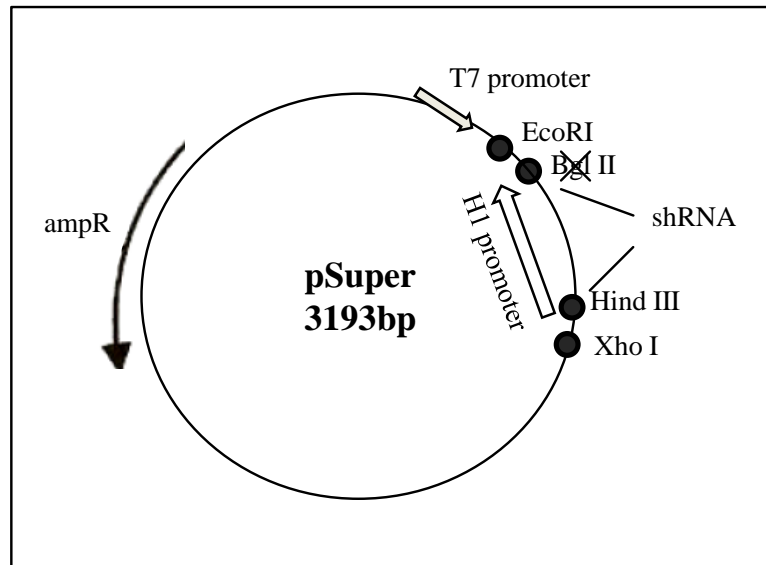
Zhao Y, Boguslawski G, Zitomer RS, DePaoli-Roach AA. (1997) "Saccharomyces cerevisiae homologs of mammalian B and B' subunits of protein phosphatase 2A direct the enzyme to distinct cellular functions." J Biol Chem. **272**(13):8256-62.
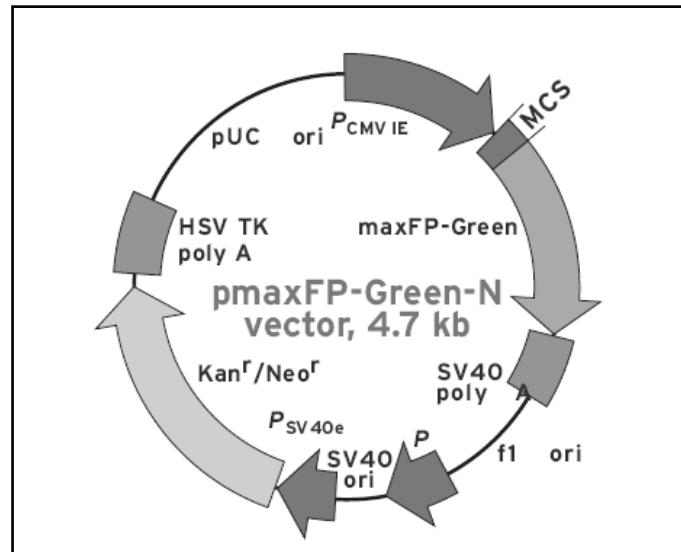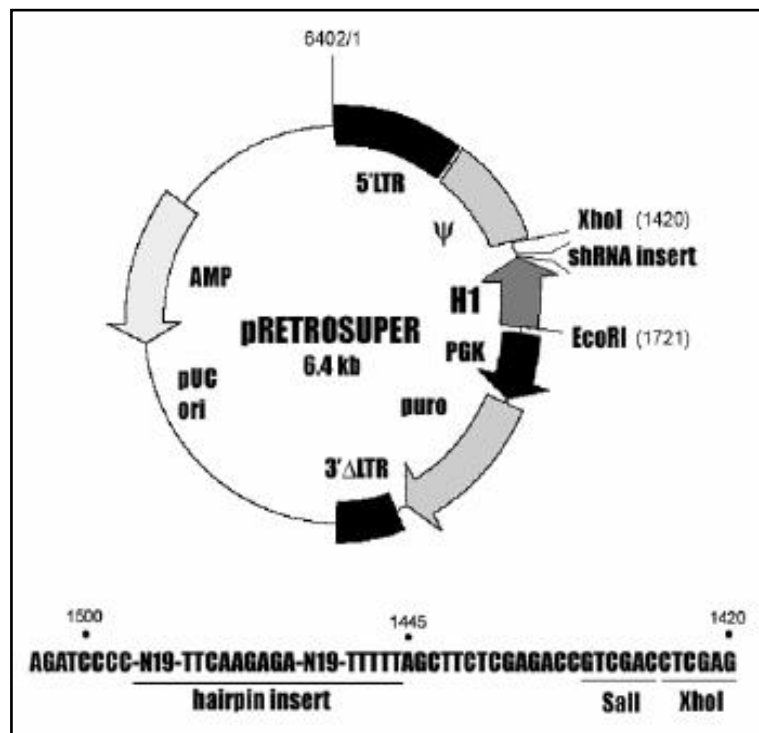
6. Appendix

pNTOneo-CT, pNTOneo-Mis:
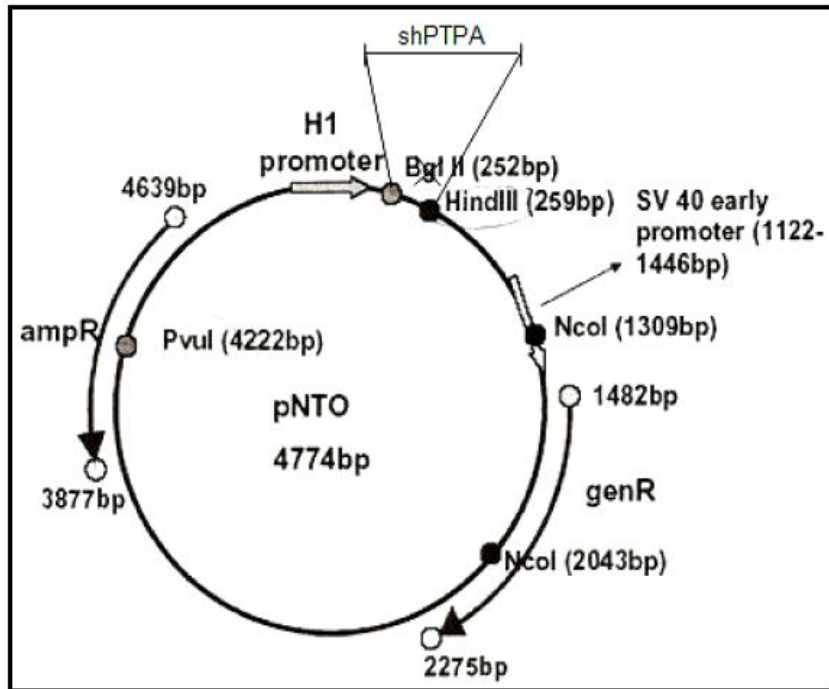
pSuper-CT, pSuper-Mis:

pmaxGFP:

pRetroSuper-CT and pRetroSuper-Mis:

Strategy: cut pSuper-CT/Mis and pRetroSuper with EcoRI and XhoI; gel elution of insert and vector (11.2.10); ligation of ~300bp –CT and –Mis of pSuper with pRetroSuper (12.2.10)

Positive clones: pRetroSuper-CT Clone 3, pRetroSuper-Mis Clone 2

Sequenced: 10.3.10 at LGC genomics with primer H1RNA pro 5´-GAATCGCGGGCCCAGTGTCA-3´

7. Acknowledgements

8. Curriculum Vitae

Personal Information

Name   Schönbauer, Sarah Maria

Address   Nussdorferstraße 40, 1090 Wien

E-mail   sarah.schoenbauer@univie.ac.at

Date of birth   December 11, 1982

Nationality   Austrian

Education

2004-2011   Study of Biology at the University of Vienna

2002-2004   Study of Medicine at the Medical University of Vienna

1993-2001   BG/BRG Ried im Innkreis